Dissertation

Identification of novel molecular components in Ripoptosome-mediated signaling pathways

Submitted to the
Combined Faculties for the Natural Sciences and for Mathematics
of the Ruperto-Carola University of Heidelberg, Germany
for the degree of
Doctor of Natural Sciences

presented by

Ramon Schilling

Dissertation

Submitted to the
Combined Faculties for the Natural Sciences and for Mathematics
of the Ruperto-Carola University of Heidelberg, Germany
for the degree of
Doctor of Natural Sciences

presented by

Ramon Schilling, Diploma in Biophysics

Born in Ludwigshafen, Germany, 16.02.1986

Oral examination: 04.08.2016

Identification of novel molecular components in Ripoptosome-mediated signaling pathways

Referees: Prof. Dr. Viktor Umansky

Prof. Dr. Petra Boukamp

Declarations according to § 8 (3) b) and c) of the doctoral degree regulations:

b) I hereby declare that I have written the submitted dissertation myself and in this process have used no other sources or materials than those expressly indicated,

c) I hereby declare that I have not applied to be examined at any other institution, nor have I used the dissertation in this or any other form at any other institution as an examination paper, nor submitted it to any other faculty as a dissertation.

Mannheim, 11.05.2016

Ramon Schilling

This PhD thesis is dedicated to my wife Martina and my daughter Helena

who gave me the strength to surpass my own limits

and bring light into my life every day.

Table of Content

I. List of Figures

II. List of Tables

III. Abstract

Programmed cellular execution is one of the hallmarks of cellular homeostasis as well as the development of multicellular organisms. To date, two major signaling pathways for programmed cell death have been elucidated, namely apoptosis and necroptosis. The induction of these two regulated cell death programs can be initiated by a variety of extrinsic as well as intrinsic stimuli, like genotoxic stress, death receptor activation, pathogen infection or the depletion cIAPs. Apoptosis thereby relies on the activation of caspase-8, which induces a downstream caspase cascade, finally leading to apoptotic execution. In contrast, caspase-independent necroptosis relies on the activation of the kinases RIP1 and RIP3, resulting in the phosphorylation of the pseudokinase MLKL. This finally leads to necroptotic plasma membrane permeabilization. Additionally, recent studies highlighted that certain cellular conditions can induce the formation of an intracellular 2 MDa multi-protein complex, called Ripoptosome, which can lead to apoptosis as well as necroptosis based on the stoichiometric composition. This protein complex consists of FADD, caspase-8, cFLIP and the name giving RIP1. However, it is still unclear, if all components or interacting proteins have been identified.

In this study purified Ripoptosome complexes were analyzed for the identification of novel components by mass spectrometry. Interestingly, the non-canonical IKKs; TBK1 and IKK-ε as well as TRAF2 could be identified as integral elements of the complex. The association of these molecules with the Ripoptosome was observed upon TNF treatment or TLR3 stimulation or the overexpression of RIP1 as the initial stimulus. Moreover, the non-canonical IKKs were highly phosphorylated in the complex, arguing for substantial activation. The cell death regulating function of the Ripoptosome was not affected by the loss of TBK1 and IKK-ε, indicating that these molecules could play a pivotal role in non-cell death signaling pathways. In contrast, decrease of TRAF2 resulted in a sensitization against apoptotic cells death. This was true for the expression of RIP1 as well as the combined treatment of poly (I:C) or TNF with IAP antagonists. Additionally, RIP1-induced Ripoptosome formation could be linked to the activation of NF-κB and the induction of inflammatory cytokines. The reduction in TBK1 and IKK-ε protein levels was leading to a decrease in the RIP1-regulated gene induction. Additionally, the formation of the Ripoptosome was inducing the phosphorylation of autophagy receptors optineurin and sequestosome-1. This activation was highly depending on the kinases TBK1 and IKK-ε, indicating a possible Ripoptosome-dependent activation of the autophagy machinery. The novel identified components highlighted the Ripoptosome as a key complex not only for cell death regulation, but also for cell death-independent signaling pathways such as inflammatory responses and autophagy.

IV. Zusammenfassung

Programmierter Zelltod (PCD) ist ein Bestandteil der zellulären Homöostase, sowie der Entwicklung vielzelliger Organismen. Bis heute wurden hauptsächlich zwei PCD Signalwege detailliert beschrieben, und zwar die Apoptose und die Nekroptose. Die Induktion dieser Zelltodprogramme kann durch eine Vielzahl von extrinsischen und intrinsischen Stimuli, wie genotoxischem Stress, der Aktivierung von Todesrezeptoren, pathogenen Infektionen oder der Depletierung von cIAPs (inhibitor of apoptosis protein) ausgelöst werden. Die Apoptose beruht dabei im Wesentlichen auf der Aktivierung der Initiator-Caspase-8, welche eine nachgeschaltete Caspase-Kaskade auslöst, was schließlich zur apoptotischen Exekution führt. Im Gegensatz dazu hängt die Caspase-unabhängige Nekroptose von der Aktivierung der Kinasen RIP1 und RIP3 ab. Nach der Aktivierung phosphoryliert RIP3 die Pseudokinase MLKL, was letztendlich zur nekroptotischen Permeabilisierung der Plasmamembran führt. Zusätzlich haben neue Studien gezeigt, dass bestimmte zelluläre Umstände zur Bildung eines 2 MDa Komplexes, dem Ripoptosom, führen können, der basierend auf seiner stöchiometrischen Beschaffenheit zu Apoptose sowie Nekroptose führen kann. Dieser Proteinkomplex besteht aus FADD, Caspase-8, cFLIP und dem namengebenden RIP1. Allerdings ist noch immer unklar, ob neben den bekannten Ripoptosomkomponenten noch weitere Proteine vorhanden sind oder mit dem Ripoptosom interagieren.

In dieser Studie wurden gereinigte Ripoptosomkomplexe massenspektrometrisch auf mögliche neue Komponenten untersucht. Interessanterweise konnten TBK1 und IKK-ε, sowie TRAF2 als Bestandteile dieses Komplexes identifiziert werden. Die Assoziation dieser Moleküle mit dem Ripoptosom konnte nach TNF Stimulation, TLR3 Aktivierung und nach Überexpression von RIP1 gefunden werden. Weiterhin waren TBK1 und IKK-ε im Komplex stark phosphoryliert. Die Ripoptosom-vermittelte Zelltodantwort wurde durch den Verlust dieser Proteine nicht beeinflusst. Im Gegensatz dazu führte die Reduktion von TRAF2, sowohl nach Expression von RIP1, als auch nach kombinierter Behandlung mit poly (I:C) oder TNF und IAP Antagonisten, zu einer Sensitivierung gegenüber apoptotischem Zelltod. Des Weiteren konnte die RIP1-induzierte Komplexformierung mit der Aktivierung von NF-κB und der Induktion inflammatorischer Zytokine verknüpft werden. Die Reduktion der TBK1 und IKK-ε Proteinlevel führte zu einer Abnahme der RIP1-vermittelten Geninduktion. Weiterhin wurde durch Ripoptosomformierung die Phosphorylierung von Autophagierezeptoren, wie Optineurin und Seqestosome-1, induziert. Diese Aktivierung war abhängig von den Kinasen TBK1 und IKK-ε. Somit beleuchten die neu identifizierten Komponenten das Ripoptosom als Schlüsselkomplex, nicht nur für die Zelltodregulation sondern auch für zelltodunabhängige Signalwege, wie Inflammation oder Autophagie.

V. Introduction

V.1. Programmed Cell Death – a regulated way to die

Multicellular organisms have developed the ability to remove excessive, abnormal and potentially dangerous cells in a highly regulated manner. Therefore, they use specific forms of programmed cell death (PCD), which can be triggered through intracellular sensors as well as through extracellular stimuli. To date, there are two described intracellular signaling pathways, named apoptosis and necroptosis, whose stimulation can lead to directed cell execution. Both differ in morphological appearance as well as in their biochemical behavior. Recent studies highlighted the essential role of both forms of execution, as disorganization of these processes can lead to embryonic lethality, autoimmune diseases or cancer development.

V.1.1. Apoptosis – a caspase-dependent, regulated cell death program

The importance of regulated cell death for cellular homeostasis was first described by the German Scientist Karl Vogt in 1842[1]. However, the importance of this discovery was not recognized until 1965 when John Foxten Ross Kerr was able to distinguish regulated cell death from traumatic cell execution[2,3]. In 1972, Kerr, Whyllie and Currie finally defined the term apoptosis for the observed regulated form of cell death[4]. The regulated removal of cells through apoptosis is normally conferring advantages during an organism's lifecycle. Whenever certain cells become abnormal and thereby potentially dangerous, for example through genetic mutations occurring during cell proliferation or after pathogen infection, they have to be removed in order to protect the surrounding tissue or the whole organism. Moreover, it was shown that apoptosis is a necessity for embryonic development[5]. This can for example be seen, when the excessive cells in the interdigital zone have to be eliminated in an ordered fashion to separate the single fingers[6].

Cells undergoing apoptosis show characteristic morphological changes that can be divided in the following steps: First, cell shrinkage and rounding is observed as a cause of the caspase-triggered breakdown of the cytoskeleton[7]. This is followed by the condensation of chromatin[8]. The DNA is fragmented and the nucleus breaks into several so-called chromatin bodies[8]. The cell membrane loses the round structure and irregular blebs become visible (known as membrane blebbing)[9]. The cell breaks into several vesicles (called apoptotic bodies) which are then eliminated through phagocytosis[10,11]. Once activated, apoptosis is resulting in the activation of an intracellular regulatory protein cascade, where cystein-aspartatic proteases

(caspases) play the major role in downstream propagation of the death signal[12]. The caspases can be divided into initiator-caspases (2, 8, 9, and 10), effector-caspases (3, 6, and 7) and inflammatory-caspases[13]. Caspases are always synthesized in their inactive proform, called zymogen or procaspase, which can be brought into its active state by autocatalytic cleavage or via fission through other caspases. The prodomain of initiator caspases consists of complex binding motives like the death effector domain (DED) or the caspase recruiting domain (CARD), which are essential for the recruitment of these caspases into multiprotein complexes[13]. The initiation of apoptotic execution can be divided into two major signaling pathways: the intrinsic or mitochondrial pathway and the extrinsic or death receptor (DR) pathway[14], which will be discussed in the following chapters.

V.1.1.1. The intrinsic apoptotic signaling pathway

Pathogen infections or inflammatory cytokines as well as intracellular stimuli like DNA (Deoxyribonucleic acid) damage or the production of reactive oxygen species (ROS) are able to induce the intrinsic apoptotic signaling pathway[14,15]. The above-mentioned stress factors result in the activation of the BH3-only (B-cell lymphoma-2 (Bcl-2) homology 3 (BH3)-only) proteins[16,17]. These proteins in turn activate the pro-apoptotic proteins Bak (Bcl-2 homologues antagonist killer) and Bax (Bcl-2 associated X protein). Both proteins are able to integrate and form porous structures in the mitochondrial outer membrane[18]. This process results in the release of apoptogenic factors, e.g. Cytochrome-c or Smac/Diablo (second mitochondria-derives activator of caspases/direct IAP binding protein with low pI) from the mitochondrial inter membrane space (IMS)[19]. The release of Cytochrome-c allows the formation of the so-called Apoptosome, consisting of Apaf-1 (apoptotic protease activation factor 1)[20], Cytochrome-c[21] and procaspase-9[22]. Activation of caspase-9 in the Apoptosome enables the activation of downstream executioner-caspases-3 and -7. These caspases further activate endonucleases such as the caspase-activated DNase (CAD) in line with the cleavage of cytokeratins, as well as nuclear- and plasma membrane cytoskeletal proteins, finally leading to the previously described DNA fragmentation and breakdown of the nuclear structure[23,24].

One can easily envision that the described mechanisms have to be controlled very tightly in order to inhibit spontaneous apoptosis through Apoptosome formation or activation of executioner caspases-3 and -7. Therefore, the apoptotic inhibitor XIAP (X-linked inhibitor of apoptosis protein)[25] is normally binding and thereby inhibiting the caspases-3, -7 and -9[26]. Once the intrinsic apoptotic pathway is activated, the release of the above-mentioned protein Smac/Diablo from the IMS is sequestering the protective function of XIAP by direct inactivation[27,28] (Figure 1).

V.1.1.2. The extrinsic apoptotic pathway

The activation of cell death by the extrinsic apoptotic pathway relies on the stimulation of death receptors, like CD95 (cluster of differentiation 95), which are located on the cell surface. After binding of specific death ligands (DL), these receptors initiate the formation of cytosolic, death inducing signaling complexes (DISC). The stimulation of the receptor results in the intracellular binding of the adaptor molecule FADD (Fas-associated protein with death domain)[29] via its death domain (DD) to the intracellular DD of the trimerized receptor[30]. FADD in turn recruits procaspase-8 via mutual interaction of the DEDs harbored by both proteins[31]. The local increase of procaspase-8 level induces the autocatalytic cleavage of the large and small catalytic subunit following the formation of the active caspase-8 homodimer. Active caspase-8 can now propagate the apoptotic signal by the cleavage of effector-caspases, e.g. caspase-3 and -7[32], which in turn can cleave their target substrates for apoptotic execution (Figure 1).

V.1.1.3. Crosstalk between the intrinsic and the extrinsic apoptotic pathway

Cell execution, carried out by the above-mentioned pathways, is not strictly following only one signaling cascade. There is rather a dynamic crosstalk that is mainly depending on the pro-apoptotic Bcl-2 family member BH3 interacting-domain death agonist (Bid)[33,34]. Bid is a direct substrate of caspase-8[35]. Cleavage of Bid through caspase-8, results in the truncated form of Bid (tBid). tBid is subsequently activating Bak and Bax, resulting in the above-mentioned release of apoptogenic factors, like Cytochrome-c[36] and Smac/Diablo from the IMS, thereby increasing the apoptotic signal. Furthermore activated caspase-6, a protein classically found in the intrinsic pathway, can cleave procaspase-8[37], providing a cellular feedback loop, again resulting in the reinforcement of apoptotic cell death (Figure 1).

V.1.2. Necroptosis – a caspase-independent form of programmed cell death

The last years have shown that besides the dominant apoptotic cell death, another PCD pathway is present. It was termed necroptosis to stress the morphological similarity to the classical phenotype of unregulated necrotic cell death[38]. When apoptosis is blocked by the inhibition of caspase activity, necroptosis can act as a backup mechanism[39], ensuring cellular execution due to pathogen infections or cellular pathophysiology. Therefore, the induction of necroptotic cell death can be triggered by the same stimuli as apoptosis, namely DR activation or genotoxic stress[40].

As mentioned above, the morphology is similar to the one found during unregulated necrotic cell death. As a first step cell rounding is observed, followed by cytoplasmic swelling. This

finally results in the disintegration of intracellular compartments as well as the rupture of the plasma membrane, resulting in the spilling of intracellular content[41].

On the molecular level, the propagation of necroptosis is, in contrast to apoptosis, completely caspase-independent. Instead, the necroptotic signaling pathway relies on the stabilization and activation of the kinases RIP1 (Receptor Interacting Protein 1) and RIP3 (Receptor Interacting Protein 3)[42]. Under physiological conditions, both kinases are regulated by active caspase-8 homodimers. RIP1 and RIP3 can be directly cleaved and thereby inactivated by caspase-8[43,44]. Moreover, cellular inhibitors of apoptosis proteins (cIAP) are important regulators of RIP1. cIAPs (especially cIAP1/2) are classically defined as anti-apoptotic proteins, as they harbor, in line with XIAP, the ability to bind and thereby inactivate the executioner-caspases-3, -7 and -9[45]. Additionally, the mentioned cIAP1/2 proteins are responsible for constitutive RIP1 ubiquitination, which in turn leads to proteasomal RIP1 degradation[46]. Summarized, both regulatory mechanisms ensure the prevention of necroptotic cell death by the tight regulation of the intracellular RIP1 and RIP3 level. Cellular conditions, especially genotoxic stress or ROS production, might lead to the depletion of the cellular pool of cIAPs, which in combination with the inhibition of caspase activity, results in increased RIP1 and RIP3 level and the propagation of necroptotic cell death[40,42]. Stabilization of RIP1 promotes the binding of RIP3[47]. This leads to the formation of the so-called Necrosome. Within this complex, RIP3 can be phosphorylated and thereby activated by RIP1[48]. The activated form of RIP3 is now able to further phosphorylate the pseudokinase MLKL (Mixed Lingase Kinase Ligase)[49]. The activation of MLKL results in the homodimerization of the pseudokinase, engaging the formation of porous structures[50,51]. These structures are finally guided to intracellular membranes as well as the plasma membrane[52,53], leading to their disruption and thereby cell execution[50] (Figure 1).

The concept of necroptosis was always extensively discussed as many people argued that the depletion of cIAPs in combination with caspase inhibition displays a rather unphysiological condition. However, recent studies showed that mice, lacking RIP1, one of the main components of this PCD, are born normal but die at the age of 1-3 days, due to high TNF driven apoptosis[54]. Moreover, knockout studies in mice have revealed that the regulation of necroptotic cell death plays a direct role in the inflammatory responses due to viral infections[48,55].These findings show that besides the backup function, there is a physiological relevance for necroptotic cell death, especially during inflammatory events[56].

V.1.3. Autophagy – a cellular recycling program with the ability to kill

The term autophagy normally refers to the process of autodigestion of cellular components. It is the only mechanism that enables the recycling of cellular organelles, such as the mitochondria, in order to eliminate deficient structures and, more important, to provide nutrients to prolong a cells life cycle[57]. Thereby, the ubiquitination of damaged structures or protein aggregates is the major trigger for autophagy induction. Optineurin (OPTN), for example, is recruited to ubiquitinated sites on damaged mitochondria, thereby targeting the autophagic machinery to the deficient organelle[58]. In respect to misfolded proteins, the autophagic receptor sequestosome-1 (SQSTM1 or p62) co-localizes with ubiquitinated protein aggregates in a similar way, thereby again labels them for autophagic degradation[59]. Altogether, certain cellular conditions like high temperature[60], starvation or even bacterial infections[61] can provoke autophagy initiation by the formation of double membrane cytosolic vesicles, called autophagosomes[62]. They are able to engulf cellular components or pathogens, which are then targeted to the lysosomes for digestion. This autophagic process guarantees the availability of important nutritious components, which are necessary for cell viability, and induces the clearance of damaged or misfolded structures. Meaning that autophagy classically functions as a pro-survival program, ensuring cell maintenance under stress conditions[63]. On the other site, there are some recent studies highlighting the presence of an autophagy related PCD program. This autophagic cell death is still controversially discussed, because it is not conclusively clarified whether autophagic activity in dying cells is the cause of death or a prevention mechanism, trying to rescue the cells[64]. However, cells lacking the pro-apoptotic proteins Bak and Bax, meaning that these cells are sequestered in their apoptotic response, show the formation of autophagosomes when treated with apoptosis inducing stimuli[65]. The same effect was achieved by the overexpression of the apoptosis inhibitors Bcl-2 or Bcl-x_L in WT (wild type) cells[65,66]. Of note, autophagic death was not observed in WT cells when caspases were inhibited, arguing that autophagic death is not a direct consequence of apoptosis inhibition but rather regulated by proteins of the Bcl-2 family. This form of cell death is directly depending on the formation of the autophagic vesicles. Pharmacological autophagy inhibitors such as 3-methyladenin or gene silencing of critical components of the autophagy machinery such as Atg5 (autophagy related 5) and Atg6 (autophagy related 6)[65], result in the repression of this form of PCD. Even if the evidence for autophagic cell death is still under controversial discussion, there are a lot of crossroads between cell death pathways and autophagy[67,68].

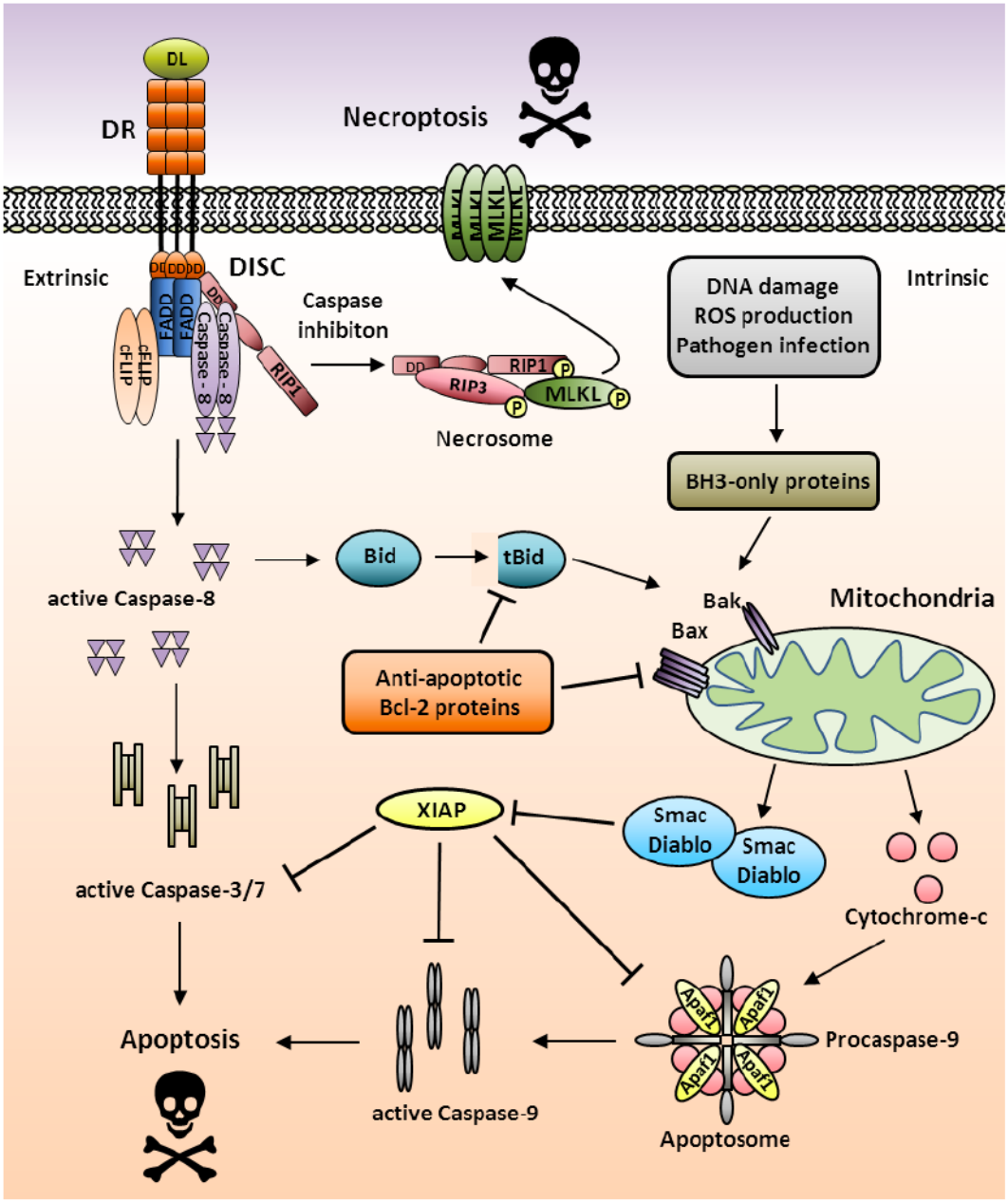

Figure 1 Propagation of extrinsic and intrinsic apoptotic and necroptotic signaling pathways.

The activation of the extrinsic apoptotic signaling pathway relies on binding of death ligands to their specific receptor. This induces the formation of intracellular death inducing signaling complexes (DISC). Activation of initiator-caspase-8 in this complex is leading to downstream activation of effector caspases-3 and -7 and finally apoptosis. Following DNA damage, ROS production or pathogen infection the intrinsic apoptotic pathway can be initiated by the activation of BH3-only proteins. They in turn activate Bak and Bax, leading to the permeabilization of the mitochondrial outer membrane. This results in the release of pro-apoptotic factors like Cytochrome-c or Smac/Diablo. These factors on the one hand inhibit the anti-apoptotic XIAP (Smac/Diablo) and on the other hand promote the formation of the Apoptosome (Cytochrome-c). Within the Apoptosome caspase-9 is activated, subsequently leading to the activation of caspase-3 and -7 and finally to apoptotic execution. The extrinsic and intrinsic pathways are connected via the protein Bid, which is a direct substrate of caspase-8. After cleavage, tBid can also activate Bak and Bax, accelerating the apoptotic signal. This process is tightly controlled by the anti-apoptotic Bcl2-proteins and XIAP, which either bind to the pro-apoptotic factors tBid and Bak/Bax or inhibit the function of the caspases-3, -7 and -9. When caspase activity is inhibited, RIP1 is stabilized, and binds to RIP3, forming the so-called Necrosome. Within the Necrosome, RIP3 is phosphorylated, enabling the further phosphorylation and thereby activation of MLKL. Active MLKL is forming porous structures, which are leading to plasma membrane disruption and finally necroptotic execution.

V.2. Formation of multiprotein complexes is the starting point of programmed cell death signaling

V.2.1. TNF complex I/II

About 30 years ago, it was found that a specific cytokine named TNF (tumor necrosis factor), which was released from immune cells after stimulation, showed significant cytotoxicity on a variety of tumor cell lines [69,70]. To date, it is known that there are two specific receptors on the cell surface, named TNF receptor 1 and 2 (TNFR1/2), which are responsible for the TNF binding and the intracellular signal transduction[71,72]. TNFR1 is constitutively expressed in most tissues, whereas TNFR2 is highly regulated and mostly found in cells of the immune system. Therefore, TNFR1 signaling will be discussed in detail in the following section.

TNFR1 activation executes a large spectrum of bioactivities. However, the most striking ones are the induction of inflammatory responses and, depending on the cellular conditions, the induction of apoptosis or necroptosis[73–75]. The binding of TNF to TNFR1, leads to the trimerization of the receptor, which in turn creates an intracellular cluster of death domains (DD). This cluster is used as a docking station for the formation of a receptor bound multiprotein complex. This so-called complex I consists of the adaptor molecule TRADD (TNFR 1-associated death domain protein), RIP1, TRAF2 (TNF associated factor 2), cIAP1 and cIAP2. TRADD is recruited via its DD to the intracellular part of the receptor[76]. This enables the binding of RIP1 to the DD of TRADD. Additionally TRAF2, an E3 ubiquitin ligase that interacts with cIAPs, is recruited to the receptor via TRADD[76]. TRAF2 and the cIAPs are now responsible for the addition of K63-linked polyubiquitin chains to RIP1 and other components of the complex. This in turn enables the recruitment of LUBAC (linear ubiquitin chain assembly complex), which is adding M1-linear polyubiquitin chains to RIP1[77,78]. These linear ubiquitin chains are essential for the recruitment of the IKK-complex and thereby NF-κB (nuclear factor of kappa-light-chain-enhancer of activated B-cells) activation[79] (Figure 2).

However, it was shown that the depletion of cIAPs in combination with TNF stimulation can induce programmed cell death. The lack of cIAPs massively decreases the NF-κB response, due to the inability to recruit LUBAC[77]. Instead, the signaling complex can be released from the receptor, leading to the recruitment of caspase-8, cFLIP (cellular FLICE (FADD-like IL-1β-converting enzyme)-like inhibitory protein)) and FADD[80]. This cytosolic complex is referred to as complex IIa[46]. Within the complex, procaspase-8 can be cleaved into its active form, resulting in the propagation of apoptotic cell death[80]. Depending on the cFLIP status (described in a separate chapter) or when caspase activity is now additionally inhibited, RIP1 is stabilized [81]. This triggers the binding of RIP3 to form the Necrosome, which is also

referred to as complex IIb (Figure 2). Within this complex, RIP1 and RIP3 are subsequently activated, promoting the phosphorylation of MLKL. Active MLKL can now homodimerize and build up porous structures, which finally lead to necroptotic execution[50] (Figure 2).

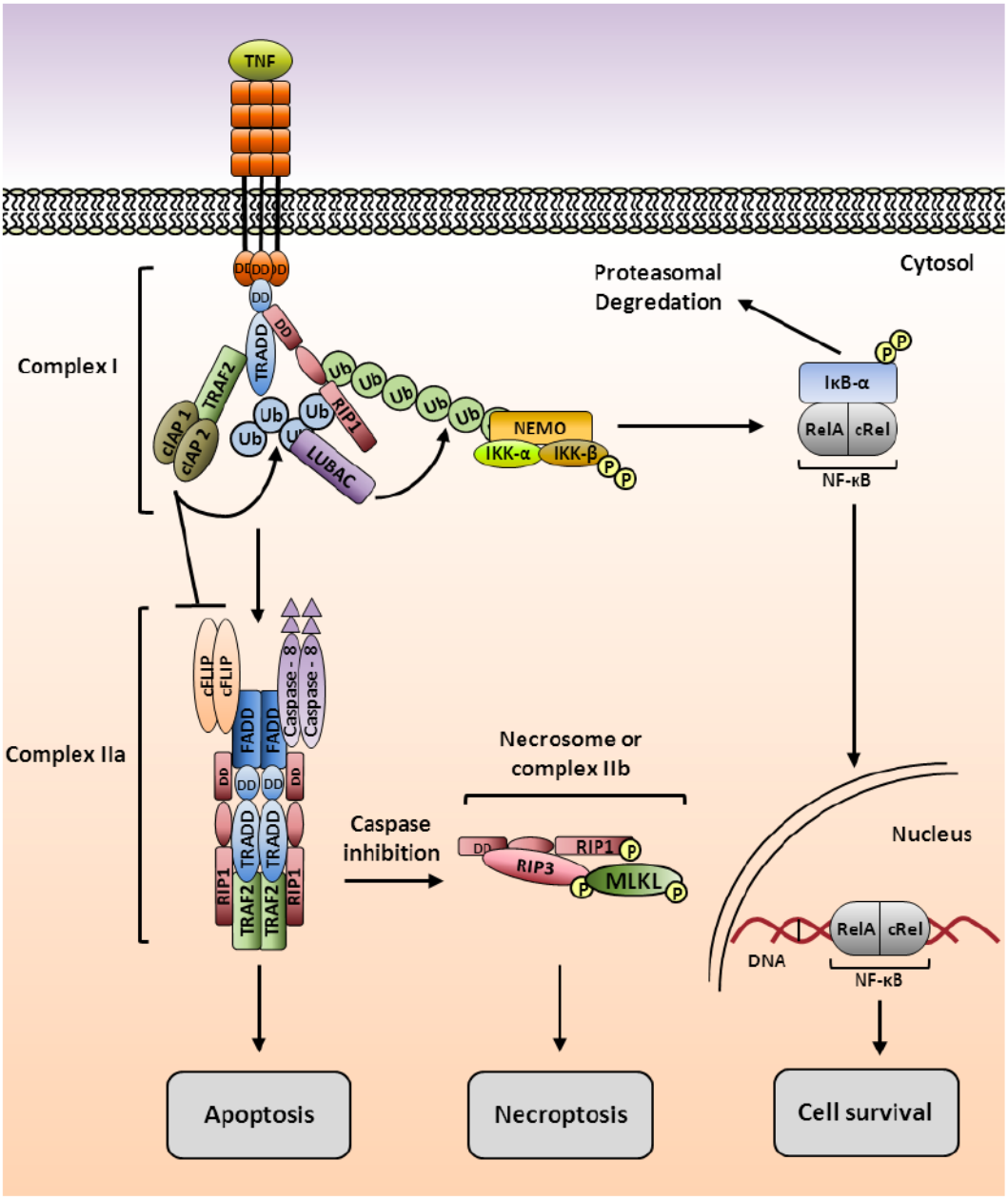

Figure 2 TNF receptor 1 signaling.
TNFR1 stimulation results in the intracellular recruitment of TRADD, followed by the binding of RIP1, TRAF2 and cIAPs to form the TNF complex I. With the help of LUBAC, linear ubiquitin (Ub) chains are attached to RIP1, to enable the recruitment of the IKK complex, resulting in the activation of NF-κB. Under conditions where cIAPs are lacking, complex I is dissociating from the receptor, to recruit FADD, cFLIP and caspase-8. This cytosolic complex is now referred to as complex IIa. The activation of caspase-8 in this complex finally results in the propagation of apoptotic cell death. Under conditions of inhibited caspase activity, RIP1 and RIP3 are forming the Necrosome, also referred to as complex IIb. Within the Necrosome RIP3 is phosphorylated, allowing the further phosphorylation of the pseudokinase MLKL, finally resulting in necroptosis.

V.2.2. DISC formation after CD95 receptor stimulation

In line with the above-described TNF, other death inducing receptors were identified. One of the most prominent ones is CD95, a receptor that belongs to the TNF receptor superfamily. CD95 is the prototypic death receptor, as its main and best-studied function is the induction of apoptosis. Binding of the CD95 ligand (CD95L) to the pre-organized receptor trimers on the cell surface is leading to the intracellular recruitment of the adapter molecule FADD via its C-terminal DD domains[29]. Now caspase-8 can be recruited to FADD via mutual interaction of their DED domains[82]. Additionally, RIP1[83] and cFLIP[84] are recruited to form the intracellular death inducing signaling complex (DISC)[85]. Within the DISC, procaspase-8 is subsequently activated, leading to the cleavage of downstream effector-caspases and finally to apoptotic execution[86]. In line with the TNF complex II, the CD95 DISC can also induce necroptotic cell death[87]. Depending on the cFLIP level in the complex and under repression of caspase activity, RIP1 and RIP3 can form the Necrosome to activate MLKL, promoting plasma membrane disruption and necroptosis (Figure 3). Besides the death-inducing function, the activation of the CD95 DISC can also result in the activation of the transcription factor NF-κB[88]. It was shown that IκB-α is degraded after CD95L stimulation, leading to the induction of NF-κB target genes and inflammatory cytokine production[89–91]. However, it is still unclear, how the signal is propagated from the DISC to IκB-α and whether this is carried out by the IKK complex or not (Figure 3).

V.2.3. cFLIP – a negative regulator of DISC and TNF complex II PCD signaling

The activation of caspase-8 during DISC or TNF complex signaling is negatively regulated via cFLIP. Many different isoforms have been reported, however, $cFLIP_s$ and $cFLIP_L$ are the most frequent and best studied ones. $cFLIP_L$ (cFLIP long) contains a caspase-8-like domain lacking the enzymatic activity[92]. This domain is completely absent in $cFLIP_s$ (cFLIP short). Both isoforms contain two DED domains for protein interactions. Upon complex formation, they can be recruited into multiprotein-complexes similar to caspase-8 via their DEDs to FADD[92–94]. Moreover, cFLIP can form heterodimers with procaspase-8, thereby inhibiting or modulating caspase-8 activation. The overexpression of $cFLIP_L$, for instance, was shown to completely block cell death. The formation of caspase-8/$cFLIP_L$ heterodimers is sufficient to cleave RIP1, thereby preventing necroptotic execution. However, the activity is not sufficient to activate caspase-8. Therefore, apoptosis is inhibited, leading to a complete abrogation of cell death. In terms of dominant emplacement of $cFLIP_S$ into the complex, necroptotic cell death is promoted in absence of cIAPs[87]. Caspase-8/$cFLIP_S$ heterodimers also block caspase-8 activation. In contrast to $cFLIP_L$, these dimers are not able to cleave RIP1. Thereby, RIP1 is stabilized, resulting in the activation of RIP3 and finally necroptosis[95].

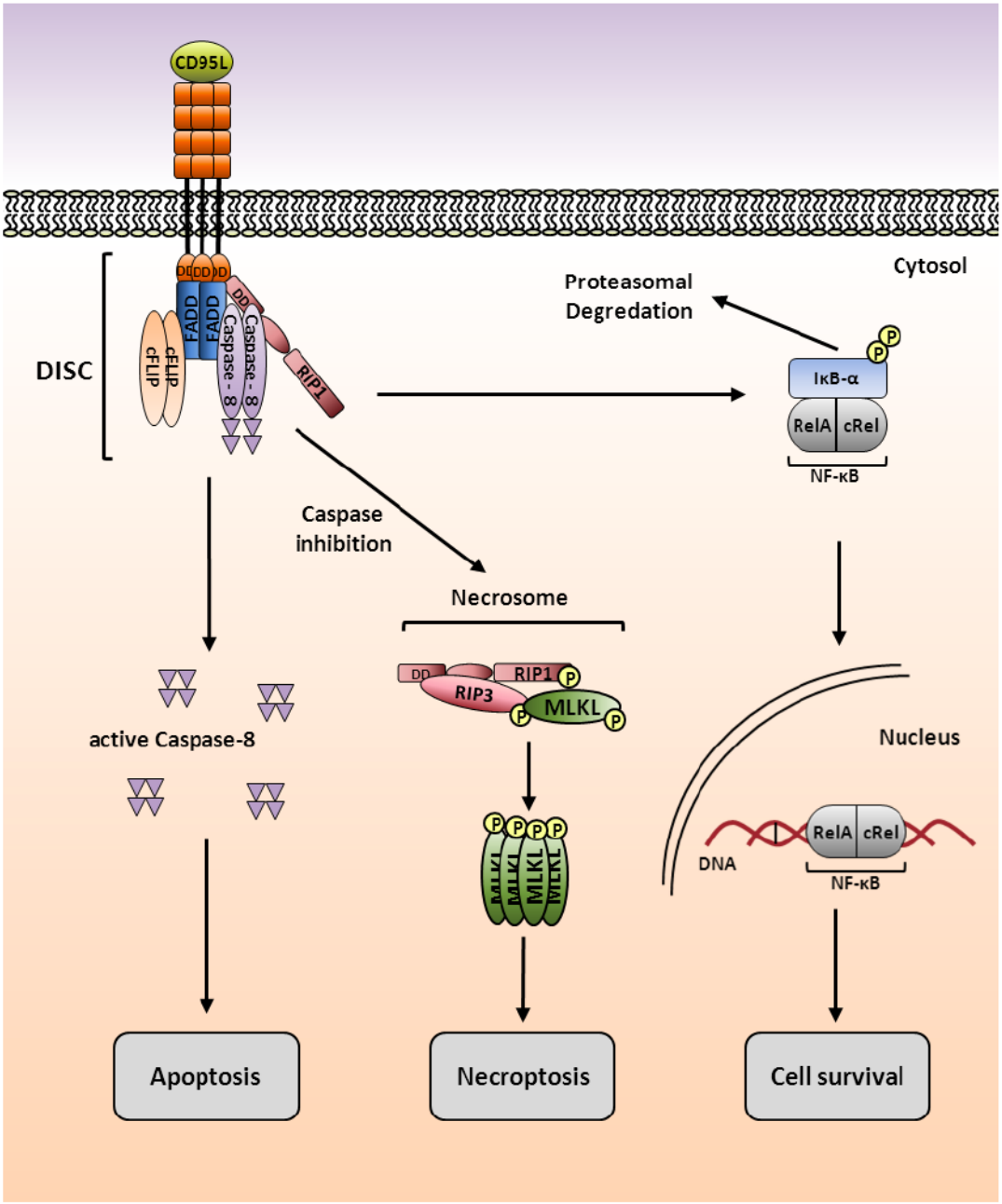

Figure 3 DISC formation and downstream signaling upon CD95 stimulation.
After binding of CD95L to the receptor, FADD is recruited intracellular via its DD. This leads to further recruitment of RIP1, cFLIP and caspase-8, to form the CD95 death-inducing signaling complex (DISC). The formation of this complex can, based on the cellular environment, either lead to gene induction via NF-κB or to cellular execution via apoptosis or necroptosis.

V.2.4. The Necrosome – Amyloid structures leading to programmed necrosis

As mentioned above, caspase-8 is constantly cleaving RIP1 in death inducing complexes to prevent necroptotic cell death[43,44]. Under conditions where caspase function is inhibited, RIP1 and RIP3 are getting stabilized and are able to bind each other to form the Necrosome[96]. Both proteins are binding each other via their RHIM domains (RIP homotypic interaction motives), resulting in the formation of amyloid structures[97,98]. These are

filamentous protein aggregates, formed by cross-β structures[97]. As mentioned above, RIP1 and RIP3, within this complex auto- and transphosphorylate each other, leading to the activation of MLKL and finally to necroptotic execution[50].

V.2.5. The Ripoptosome

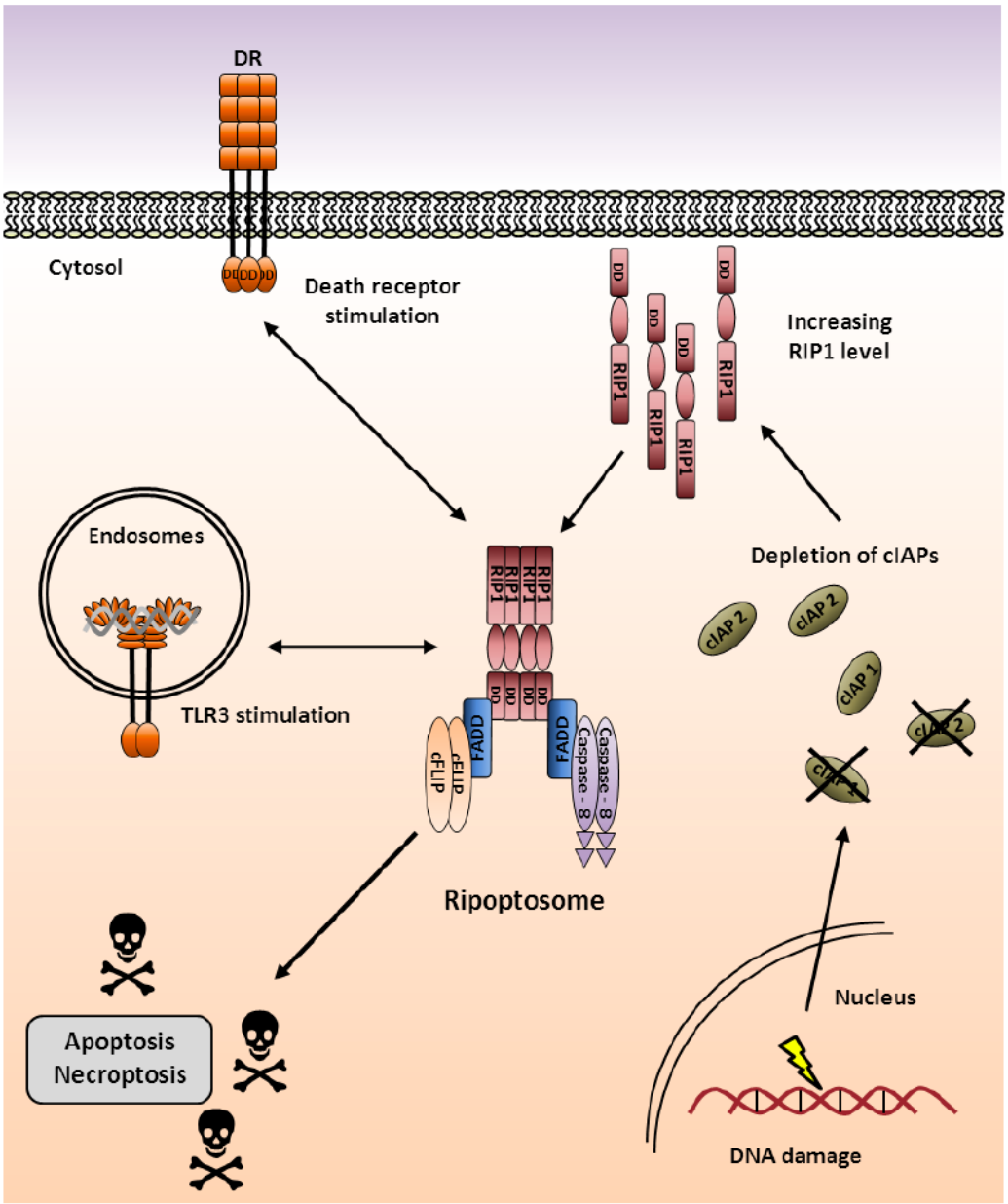

Figure 4 Genotoxic stress and depletion of cellular IAP level lead to Ripoptosome assembly.
The 2 MDa Ripoptosome consists of the proteins RIP1, FADD, caspase-8 and cFLIP. It can be induced through DNA damage or other stress signals, leading to the depletion of cIAP level, finally enhancing the active available pool of RIP1. Additional stimulation of the TLR3 receptor or activation of death receptors can allow Ripoptosome recruitment to the respective receptors when cellular IAP levels are depleted. The assembled Ripoptosome can execute apoptotic and necroptotic cell death based on the cellular conditions and complex composition.

Many important functions are executed by the above-mentioned signaling platforms, such as the death-inducing signaling complex (DISC), TNF complex I/II or the Necrosome during necroptotic execution. In the last decade many studies have provided evidence that another intracellular complex is formed after stress signaling or cell death induction. It was named Ripoptosome, because RIP1 is the central component and by inhibiting the RIP1 kinase activity the assembly of the complex can be decreased or even fully blocked[99]. The total size of the Ripoptosome is 2 MDa and it consists, besides the name giving RIP1, of the proteins FADD, caspase-8, cFLIP, cIAP1 and cIAP2. Ripoptosome formation can be induced and accelerated through a variety of extrinsic and intrinsic stimuli like DNA damage, depletion of cellular IAPs, overexpression of RIP1, TLR3 stimulation or death ligand binding to their specific receptors[99,100] (Figure 4). It was shown that the mode of cell death, that is induced by the Ripoptosome, is mainly driven by the complex composition, especially the stoichiometry of the cFLIP isoforms[92,95]. As described above, caspase-8/cFLIP$_L$ heterodimer formation promotes a total inhibition of cell death, caspase-8/cFLIP$_S$ heterodimers favour necroptosis and caspase-8 homodimerization leads to the execution of apoptosis[95].

V.2.6. TLR3 signaling

As a first line of defense against pathogens, the immune system of multicellular organisms has evolved two branches in order to recognize pathogenic microorganisms, namely the innate and the adaptive immune system. The innate immune system is phylogenetically conserved and found in almost all multicellular organisms. However, innate immunity was long time thought to be quite non-specific, with the main roles in destroying pathogens and presenting pathogenic peptides on the cell surface for recognition by the adaptive immune system. However, with the identification of the Toll pathway in *Drosophila*, the view on innate immunity changed. Until now, eleven homologues of the Drosophila Toll have been identified in mammals. They build up the so-called Toll-like receptor (TLR) superfamily[101]. All members of the superfamily harbor a conserved cytosolic TIR (toll/interleukin-1 receptor) domain, which is responsible for the binding of respective adaptor proteins like TRIF (TIR-domain-containing adapter-inducing interferon-β) or Myd88 (Myeloid differentiation primary response gene 88), which are necessary for further signal transduction[102,103], finally resulting in target gene expression. In the following section, the signal transduction of the TLR3 receptor is described exemplarily, as the stimulation of this specific receptor holds also the possibility for cell death induction and Ripoptosome recruitment.

After the binding of double-stranded viral RNA to the endosomal TLR3[104], TRIF is recruited to the cytosolic part of the receptor via its TIR domain. From this starting point, a variety of cellular signals can be switched on. TRIF can now activate the IKK-related kinases TBK1

(TANK-binding kinase 1) and IKK-ε[105]. They, in turn, phosphorylate TRIF itself, thereby enabling the recruitment of the transcription factor IRF3[106]. The close proximity allows TBK1 to phosphorylate IRF3, which can now, in its active state, enter the nucleus to induce the production of type I interferons[105].

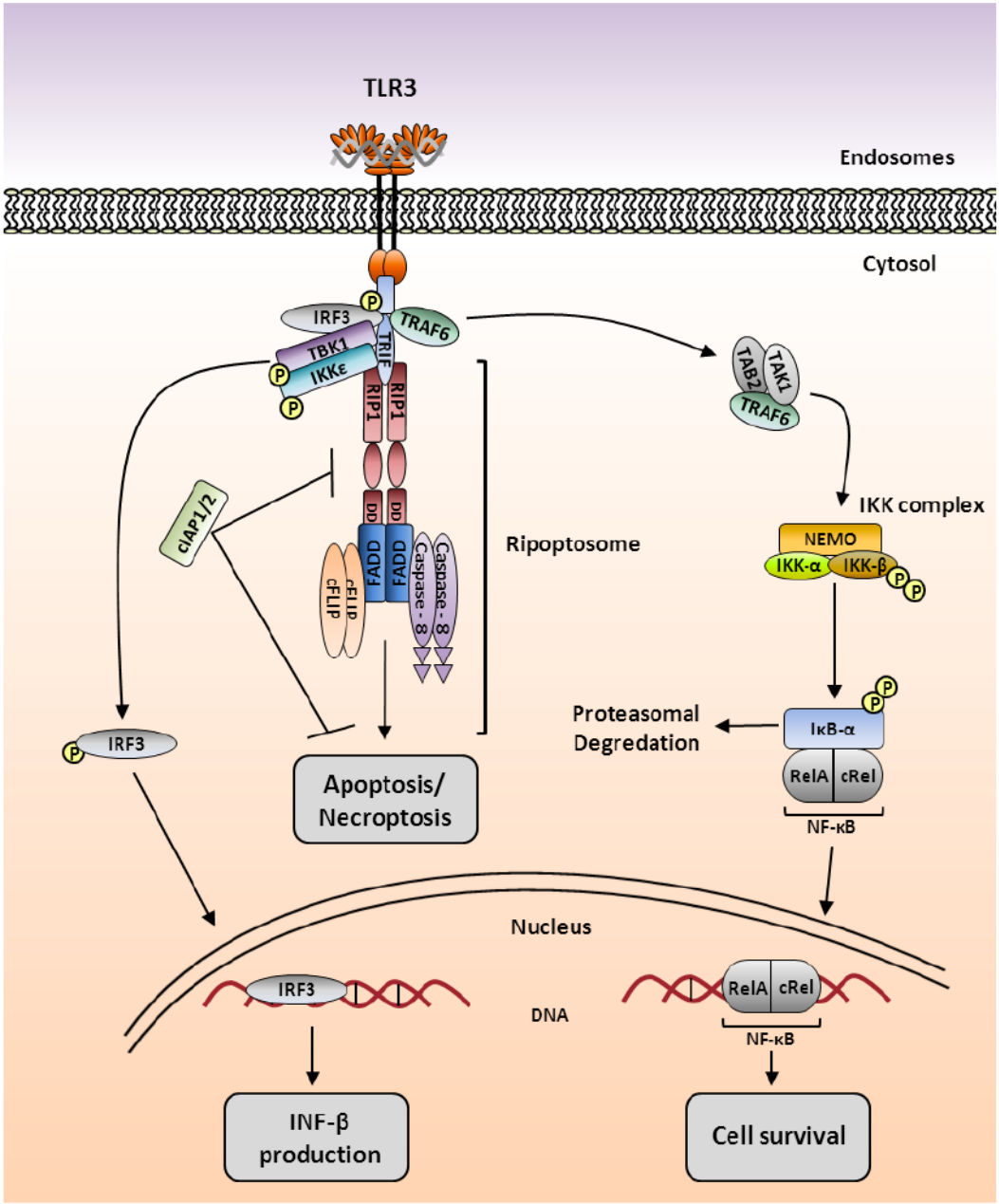

Figure 5 TLR3 receptor signaling.
Stimulation of the endosomal TLR3 receptor via double stranded DNA is inducing a variety of signaling pathways. After stimulation, TRIF is binding to the cytosolic part of the receptor. This enables the recruitment of TBK1/IKK-ε and the transcription factor IRF3 that results in the production of INF-β. In addition, TRAF6 is recruited, leading to the activation of NF-κB over a TAB2-TAK1-TRAF6 containing complex. Finally, under conditions where cIAPs are depleted, RIP1 together with caspase-8, FADD and cFLIP forms the Ripoptosome which is recruited to and interconnected with the TLR3 receptor by binding of RIP1 to TRIF via its RHIM domain. This enables the Ripoptosome for apoptotic and necroptotic cell death execution.

In parallel, the stimulation of the TLR3 receptor can induce the activation of NF-κB. Therefore, TRAF6 can be recruited and activated via TRIF. This leads to the further recruitment of TAB2 and TAK1. The TRAF6-TAB2-TAK1 complex dissociates to the cytosol, where TAK1 can be activated. This enables TAK1 to further activate the IKK complex for subsequent NF-κB activation[107] (Figure 5).

In the last years, it was also shown that TLR3 stimulation enables the induction of cell death, when cIAPs are depleted[100]. The loss of cIAPs stabilizes RIP1, which allows now for the recruitment of the main components of the Ripoptosome (FADD, caspase-8 and cFLIP)[100]. RIP1 can then bind TRIF via its RHIM domain, thereby recruiting the Ripoptosome to the TLR3 receptor. As mentioned above, the Ripoptosome can then execute apoptotic or necroptotic cell death, based on the cellular conditions (Figure 5).

V.3. The balance between life and death – cell death signaling complexes induce the production of inflammatory factors and cytokines via the transcription factor NF-κB

The transcription factor NF-κB was originally identified by playing a central role in B-cell specific gene expression[108]. Further studies showed that proteins of the NF-κB family are expressed in almost all tissues and cells[109]. They are responsible for the expression of specific genes, particularly involved in inflammation, innate immune responses or apoptosis[110]. To date, there are five known members of the NF-κB family: RelA (also known as p65), c-Rel, RelB, NF-κB1 (p105/ p50), and NF-κB2 (p100/ p52)[111,112]. RelA, c-Rel and RelB are transcriptionally active, whereas NF-κB1 and NF-κB2 are transcribed as inactive precursors of 105 and 100 kDA[113]. These precursors undergo proteolytic cleavage to form the active NF-κB p50/p52 proteins[114], which in turn form homo- or heterodimers with Rel proteins. In the inactive state, NF-κB homo- or heterodimers, stay associated with proteins of the IκB (nuclear factor of kappa light polypeptide gene enhancer in B-cells inhibitor) family, which are able to bind to the nuclear localization sequence (NLS) of NF-κB, thereby inhibiting their nuclear translocation[115]. The most important IκB family members are IκB-β, IκB-ε and the prototypical IκB-α[112]. As mentioned above, stimulation of death receptors, as exemplified for TNF or CD95L, or the activation of the TLR3 receptor can result in the expression of inflammatory genes after NF-κB activation[73,90,107,116,117]. Therefore, cell death pathways and NF-κB activation are closely connected. The activation of NF-κB is divided into two signaling pathways, namely the canonical (classical) and the non-canonical NF-κB pathway[118].

V.3.1. The canonical NF-κB pathway

The induction of the canonical NF-κB pathway responds to a variety of stimuli like antigen binding, cytokine recognition or pattern recognition. All signals converge in the activation of the so called IKK complex. This complex consists of the catalytic IκB kinases IKK-α and IKK-β[119], as well as of the regulatory subunit IKK-γ (also called NEMO)[120]. The activated IKK complex phosphorylates the inhibitory IκB-α, thereby triggering its ubiquitination and proteasomal degradation[121]. This, in turn, enables the NF-κB proteins to enter the nucleus and to activate their specific target genes (Figure 2, 3 and 5). In terms of the canonical signaling pathway activation of RelA/p50 and c-Rel/p50 NF-κB complexes is predominantly responsible for the gene inductive properties[122].

V.3.2. The non-canonical NF-κB pathway

In contrast to the canonical NF-κB activation, the non-canonical signaling pathway relies on the stabilization of NIK (NF-κB inducing kinase). Under unstimulated conditions, cIAP proteins are constantly marking NIK for proteasomal degradation via ubiquitination[123]. After the depletion of the cellular cIAP pool, NIK is stabilized and forming a complex with IKK-α[124], p100 and RelB[125]. Within this complex, p100 is phosphorylated enabling the proteolytic cleavage into the active p52 fragment[126,127]. The active p52/RelB heterodimer can than enter the nucleus to induce specific target genes.

V.3.3. The non-canonical IKKs

Whenever it comes to viral or bacterial infections, the innate immune system is the first line of cellular defense mechanisms. The mentioned pathogens are detected as ``non-self`` by a variety of cytosolic or membrane bound receptors, like RIG-I (retinoid acid-inducible gene)[128] or the Toll-like receptor (TLR) family[104]. The outcome of the receptor stimulation is the above-mentioned induction of NF-κB and the activation of interferon (IFN) regulatory factors (IRFs)[129,130]. These IRFs together with NF-κB control the expression of immune regulatory genes, like interferons and cytokines[130]. In addition to the above-mentioned IκB kinases, the two IKK-related kinases TBK1 (TANK-binding kinase 1)[131] and IKK-ε (Inhibitor of nuclear factor kappa-B kinase subunit epsilon)[132] were identified as important regulators, not only of the described NF-κB pathway, but also for the activation of IRFs[133]. TBK1 and IKK-ε were termed the non-canonical IKKs, as they share large sequence similarity to the classical IKKs and are able to phosphorylate IκB-α[134].

Importantly, in contrast to the classical IKKs, TBK and IKK-ε lack a NEMO binding domain (NBD). Instead, they form similar signaling complexes with other scaffold proteins, involved

in a variety of intracellular signaling pathways[135]. In terms of pathogen recognition, both proteins contribute to the activation of the transcription factors IRF3 and IRF7[136], which in turn, induce the production of type I interferons. Moreover, the lack of TBK1 leads to embryonic lethality, due to TNF induced liver degeneration[137]. This shows that TBK1 is indispensable for NF-κB regulation and interferon production during development. In contrast, IKK-ε knockout mice are viable[138]. However, to date it is not clearly understood what the distinct roles of TBK1 and IKK-ε are in IRF activation. Recent studies showed that the lack of TBK1 is reducing the IRF3 phosphorylation upon stimulation. In contrast, depletion of IKK-ε does not alter the IRF3 activation. But the lack of both proteins abolishes the IRF3 phosphorylation and interferon production completely[139]. Meaning that in this situation, IKK-ε can somehow compensate for the loss of TBK1, although the exact mechanism is still unclear. Both proteins are composed of a kinase domain (KD) that houses its catalytic activity and three accessory regulatory elements: a ubiquitin-like domain (ULD), a Lysine-zipper (LZ) and a helix-loop-helix domain for protein interactions[138] (Figure 6). TBK1 is expressed in nearly all cell types, whereas IKK-ε is only found in certain tissues. The IKK-ε expression can be induced after pathogen infection. Thus, IKK-ε is also called the inducible IκB kinase[140].

Additionally, further studies displayed an important involvement of TBK1 in autophagic execution. Here, TBK1 is responsible for the phosphorylation of the autophagy adaptor sequestosome-1 (also p62 or SQSTM1) and optineurin (OPTN), which is important for autophagic clearance[141]. Moreover, recent studies showed that TBK1 is especially involved in the process of mitophagy[142], where damaged detrimental mitochondria are marked for degradation. The proteins PINK (PTEN-induced putative kinase 1) and Parkin are responsible for the addition of ubiquitin chains to the damaged mitochondria. These chains provoke the association of autophagy receptors like sequestosome-1 and TBK1 to associate with the mitochondria, enabling the activation of these adaptors and mitophagic clearance[143].

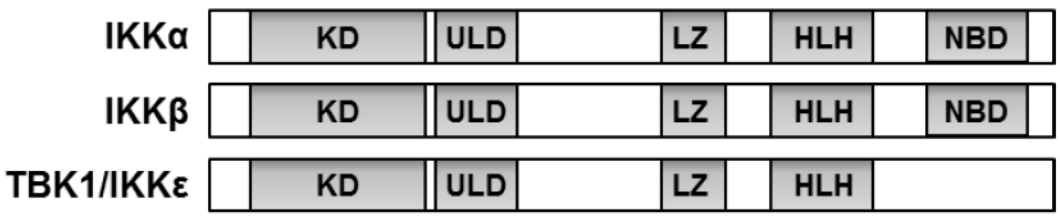

Figure 6 The non-canonical IKKs.
Structural scheme of the protein domains of the classical and non-canonical IKKs. IKK-α and IKK-β as well as TBK1 and IKK-ε consist of a kinase domain (KD), a ubiquitin-like domain (ULD), a Lysine-zipper (LZ) and a helix-loop-helix domain (HLH). TBK1 and IKK-ε lack the NEMO binding domain (NBD), harbored by the classical IKKs.

VI. Aims of the Thesis

During the last decade, the identification of the Ripoptosome and its main components enabled a novel possible target for the treatment of various diseases, including cancer. Several studies showed that genotoxic stress and the depletion of cIAPs triggered the formation of the 2 MDa Ripoptosome, containing the proteins RIP1, FADD, caspase-8 and cFLIP[99,144]. The formation of this complex can either lead to apoptotic or necroptotic cell execution based on the stoichiometric composition. During the last years, chemical compounds, so called Smac mimetics were developed in order to deplete cellular IAP levels. Indeed, several cancer identities have been shown to undergo cellular execution due to Ripoptosome formation when treated with Smac mimetics. This was for example true for glioma[145], lung cancer[146] or acute lymphoblastic leukemia (ALL) and promoted these drugs for clinical trials. In contrast, other cancer identities, like chronic lymphocytic leukemia (CLL), were quite resistant to the Smac mimetic treatment due to their inability to form a Ripoptosome[147]. These studies highlighted the importance for a better understanding of Ripoptosome regulation and formation in cancer treatment, especially to overcome other drug resistances.

However, to date it is still not fully verified, if the core components RIP1, FADD, caspase-8 and cFLIP do interact with other proteins to propagate Ripoptosome-mediated cell death or alternative signaling pathways. To generate deeper insight into the molecular mechanisms of Ripoptosome signaling, the following questions should be addressed in this thesis:

- **Are there other integral components or proteins interacting with the Ripoptosome, besides RIP1, FADD, caspase-8 and cFLIP?**
- **How do potentially novel components of the Ripoptosome influence the cell death machinery or other non-cell death related signaling pathways?**

By the use of mass spectrometric analysis, novel components of the Ripoptosome should be identified. Based on these results, the appearances and the function of these proteins and their posttranslational modifications in the complex will be examined. Thereby, their role in cell death regulation or non-cell death signaling pathways should be dissected. Moreover, with the help of genetic manipulation, such as overexpression, knockdown or knockout of the respective proteins, the role of the Ripoptosome-associated proteins will be identified for TLR3-related and DL-mediated signaling pathways.

VII. Material and Methods

VII.1. Material

Table 1 Reagents and kits

Reagents and kits	Company	Cat. No.
4-(2-Aminoethyl)-benzenesulfonyl Fluoride (AEBSF) Hydrochloride	AppliChem	A1421
Agarose Neo ultra-quality	Roth	2267.2
Ampicillin sodium salt	Roth	K029.1
Aprotinin	Roth	A162.3
BbsI	New England BioLabs	R0539S
BD OptEIA™ Human IL-8 Set	BD Biosciences	555244
BD OptEIA™ Reagent Set B	BD Biosciences	550534
Benzamidine	Sigma-Aldrich	12072-10G
Bis-Tris	Applichem	A1025,0500
Bovine Serum Albumin (BSA)	Santa Cruz	sc 2323A
Bromophenol blue	Sigma-Aldrich	B8026
Calcium chloride dihydrate	Sigma-Aldrich	C3306
Colloidal Blue Staining Kit	Thermo Scientific	LC6025
cOmplete Protease Inhibitor Cocktail Tablets	Sigma-Aldrich	11836145001
Crystal violet	Applichem	A0691.0250
di-Sodium hydrogen phosphate dihydrate	Roth	4984.1
dNTPs	Thermo Scientific	R0193
1,4-Dithiothreitol (DTT)	Applichem	A2948.0025
E.Z.N.A. FastFilter Plasmid Maxi Kit	OMEGA	D6924-04
E.Z.N.A. Gel Extraction Kit	OMEGA	D2500-02
Ethanol denatured	Roth	K928.4
Ethanol ROTIPURAN	Roth	9065.3
GeneJET Plasmid Miniprep Kit	Thermo Scientific	K0503
GeneRuler 1 kb DNA Ladder	Thermo Scientific	SM0312
GeneRuler 100bp DNA Ladder	Thermo Scientific	SM0242
Glycerin ROTIPURAN	Roth	3783.2
iBlot 2 Transfer Stacks	Life technologies	IB24001
KAPA SYBR FAST Universal	Peqlab	07-KK4600-03

LB-Agar (Lennox)	Roth	X965.2
LB-Medium (Lennox)	Roth	X964.2
Leupeptin	Sigma-Aldrich	L2884
Luminata Forte Western HRP substrate	Merck Millipore	WBLUF0500
Methanol AnalaR NORMAPUR	VWR	20847.360
Microlance 3 27 G ¾''	BD	302200
MOPS for buffer solutions	AppliChem	A1076,1000
Nancy-520	Sigma-Aldrich	01494
NuPAGE Novex 4-12% Bis-Tris Protein Gels	Invitrogen	NP0329BOX
Pacific Blue Annexin V	Biolegend	640918
PageRuler Prestained Protein Ladder	Life technologies	26617
Phusion High-Fidelity DNA Polymerase	New England BioLabs	M0530L
Pierce ECL Western Blotting Substrate	Thermo Scientific	32106
Potassium chloride	Roth	6781.3
Potassium dihydrogen phosphate	Roth	3904.1
Protein Assay Reagent A	Bio-Rad	5000113
Protein Assay Reagent B	Bio-Rad	5000114
Protein Assay Reagent S	Bio-Rad	5000115
Protein G Agarose	Roche	05015952001
Restore Western Blot Stripping Buffer	Thermo Scientific	21063
RNaseOUT Recombinant Ribonuclease Inhibitor	Invitrogen	10777-019
RNeasy Mini Kit	Qiagen	74106
SDS Pellets	Roth	CN30.3
Skim Milk Powder	Sigma-Aldrich	70166-500G
Sodium chloride (NaCl)	Roth	3957.2
Sodium citrate dihydrate	Sigma-Aldrich	W302600
Sodium hydroxide (NaOH) solution	Roth	KK71.1
Sodium orthovanadate	Sigma-Aldrich	S6508
SuperScript II Reverse Transcriptase	Invitrogen	18064-071
T4 DNA Ligase	Thermo Scientific	EL0016
Tris ultrapure	AppliChem	A1086,1000
Triton X-100	AppliChem	A1388,0500
Tween 20	Roth	9127.3
UltraPure DNase/RNase-Free Distilled Water	Invitrogen	10977-049
β-Glycerophosphate disodium salt hydrate	Sigma-Aldrich	G9422-10G
β-Mercaptoethanol	Merck Millipore	805740

Table 2 Cell culture reagents

Cell culture reagents	Company	Cat. No.
(Z)-4-Hydroxytamoxifen	Sigma-Aldrich	H7904
AllStars Negative Control siRNA	Qiagen	1027281
Dimethyl sulfoxide (DMSO)	AppliChem	A3672,0100
DMEM, high glucose, GlutaMAX	Thermo Scientific	61965-059
DPBS, calcium, magnesium	Thermo Scientific	14040-174
EDTA (Versen)	Merck Millipore	L 2113
Fetal Bovine Serum (FBS)	Thermo Scientific	10270-106
Hepes solution	Sigma-Aldrich	H0887
Hygromycin B	A&E Scientific	P21-014
Lipofectamine 2000 Transfection Reagent	Invitrogen	11668-019
Necrostatin-1	Sigma-Aldrich	N9037-25MG
Opti-MEM I Reduced Serum Medium	Thermo Scientific	31985-047
Polyinosinic–polycytidylic acid sodium salt (poly (I:C))	Sigma-Aldrich	P1530
Polyprene (Hexadimethrine bromide)	Sigma-Aldrich	H9268-5G
Puromycin Dihydrochloride	Thermo Scientific	A11138-03
RPMI 1640 Medium	Thermo Scientific	21875-091
Sodium Pyruvate	Thermo Scientific	11360-088
Sterile Cellulose Nitrate Membranes	GE Healthcare	10401170
Trypsin 2,5%	Invitrogen	15090-046
Zeocin Selection Reagent	Thermo Scientific	R250-01
z-Val-Ala-DL-Asp-fluoromethylketone (zVAD-fmk)	Bachem	N15100025

Table 3 Cytokines

Stimulatory cytokines	Source
His-Flag-TNF (TNF-HF)	P. Diessenbacher [116]

Table 4 Antibodies

Target	Species/Feature	Application	Company/Source	Cat. No.
Primary Antibodies				
Actin (A2103)	Rabbit	WB	Sigma-Aldrich	A2103
Caspase-8 (C15)	Mouse IgG2b	WB	P.H. Krammer	
Caspase-8 (C20)	Goat	IP	Santa Cruz	sc-6136
cFLIP (NF6)	Mouse IgG1	WB	Enzo Life Science	ALX-804-961-01
FADD (1)	Mouse IgG1	WB	BD Biosciences	F36620
Phospho-IRF3 (S396) (D4G4)	Rabbit	WB	Cell Signaling	4947
IκBα (C21)	Rabbit	WB	Santa Cruz	sc-371
Phospho-IκBα (S32/36) (5A5)	Rabbit	WB	Cell Signaling	9246
IKKε (D20G4)	Rabbit	WB	Cell Signaling	2905
Phospho-IKKε (S172) (D1B7)	Rabbit	WB	Cell Signaling	8766
MLKL (3H1)	Rat	WB	James Murphy	
Phospho-MLKL (S358)	Rabbit	WB	Abcam	ab187091
Phospho-p65 (Ser536) (93H1)	Rabbit	WB	Cell Signaling	3033
NF-κB2 p100/p52	Rabbit	WB	Cell Signaling	4882
RIPK1 (38)	Mouse IgG2a	WB	BD Biosciences	R41220
Phospho-RIPK1 (S166)	Rabbit	WB	P. Gough	
RIPK3	Rabbit	WB	Imgenex	IMG-5846A
TRADD (37)	Mouse IgG1	WB	BD Biosciences	T610573
TRAF2 (EPR6048)	Rabbit	WB	Abcam	ab126758
β-Tubulin (TUB 2.1)	Mouse IgG1	WB	Sigma-Aldrich	T4026
Secondary antibodies				
Mouse IgG1	Goat/HRP	WB	SouthernBiotech	1070-05
Mouse IgG2a	Goat/HRP	WB	SouthernBiotech	1080-05
Mouse IgG2b	Goat/HRP	WB	SouthernBiotech	1090-05
Rabbit	Goat/HRP	WB	SouthernBiotech	4030-05
Rat	Goat/HRP	WB	SouthernBiotech	3030-05
Goat IgG	Rabbit/HRP	WB	SouthernBiotech	6160-05

Table 5 Buffer and solutions

Buffer/Solution	Content
DISC-lysis buffer	30 mM TRIS-HCl (pH 7.5) 120 mM NaCl 10% (v/v) Glycerol, 1% (v/v) Triton X-100 2 tablets cOmplete Protease Inhibitor/100 ml
Phospho-lysis buffer	20 mM Tris-HCL (pH 7,4) 137 mM NaCl 10% (v/v) Glycerol, 1% (v/v) Triton X-100 2 mM EDTA 50 mM β-Glycerophosphate-disodium-salt-hydrate 1 mM Na-orthovanadate 1 mM AEBSF Hydrochloride 5 µg/ml Aprotinin 5 µg/ml Leupeptin 5 mM Benzamidine
5x Laemmli buffer	250 mM Tris-HCl (pH 6.8) 10% (w/v) SDS 50% (v/v) Glycerol 0.1% (w/v) Bromophenol blue
2x HBS buffer pH 7.0	280 mM NaCl 50 mM Hepes 1.5 mM Na_2HPO_4
Crystal violet dye	0.5% (w/v) crystal violet 20% (v/v) methanol
TAE buffer	40 mM Tris 20 mM acetic acid 1 mM EDTA
PBS (pH 7.4)	2.7 mM KCl 1.5 mM KH2PO4 137 mM NaCl 8 mM Na2HPO4

Table 6 Software

Software	Source
Image J	National Institute of Health (NIH)
MaxQuant (version 1.5.2.8)	coxdox.org
MxPro QPCR Software	Agilent
Primer3	Whitehead Institute for Biomedical Research
Wallac 1420 WorkOut Data Analysis software	PerkinElmer

Table 7 Devices

Device	Company
Curix 60	AGFA
EASY-nLC 1000	Thermo Scientific
Gel iX20 Imager	INTAS
Mx3005P QPCR System	Agilent
NanoDrop 2000 Spectrophotometer	Thermo Scientific
Q Exactive Plus	Thermo Scientific
T100 Thermal Cycler	BioRad
VICTOR^3 1420 Multilabel Reader	PerkinElmer

VII.2. Methods

VII.2.1. Cell culture

Table 8 Cell lines

Cell line	Origin
HaCaT	Keratinocytes
HeLa	Cervical carcinoma
Jurkat	T-Lymphocytes
HEK293T	Embryonic kidney cells

Cell lines used in this study (Table 8) were cultured at 37°C under 5% CO_2. Jurkat cells were cultured in RPMI 1640 medium containing 10% heat inactivated fetal calf serum (FCS). This suspension cell line was split when a confluence of 1x 10^6 cells/ml was reached. Therefore,

cells were sedimented by centrifugation at 400x g for 5 min followed by resuspension in fresh medium and dilution with a maximum ratio of 1:10, depending on the period of cultivation. All other cell lines were cultured in DMEM medium (Dulbecco´s Modified Eagle Medium) containing 4,500 mg/l glucose and 4 mM L-glutamine, additionally supplemented with 1% Hepes, 1% sodium pyruvate and 10% FCS. The adherent cell lines were split when they reached a confluence of 80-100%. Therefore, cells were washed with DPBS followed by detachment via 2.5% Trypsin solution. Trypsinisation was stopped by addition of DMEM containing 10% FCS. Cells were resuspended until a homogenous cell suspension was reached. The cells were sedimented by centrifugation with 400x g for 5 min at room temperature (RT). After removal of the supernatant, the cell pellet was resuspended in fresh medium and diluted depending on the period of cultivation. HaCaT cells were diluted with a maximum ratio of 1:5, whereas HeLa and HEK293T cells were diluted with a ratio up to 1:15.

VII.2.2. SDS-PAGE and Immunoblotting

For the creation of cellular protein lysates, cells were washed with DPBS followed by extraction with DISC-lysis buffer. Therefore, cells were lysed for 45 min on ice. The cell extracts were centrifuged for 30 min with 20,000x g at 4°C to sediment cellular debris. The protein concentration was determined using the DC™ Protein Assay (BioRad) according to manufacturer´s instructions. Protein samples were prepared under reducing conditions by the addition of Laemmli buffer and 5% 1 M DTT. Lysates were diluted to a final concentration of 0.5-1 µg/µl, followed by boiling at 96°C for 10 min. Samples were finally loaded on NuPAGE 4-12% BisTris gels (Invitrogen) and proteins were separated in MOPS buffer according to manufacturer´s protocol. Additionally, PageRuler Prestained Protein Ladder (Life Technologies) was loaded on each gel to visualize the molecular weight and protein separation.

For Western Blot analysis, separated proteins were transferred to polyvinylidene difluoride (PVDF) membranes using the iBlot2 Transfer Stacks (Life Technologies) according to manufacturer´s instructions. After blotting, membranes were blocked with 5% non-fat dried milk in PBS plus 0.1% Tween20 (from here on referred as PBST) for 1 h at RT. Primary antibodies were diluted in 5% milk in PBST or 5% BSA (bovine serum albumin) in PBST with the respective concentrations. Membranes were incubated with the primary antibodies on a rocker shaker overnight at 4°C. Membranes were brought to RT and washed four times in PBST. The respective secondary antibodies were diluted 1:10000 in 5% milk in PBST and incubated with the membranes for 1 h at RT. Membranes were washed three times in PBST and once in PBS only. Protein signals were visualized depending on their respective strength

using Pierce ECL Western Blotting substrate (Thermo Scientific) or Luminata Forte Western blot HRP (Millipore) and the Curix 60 (AGFA) developing machine.

VII.2.3. Detection of Phosphoproteins

Cells were stimulated and harvested as described before. To visualize protein modifications, especially phosphorylation of serine residues, cells were quickly homogenized by pushing the cell pellet three times through a 0.4 mm Microlance needle (BD). This was performed in the special Phopho-lysis buffer, containing different phosphatase inhibitors.

VII.2.4. Transfection and Transduction

In order to reach an optimal transfection and transduction efficiency, cells were seeded at the respective concentrations to receive a confluence of 60-70% at the day of transfection or transduction.

VII.2.4.1. siRNA-mediated knockdown

For transient knockdown experiments, the following siRNA duplexes were used:

- Dharmacon siGenome set of 4 human TBK1 siRNA (Cat. No.: MU-003788-02-0002)
- Dharmacon siGenome set of 4 human IKBKE siRNA (Cat. No.: MU-003723-02-0002)
- Quiagen AllStars Negative Control siRNA (Cat. No.: 1027281)
- FlexiTube Gene Solution for TRAF2 (Cat. No.: GS7186)

For siRNA mediated gene knockdown, 2x 10^5 cells were seeded per well of a 6-well plate, one day prior to the planned transfection. The next day, 5 µl Lipofectamine 2000 was added to 300 µl Opti-MEM medium and incubated 10 min at RT. In a separate tube, 5 µl of the respective 10 µM siRNA stock solution was mixed with 300 µl Opti-MEM. The two solutions were combined and incubated for 20 min at RT, in order to allow for siRNA/Lipofectamin complex formation. Meanwhile, the old medium was discarded from the cells and 1.4 ml fresh Opti-MEM medium was added. Finally, the transfection mixture containing the siRNA was added dropwise to the cells. Knockdown was monitored 72 h after transfection by Western Blot analysis.

VII.2.4.2. Generation of lentiviral particles

For the generation of lentiviral particles, HEK293T cells were cultured in 10 cm dishes and grown to 60-70% confluence. The cells were transfected using calcium phosphate transfection and the 2nd generation packaging system. Therefore, 3 µg pMD2.G, 7.5 µg pSPax2, and 3 µg pcDNA3.1/p35 of lentiviral packaging vectors were co-transfected together with 10 µg of the transfer vector. The transfer plasmid was either pF Super PGK Hygro (Gev16) providing the 4-HT-dependent expression of Gal4 or pF 5x UAC MCS W SV40 containing the cDNA sequence of interest[95,116]. This inducible transfer plasmid expresses the gene of interest in a Gal4-dependent fashion. For the calcium phosphate transfection, medium was removed from the cells and 6 ml fresh medium containing 25 µM chloroquine was added, followed by 2 h incubation at 37°C. Meanwhile, the above-mentioned plasmid DNA was diluted in a total volume of 500 µl containing 250 mM $CaCl_2$. Additionally, 500 µl 2x HBS buffer were prepared in a separate tube. In order to increase the surface and the oxygen uptake, air bubbles were carefully created in the HBS buffer by constant airflow from a pipette controller. The DNA $CaCl_2$ solution was carefully added dropwise into the air bubbled HBS buffer. The combined solution was incubated for 25 min at RT. The transfection solution was added dropwise to the cells and they were incubated overnight at 37°C. On the next day, medium containing the retroviral particles was collected, filtered (0.45 µm), shock frozen in liquid nitrogen, and finally stored at -80°C. Again, 6 ml fresh medium was added to the cells for a second collection of viral supernatants on the following day. All steps described were carried out according to the safety class two requirements.

VII.2.4.3. Generation of stable cell lines

For the generation of stable cell lines, the above-described viral particles were thawed and 5 µg/ml polybrene was added. The viral polybrene solution was added to cells, followed by spin-infection (2300 rpm) for 1.5 h at 30°C. The day after, cells were washed three times with PBS and reincubated with fresh DMEM at 37°C. On the second day after transfection, successfully transduced cells were selected using the respective antibiotic resistance harbored by the transduced plasmid. Therefore, cells were cultured in medium containing 1µg/ml Puromycin (pF 5x UAC MCS W SV40) or 300 µg/ml Hygromycin (pF Super PGK Hygro (Gev16)). Selection was completed, when 100% of untransduced control cells were killed, which was normally the case in 4-10 days. All steps were carried out according to the safety class two requirements until the cells were washed at least six times in virus free medium after transduction.

VII.2.5. Agarose gel-electrophoresis and gel-extraction

For the visualization of plasmid DNA or DNA fragments, agarose based gel-electrophoresis was used. Therefore, 1% agarose gels, containing 0.5x Nancy-520 (Sigma-Aldrich) were prepared from TAE buffer and low melt agarose (Roth). DNA samples were separated using electrophoresis and visualized by UV light. Successfully digested vector fragments were cut out from the gel and purified using the E.Z.N.A. Gel Extraction Kit (Omega). Purification was carried out according to manufacturer´s instructions and final DNA fragments were eluted in DNase free water. DNA quality and concentration were measured using a NanoDrop 2000 spectrophotometer.

VII.2.6. CRISPR/Cas9-mediated knockout of target genes

VII.2.6.1. Primer design and annealing for gRNA insert preparation

CRISPR gRNA sequences were generated using the open access software provided on the http://crispr.mit.edu/ webpage. For the design of the forward primer, a G was added in front of the 20 bp (base pair) gRNA sequence. The sequence including the G was used for the reverse complement building the reverse primer. Additionally, a CACC overhang for BbsI recognition was added in front of the G for the forward primer. AAAC was added as BbsI recognition site on the reverse primer.

Table 9 Primer for CRISPR gRNA ligation with BbsI sites

Primer	forward	reverse
TBK1 gRNA #1	CACCGGCTACTGCAAATGTCTTTCG	AAACCGAAAGACATTTGCAGTAGCC
TBK1 gRNA #2	CACCGTTTGAACATCCACTGGACGA	AAACTCGTCCAGTGGATGTTCAAAC
IKK-ε gRNA #1	CACCGGTTGCGGGCCTTGTACACAC	AAACGTGTGTACAAGGCCCGCAACC
IKK-ε gRNA #2	CACCGCATTGTCAAGCTCTTTGCGG	AAACCCGCAAAGAGCTTGACAATGC
TRAF2 gRNA #1	CACCGATATATGCCCTCGTGAACAC	AAACGTGTTCACGAGGGCATATATC
TRAF2 gRNA #2	CACCGGCAGCTAGCGTGACCCCCCC	AAACGGGGGGGTCACGCTAGCTGCC

The forward and reverse primer (100µM) were mixed in a 1:1 ratio. For annealing of the two oligos, the mixture was boiled at 100°C for 5 min, followed by cooling down at RT. The annealed oligos were diluted 1:300.

VII.2.6.2. Restriction enzymatic digestion

The empty pSpCas9(BB)-2A-GFP (PX458) plasmid (Addgene, kindly provided by the lab of Prof. Pascal Meier, ICR London, UK) was digested with the restriction enzyme BbsI (New England Biolabs) for cloning of the respective gRNA. Therefore, 1-2 µg of the plasmid was mixed with 1 µl of BbsI and 2 µl 10x NEB buffer 2. The volume was adjusted to a final volume of 20 µl. The reaction was performed for 2 h at 37°C. The digested vector was cleaned up *via* agarose gel electrophoresis and gel-extraction as described above.

To combine the gRNA oligos and the digested plasmid, 10 µl ligation reaction was prepared for each gRNA. Therefore, 1 µl of the digested plasmid, 1 µl of the diluted gRNA Oligos, 1 µl T4 DNA ligase, and 1 µl ligation buffer (New England Biolabs) were incubated 3 h at RT.

VII.2.6.3. Transformation and plasmid isolation

The ligated plasmids were transformed into chemical competent TOP10F *E. coli* (Invitrogen) bacteria. Therefore, the whole 10 µl ligation mixture was mixed with 100 µl bacteria and incubated on ice for 30 min. Afterwards, cells were heat shocked shortly for 45 sec at 42°C, followed by an additional incubation on ice for 2 min. 500 µl lysogeny broth (LB) medium was added to each sample, followed by a gently shaking incubation for 1 h at 37 °C. Transformed bacteria were finally plated on LB agar plates containing 100 µg/ml ampicillin and incubated overnight at 37°C. Single colonies were picked and transferred into 15 ml Falcon reaction tubes containing approximately 3-5 ml LB medium containing 100 µg/ml ampicillin (LB_{Amp}). The tubes were again gently shaking incubated overnight at 37°C. Plasmid DNA was isolated using the GeneJET Plasmid Miniprep Kit (Thermo Scientific) according to manufacturer´s instructions. The constructs were verified by sequencing and successfully generated plasmids were again transformed into bacteria as described above. After growing them on LB agar plates, single colonies were picked and inoculated in sterile Erlenmeyer flask containing 200 ml LB_{Amp} overnight at 37°C. Plasmids were isolated using the E.Z.N.A Fastfilter Plasmid Maxi Kit (Omega) according to manufacturer´s instructions. Plasmids were eluted in 1.5 ml DNase free water and analyzed with a NanoDrop 2000 spectrophotometer.

VII.2.6.4. CRISPR knockout of RIP1

RIP1 deficient HeLa cells were generated using the CRISPR/Cas9 system. Therefore, 1x 10^5 HeLa cells were seeded per well in 6-well plates. The next day, 600 ng pBluescript CRISPR plasmid, containing the gRNA targeting *RIP1* (kindly provided by the lab of Prof. Pascal Meier ICR London, UK) and 1 µg of the Dharmacon mKate-Cas9 Nuclease expression plasmid were co-transfected, using 1 µl Dharmafect Duo Transfection reagent per 6-well. The RIP1 target sequence is shown in Table 10. Two days after transfection, cells were

sorted via BD FACSAria I (BD Bioscience) for mKate expression and plated as single cell clones in 96-well plates. Arising clones were cultured for 2-3 weeks and analyzed for successful RIP1 knockout by Western blotting.

VII.2.6.5. CRISPR knockout of TBK1, IKK-ε and TRAF2

For the knockouts of TBK1, IKK-ε and TRAF2 second generation CRISPR plasmids containing the Cas9 nuclease as well as the gRNA were used. CRISPR gRNA sequences were generated using the Zhang's lab open access gRNA generation software (http://crispr.mit.edu/). The first 100 bp of the target gene mRNA were pasted into the software. Two CRISPR sequences were used for each gene to avoid off-target effects.

Table 10 Sequences of the single CRISPR gRNAs

Primer	forward
TBK1 gRNA #1	GCTACTGCAAATGTCTTTCG
TBK1 gRNA #2	TTTGAACATCCACTGGACGA
IKK-ε gRNA #1	GTTGCGGGCCTTGTACACAC
IKK-ε gRNA #2	CATTGTCAAGCTCTTTGCGG
TRAF2 gRNA #1	ATATATGCCCTCGTGAACAC
TRAF2 gRNA #2	GCAGCTAGCGTGACCCCCCC
RIP1 gRNA	TCGGGCGCCATGTAGTAG

The identified target sequences were cloned into the pSpCas9(BB)-2A-GFP (PX458) plasmid, as described above. 1x 10^5 HeLa cells were seeded per well in a 6-well plate. The next day, the cells were transfected with 500 ng pSpCas9(BB)-2A-GFP containing the respective gRNA, using 5 µl GeneJuice Transfection reagent (Merck/Millipore). Two days after transfection, cells were separated via BD FACSAria I (BD Bioscience). Single cell clones expressing GFP were plated as single cell clones in 96-well plates. Arising clones were cultured for 2-3 weeks and analyzed for a successful knockout of the target gene by Western blotting.

VII.2.7. Gel-filtration

The described gel-filtration was kindly done by our cooperation partner in Leicester (Prof. Marion MacFarlane from the Molecular Mechanisms of Cell Death section, MRC Toxicology Unit) as described before[148]. In brief, HaCaT RIP1 WT cells (~1x 10^8) were treated 6 h with

100 nM 4-HT to induce Ripoptosome formation. Thereafter, the cells were lysed in 2 ml DISC-lysis buffer before being cleared by centrifugation. The cleared lysate was then loaded onto an agarose matrix (Superrose 6) and forced through the column using low pressure. Small fractions, containing size separated protein fractions, were collected and analyzed via Western Blot analysis.

VII.2.8. Caspase-8 Immunoprecipitation (IP)

The respective cell lines were seeded in T175 flasks and grown to 80-90% confluence (~ 1.5x 10^7 cells). After appropriate stimulation, the cells were washed once with cold PBS, following solubelization with 5 ml 2.5% Trypsin. Once the cells were detached, 5 ml of DMEM medium with 10% FCS was added in order to stop the trypsinization. The cell suspension was centrifuged 5 min with 400x g and the pellet was resuspended in PBS. After another round of centrifugation (5 min at 400x g), cells were lysed on ice by the addition of 1.5 ml DISC-lysis buffer. After 45 min of lysis, the lysates were centrifuged at 20,000x g for 30 min, respectively, to remove cellular debris. The protein concentration of the cleared lysates was determined by Bradford assay. A small fraction of 100 µg from each lysate was used as an input control, named TL (total lysate). For the immunoprecipitation, 30 µl protein G-agarose beads and 1 µg caspase-8 antibody (C20) was added to 2 µg of the total protein lysates. All samples were incubated overnight on an overhead shaker at 4°C. The next day, the supernatants were discarded and the beads with the bound affinity precipitates were washed 5x with 1 ml of DISC-lysis buffer. The bound proteins were eluted from the dried beads by addition of standard reducing sample buffer and boiling for 10 min at 95°C. Subsequently, protein samples were separated by SD-PAGE on 4-12% NuPAGE gradient gels and precipitated proteins were visualized by Western Blot analysis.

VII.2.9. Cell death analysis by crystal violet staining

1-1.5x 10^4 cells of the different cell lines were seeded per well in a 96-well plate. The next day, the cells were stimulated in triplicates with the respective ligands and incubated for the appropriate time at 37°C. After the stimulation, the supernatant was discarded and the cells were carefully washed two times with PBS to remove detached cells. 50 µl of crystal violet solution was added per well, respectively. The plate was incubated for 20 min at room temperature on a platform tumbling shaker. For removal of the Crystal violet, cells were washed with tap water until the excessive dye was removed completely. The stained cells were put upside down on a paper towel and dried for minimum 2 h at RT to get rid of remaining liquids. To dissolve the crystal violet dye, 200 µl Ethanol per well was added and

the plate was incubated 20 min at RT on a platform tumbling shaker. Optical density of the single wells was measured with a VICTOR3 1420 Multilable Reader and optical density of control conditions (cells treated with diluents) was set to 100% to allow comparison. For statistical analysis, mean values of three independent experiments were assessed. To accommodate experimental deviations, the standard error of mean (SEM) was calculated using Excel.

VII.2.10. RNA Isolation

For the isolation of total cellular RNA, the respective cell pellets were treated according to manufacturer´s instructions of the RNeasy Mini Kit (Quiagen). Therefore, cells were washed in PBS, followed by lysis in RLT buffer containing 1% β-mercaptoethanol. RNA was extracted using spin column purification. The purified RNA was washed twice, followed by elution with RNase free water. RNA quality and concentration was measured using a NanoDrop 2000 spectrophotometer. For the reverse transcription reaction, 1.5 µg RNA of each sample was diluted in RNase free water to a final volume of 9.8 µl. The diluted RNA was mixed with 1 µl 10 mM deoxynucleoside triphosphate (dNTP), 1 µl 100 µM random nanomers and 0.2 µl 100 µM oligo dT primer. The probes were incubated in a thermocycler for 5 min at 65°C. Afterwards, the samples were taken out from the thermocycler and 4 µl 5x First Buffer, 2 µl 0.1 M DTT, 0.5 µl RNase out (Life Technologies), and 0.5 µl Superscript II (Life Technologies) was added into each reaction tube. The samples were further incubated in the thermocycler for 2 min at 42°C, 12 min at 25°C, 50 min at 42°C, and finally 15 min at 70°C. The synthesized cDNA was finally diluted to a concentration of 100 ng/µl.

VII.2.11. Quantitative real time polymerase chain reaction (qPCR)

For the analysis of gene expression qPCR analyses were performed. Primer for the respective target genes were designed using the open source program Primer3. The Primers were diluted to a final concentration of 20 µM. Each single sample was prepared with a final volume of 20 µl, containing 8.8 µl cDNA (100 ng/µl), 10 µl. KAPA SYBR FAST (Peqlab), 0.4 µl ROX (Peqlab), 0.4 µl forward and reverse primer. Single cDNAs or conditions were always analyzed in triplicates. qPCR analyses were performed using a Mx3005P QPCR System (Agilent). Equal cycling conditions were used to amplify the genes of interest.

Melting curve analysis was used to confirm the specific amplification of single products of the expected size. Furthermore, all primers used for qPCR studies have been tested before by cDNA dilution curves to show efficiency within 80-110%. All samples were tested to have a low variance in the housekeeping gene (*GAPDH*) expression, which was set as a calibrator in the MxPro software. The relative fold induction was determined by using the relative

quantification to the calibrator (dRn), calculated by the MxPro software. Unstimulated Ctrl samples were set to 1 and the respective samples of interest were calculated by dividing the dRn values of interest through the value of the Ctrl sample.

The qPCR program was set as follows:

- 50°C for 2 min
- 95°C for 10 min

Followed by 42 cycles of:

- 95°C for 30 sec
- 60°C for 1 min

Ended with a final cycle of:

- 95°C for 1 min
- 65°C for 30 sec
- 95°C for 1min

VII.2.12. Microarray analysis

For the analysis of gene expression profiles, 2x 10^5 HaCaT RIP1 WT cells were seeded per well of a 6-well plate. The next day, cells were transfected with Ctrl, TBK1 and IKK-ε siRNAs as described above. Three days after transfection, cells were starved for 3 h in DMEM medium without FCS, followed by stimulation with 50 µM Necrostatin-1 (Nec-1) for 1 h. RIP1 expression was induced by the addition of 4-HT for 8 h. RNA was isolated, using the Qiagen RNeasy Mini Kit as described above. Gene expression of the single samples was analyzed by microarray analysis in three independent biological replicates. The array analysis was kindly done by the lab of Martin Sprick (DKFZ, Heidelberg) and the Genomics and Proteomics Core Facility of the German Cancer Research Center (GPCF DKFZ, Heidelberg), as described in recent publications[149]. In brief, RNA (500 ng per sample) was labeled, using the Illumina TotalPrep RNA Amplification Kit according to the manufacturer's instructions. cRNA was hybridized to human whole-genome Illumina HumanHT-12 V4.0 expression BeadChip (Illumina, Inc.). BeadChips were scanned with an Illumina iScan system (Illumina Inc.). Scanning and feature extraction was performed using BeadScan and BeadStudio software (Illumina) with standard settings for the chips used. Quantile normalization was performed with the Illumina BeadStudio.

VII.2.13. SILAC labeling and mass spectrometry

The SILAC in this study was kindly done by the group of Prof. Ivan Dikic from the Institute of Biochemistry II, Goethe University Medical School in Frankfurt as described before[150]. In brief, HeLa RIP1 WT and TBK/IKK-ε KO RIP1 WT cells were grown in medium containing heavy (HeLa WT) or light (TBK/IKK-ε KO) isotope labeled amino acids. Cells were maintained in custom-made SILAC DMEM (heavy/medium/light) for 10 days, and incorporation of labeled amino acids to more the 95% was verified. Cellular lysates of both cell lines were generated and mixed in 1:1 ratio. Protein lysates were loaded onto a 4-12% gradient SDS/PAGE gel and proteins were stained using the Colloidal Blue Staining Kit (Thermo Fisher) and digested in-gel, using trypsin. Peptides were extracted from the gel and desalted on reversed phase C18 StageTips. Peptide fractions were analyzed on a quadrupole-Orbitrap mass spectrometer (Q Exactive Plus; Thermo Scientific) equipped with an ultrahigh-performance liquid chromatography (UHPLC) system (EASY-nLC 1000; Thermo Scientific). Raw data files were analyzed using MaxQuant (version 1.5.2.8) and compared for protein phosphosites.

VIII. Results

VIII.1. Spontaneous Ripoptosome formation and cell death induction depends on intracellular RIP1 level

Many studies have highlighted that RIP1 is one of the key players in cellular PCD signaling pathways[151–153]. The dual function of RIP1 is reflected by the death receptor-mediated NF-κB activation, as described in detail for TNFR1, thereby promoting cell survival[151,154]. In contrast, RIP1 is one of the key mediators of the necroptotic signaling cascade, where it is responsible for the activation of RIP3[40,47,56]. Moreover, RIP1 is the central component of the Ripoptosome, whose formation can lead to apoptosis as well as necroptosis[95,99,100,144]. Hence, the intracellular protein level and the activation of RIP1 have to be tightly regulated in order to maintain normal cellular viability and function.

VIII.1.1. Expression of RIP1 induces kinase-dependent cell death in HaCaT and HeLa cells

As mentioned above, changes in the intracellular RIP1 level could have severe effects on cellular signaling pathways and thereby cell viability. In order to investigate the role of RIP1 for cell death regulation as well as cell death-independent signaling pathways, cell models with a 4-Hydroxy-Tamoxifen (4-HT) inducible RIP1 expression were established. Therefore, HaCaT and HeLa cells were transduced with recombinant lentiviral particles, containing cDNAs specific for Gev16 and RIP1 WT as described in former publications[95,116]. The newly generated cell lines were named HaCaT RIP1 WT and HeLa RIP1 WT. To determine the optimal point of time for substantial RIP1 protein expression upon 100 nM 4-HT stimulation, a time-dependent kinetic was performed (Figure 1A). Substantial increase in RIP1 level was detected four hours after stimulation. The expression level of the kinase was comparable in both cell lines. In order to rule out side effects of the 4-HT stimulation in respect to PCD related components, Western Blot analyses of the respective proteins were performed. HaCaT cells showed no significant changes in the expression level of the proteins FADD, MLKL or RIP3 (Figure 1A). cFLIP was not shown as HaCaT cells harbor very low level of this protein, which are under the detection limit of the used antibody. In contrast, caspase-8 levels were reduced over time in line with the RIP1 expression, most probably due to caspase-8 cleavage, indicating activation and cell death induction. HeLa cells showed the cleavage of cFLIP in line with the increasing RIP1 level, indicating that increased RIP1

activity leads to caspase-8 activation that finally targets cFLIP (cleavage) and promotes the induction of cell death (Figure 1C). Interestingly, the caspase-8 protein level seems to be rather unchanged, indicating that the cell death induction is weaker when compared to HaCaT cells. FADD and MLKL showed no significant differences in their protein level upon RIP1 expression (Figure 1C). RIP3 was not shown in HeLa cells as these cells are RIP3 negative.

The indicated induction of cell death by the observed reduction of caspase-8 level and cFLIP cleavage was further functionally analyzed by crystal violet staining. This assay measures changes in cell attachment in respect to certain stimulations. Therefore, this assay can be used as an indicator for cell death, although the observed differences could also be due to growth inhibitory effects. In the following, the detected cell detachment was set equal to cell execution, although the described crystal violet assays do not measure cell death directly. In order to distinguish between caspase-dependent (apoptotic) and caspase-independent (necroptotic) cell execution, both cell lines were prestimulated with the caspase inhibitor carbobenzoxy-valyl-alanyl-aspartyl-[O-methyl]-fluoromethylketone (zVAD-fmk)[155–157] and the RIP1 kinase inhibitor Necrostatin-1 (Nec-1)[158]. RIP1 expression was induced by a 20-hour stimulation with increasing concentrations of 4-HT (Figure 1B and 1D). Both cell lines showed substantial decrease in cell attachment, indicating an increased cell death response in line with the expression of RIP1 (Figure 1B and 1D). The combination of zVAD-fmk and Nec-1 completely blocked cell death compared to the unstimulated control (Ctrl) after the overexpression of RIP1. The addition of the RIP1 kinase inhibitor Nec-1 could only partially (about 20%) rescue from detachment. The caspase inhibitor zVAD-fmk could completely abrogate cell death in HeLa cells, arguing for the exclusive appearance of apoptotic cell death. This was expected, as these cells lack the necroptotic relevant RIP3. In contrast, the protection by zVAD-fmk in HaCaT cells reached only 80% (Figure 1B, red curve), indicating the appearance of a caspase-independent, potentially necroptotic cell death. In general, HaCaT cells were more sensitive to cell death (100% dead cells after 20 hours stimulation with 50 nM 4-HT) induced by RIP1 expression when compared to HeLa cells, which showed a maximum of 40% dead cells after 20 hours with 200 nM 4-HT. Altogether, these data show that RIP1 expression induces caspase-dependent and -independent execution in HaCaT cells. HeLa cells undergo solely caspase-dependent death due to the lack of RIP3. Moreover, HeLa cells are more resistant to RIP1-induced cell death, when compared to HaCaT cells.

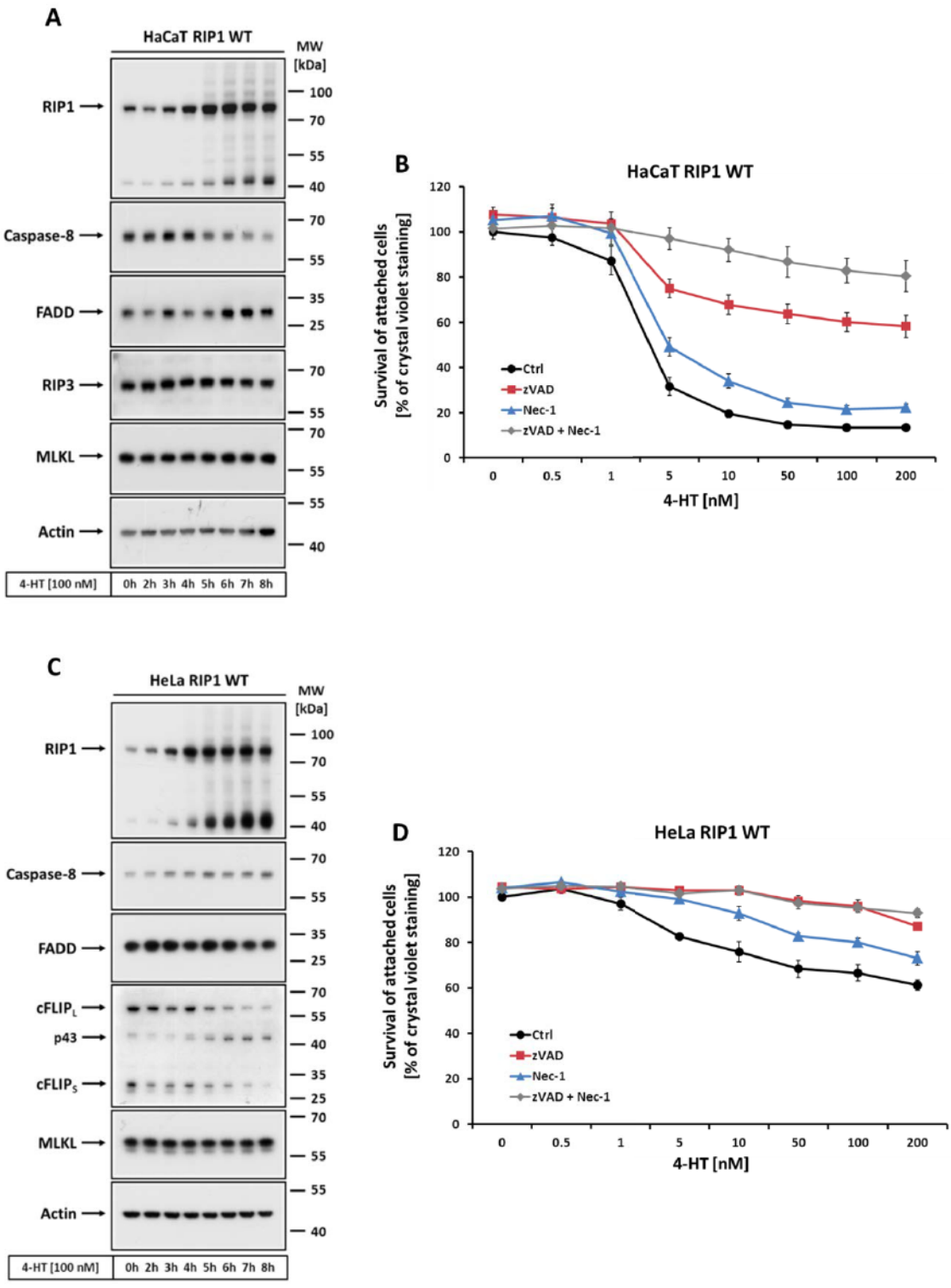

Figure 7 Inducible RIP1 expression promotes cell detachment in HaCaT and HeLa cells.
For expression of RIP1 WT, HaCaT (A) and HeLa (C) cells were stimulated with 100 nM 4-HT for the indicated point of time. 10 µg total protein lysates were separated via SDS-PAGE. Expression of PCD-related proteins (RIP1, FADD, caspase-8, cFLIP, MLKL and RIP3) were analyzed by Western Blot analysis. (A and C). Cell detachment induced by the RIP1 expression was monitored via crystal violet assay (B and D). Viable attached cells were stained with crystal violet after 20 h stimulation with different concentrations of 4-HT. Figure B and D display the mean values of three independent experiments. Error bars were calculated with the standard error of mean (SEM).

VIII.1.2. Expression of RIP1 leads to kinase-dependent formation of the Ripoptosome

As shown in recent publications[95], the observed cell death most likely is induced by the formation of a Ripoptosome-like complex, which is able to regulate apoptotic and necroptotic cell death responses based on the molecular constitution[95,100]. To investigate the role of RIP1 expression and regulation in respect to Ripoptosome formation, immunoprecipitations (IP) of caspase-8, a central component of the complex, were performed and analyzed for the co-precipitation of other Ripoptosome-associated components. Moreover, the impact of caspase activation and RIP1 kinase activity in respect to Ripoptosome formation were analyzed by the addition of the above-mentioned inhibitors. Therefore, the generated HaCaT and HeLa RIP1 WT cells were prestimulated with zVAD-fmk and Nec-1, followed by the addition of 100 nM 4-HT. After six hours cellular lysates were generated and caspase-8-associated complexes were immunoprecipitated as described in the material and methods section.

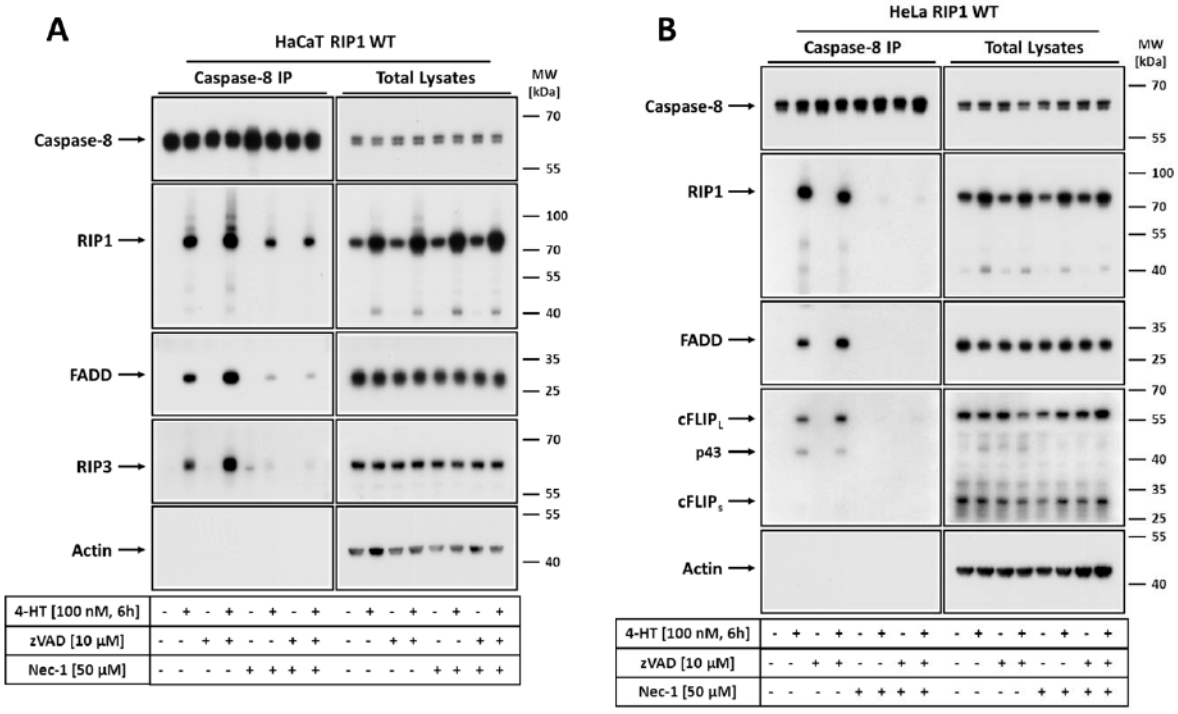

Figure 8 Expression of RIP1 induces spontaneous RIP1 kinase-dependent Ripoptosome formation in HaCaT and HeLa cells.
HaCaT (A) and HeLa (B) RIP1 WT cells were prestimulated with 10 µM zVAD-fmk and 50 µM Nec-1 for 1 h. RIP1 expression was induced by the incubation with 100 nM 4-HT for 6 h. Cells were lysed in DISC-lysis buffer and caspase-8 and caspase-8-associated complexes were precipitated from 2 mg of total cellular lysates. Total protein lysates and caspase-8-bound complexes were separated by SDS-PAGE and analyzed via Western Blot for caspase-8-associated components of the Ripoptosome (caspase-8, RIP1, FADD, cFLIP and RIP3).

HaCaT and HeLa cells both showed a strong association of caspase-8 with RIP1 and FADD (Figure 8A and 8B). Additionally, cFLIP was precipitated together with caspase-8 in HeLa cells. Moreover, RIP3 was found to be part of the complex in HaCaT cells (Figure 8A). The addition of the caspase inhibitor zVAD-fmk slightly increased the co-precipitation of the above-mentioned proteins with caspase-8 (especially seen in HaCaT cells). This was rather expected, as caspase inhibition results in the stabilization of caspase-8-containing complexes[100,144]. The inhibition of RIP1 kinase activity through Nec-1 largely suppressed Ripoptosome formation as well as the appearance of higher molecular weight modifications on RIP1 (especially seen in HaCaT cells). RIP1 is post translationally modified via phosphorylation and ubiquitination at several sites[152]. As the inhibition of the kinase activity by Nec-1 suppresses these modifications, the seen laddering is most likely driven by autophosphorylation due to high local RIP1 concentrations, finally resulting in the phosphorylation-dependent ubiquitination followed by proteasome-dependent degradation. Summarized, these data suggest that the overexpression of RIP1 leads to the formation of the Ripoptosome, containing the proteins caspase-8, RIP1, FADD, cFLIP (in HeLa cells) and RIP3 (in HaCaT cells). Moreover, the kinase activity of RIP1 was crucial for the formation of this complex, as the addition of Nec-1 largely suppressed the association of the above-mentioned proteins with caspase-8.

It is well known that the RIP1 inhibitor Nec-1 has additional effects apart from inhibiting RIP1 activity. Several studies showed that the compound for example also suppresses the function of the indoleamine-2,3-dioxygenase (IDO)[158,159]. To confirm that the observed complex inhibitory properties of Nec-1 were not simply due to off-target effects, another specific RIP1 inhibitor (GSK'481) was tested[160]. Moreover, to investigate if RIP3 kinase activity is of relevance for Ripoptosome formation, a specific RIP3 inhibitor (GSK'840) was used. This second inhibitor blocks necroptotic cell death downstream of RIP1[160]. Therefore, HaCaT RIP1 WT cells were prestimulated with GSK'481 and GSK'840 for one hour. RIP1 expression was again induced by the addition of 100 nM 4-HT for six hours. Cellular lysates were assessed for complex formation by caspase-8 IP as described above. Expression of RIP1 again resulted in the association of RIP1, FADD and RIP3 with caspase-8. RIP1 kinase inhibition through GSK'481 resulted in a dramatic decrease in complex formation and the inhibition of higher molecular weight modifications of RIP1. Inhibition of RIP3 downstream of RIP1 by GSK'840 had no effect in terms of Ripoptosome formation (Figure 9). These data confirmed the findings from the last section. Kinase activity of RIP1 is required for substantial Ripoptosome formation. Inhibition of downstream necroptotic signaling by the RIP3 inhibitor GSK'840 had no effect on the complex formation, indicating that RIP3 kinase activity is not of critical relevance for Ripoptosome formation.

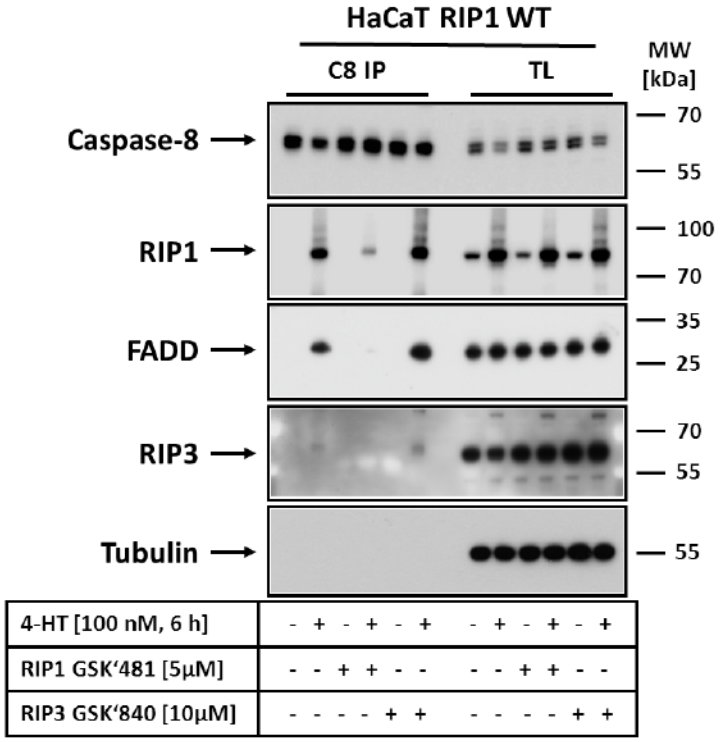

Figure 9 Impact of RIP1 and RIP3 kinase inhibitors on RIP1-induced Ripoptosome formation.
HaCaT and HeLa RIP1 WT cells were prestimulated with 5 µM of the RIP1 inhibitor GSK'481 and 10 µM of the RIP3 inhibitor GSK'840 for 1 h. RIP1 expression was induced with 100 nM 4-HT for 6 h. Cells were lysed in DISC-lysis buffer and caspase-8 and caspase-8-associated proteins were precipitated from 2 mg of total cellular lysate. Total cellular lysates and caspase-8-bound complexes were separated by SDS-PAGE. Association of Ripoptosome components (caspase-8, RIP1, FADD and RIP3) with caspase-8 was visualized via Western Blot analysis.

VIII.2. TBK1, IKK-ε and TRAF2 are novel components of the Ripoptosome

Thus far, formation and downstream signaling of the Ripoptosome has only been linked to cell death induction[95,144,161]. However, it is very likely that the formation of such an intracellular protein complex can also induce non-cell-death signaling cascades, like the expression of inflammatory genes through the activation of NF-κB. This is a very common concept in intracellular stress signaling, as seen for the TNF complex I, DISC signaling or TLR3 stimulation[73,107,112]. Therefore, further analyses of the Ripoptosome could reveal novel components and interacting proteins, which might be responsible for the propagation of such signaling pathways. Therefore, highly purified Ripoptosome complexes should be dissected by mass spectrometry and analyzed for thus far unknown components. In this respect, the above-described necroptotic potent HaCaT system was used, as the expression of RIP1 induces a strong, kinase-dependent association of the Ripoptosome components RIP1,

FADD and RIP3 with caspase-8. Moreover, the expression of the central RIP1 kinase is the only trigger for complex formation and downstream signaling, ruling out site effects from different stimuli, like death ligands or Smac mimetics.

VIII.2.1. Mass spectrometric analysis revealed TBK, IKKε and TRAF2 as integral components of the RIP1-induced Ripoptosome

Novel components of the purified RIP1-induced Ripoptosome should be determined with the help of mass spectrometric complex dissection. Therefore, HaCaT RIP1 WT cells were kindly analyzed, by our cooperation partner in Leicester (Prof. Marion MacFarlane from the Molecular Mechanisms of Cell Death section, MRC Toxicology Unit) as described before[148]. After the induction of RIP1 with 4-HT for six hours, cellular lysates were separated using a Gel-filtration matrix. Therefore, cellular lysates were forced through an agarose column, enabling the size-dependent separation of unbound proteins and higher molecular protein complexes (Figure 10A). When cells were stimulated with zVAD-fmk alone as our control condition for analysis of complex formation, RIP1 and caspase-8 were exclusively found in lower molecular weight fractions (Figure 4A, bottom) and no high molecular weight complexes were observed. In contrast, when RIP1 expression was induced by 100 nM 4-HT, a large portion of both proteins was shifted to the high molecular weight fractions (Figure 4A top lane 1-5, marked in red). This indicates the association of RIP1 and caspase-8 in a high molecular weight complex, which we know is the Ripoptosome[100]. In order to isolate the caspase-8-containing complex from non-complexed proteins, the Ripoptosome containing fractions 1-5 were pooled and a caspase-8 immunoprecipitation was performed. The caspase-8-bound proteins were separated via SDS-PAGE, followed by coomassie staining (Figure 10B). Finally, the protein bands shown in Figure 10B, were analyzed by mass spectrometry. The mass spectrometric analysis revealed the already known components RIP1, cIAP2 and caspase-8 (Table 1 marked in grey). Surprisingly, it was never possible to detect the adapter molecule FADD. However, this could most probably be explained with the small molecular weight of this protein and thereby the detection limit of the technique due to the trypsin digestion or via the low required quantities of FADD, as the incorporated amounts of FADD during Ripoptosome formation are rather low, when compared to other components[100,162]. Aside from the already known Ripoptosome components, some contaminating proteins, like the heat shock and stress proteins (HSPA9, HSPA1A, HSPA5 or HSPA8), which are often seen in mass spectrometric analysis, were found. Interestingly, substantial amounts of the non-canonical IKKs, namely TBK1 and IKK-ε, together with the E3-ubiquitin ligase TRAF2 were identified (Table 11 marked in red).

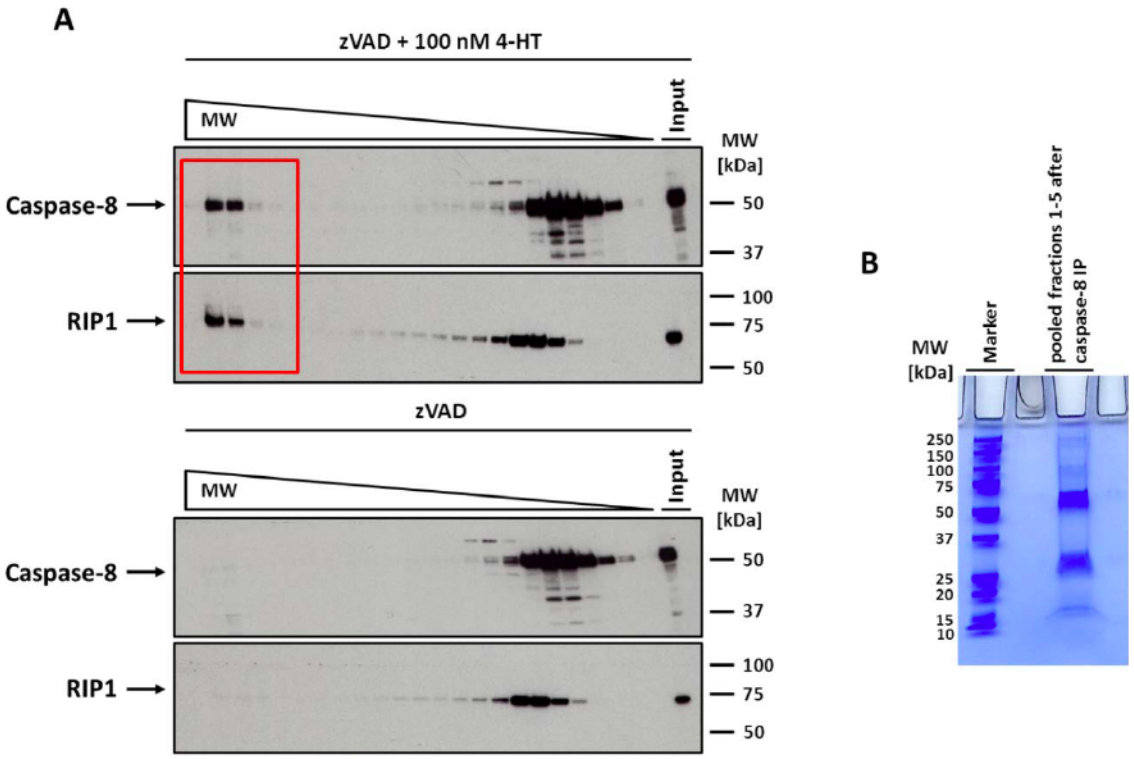

Figure 10 Gel-filtration and immunoprecipitation of the purified Ripoptosome.
(A) HaCaT RIP1 WT cells were stimulated for 6 h with 100 nM 4-HT plus zVAD-fmk (top) or with zVAD-fmk alone (bottom). Cellular lysates of the respective cells were separated into size specific fractions by gel-filtration using Superose 6 agarose columns. Samples of the different fractions were analyzed via Western Blot for Ripoptosome-associated proteins (RIP1 and caspase-8). (B) Ripoptosome-containing fractions 1-5 (marked in red) were pooled and caspase-8 was immunoprecipitated. The caspase-8-bound proteins were separated by SDS-PAGE and visualized by coomassie staining. The experiments were kindly done and provided by the lab of Prof. Marion MacFarlane from the Molecular Mechanisms of Cell Death section, MRC Toxicology Unit in Leicester.

To confirm the precipitation of TBK1, IKK-ε and TRAF2 within the Ripoptosome, these proteins were analyzed in RIP1-induced complexes by Western Blot analysis. Moreover, the influence of caspase activity as well as RIP1 kinase activity were analyzed in respect to the association of the novel identified components. Therefore, RIP1 WT HaCaT (Figure 11A) and HeLa (Figure 11B) cells were stimulated with zVAD-fmk and Nec-1, followed by RIP1 expression induced by 100 nM 4-HT for six hours. Caspase-8 was precipitated from cellular lysates as described above. Furthermore, the coprecipitation of TBK1, IKK-ε and TRAF2 with caspase-8 was analyzed by Western Blotting (Figure 11). Confirming the mass spectrometric results, all three novel components were found associated with caspase-8 in the IP samples. The association was, in line with the above-mentioned results, clearly RIP1 expression-dependent. Moreover, the Western Blot, shown in Figure 11, displays the already seen inhibition of complex formation when kinase activity was blocked by Nec-1. The addition of zVAD-fmk could, as expected, slightly increase the complex formation.

Table 11 Mass spectrometric results of the RIP1-induced purified Ripoptosome

Identified Proteins	Symbol	Molecular Weight [kDa]	Coverage
Stress-70protein, mitochondrial OS=homo sapiens GN=HSPA9 PE=1 SV=2	HSPA9	74	17
Caspase-8 OS=homo sapiens GN=CASP8 PE=1 SV=1	CASP8	55	24
Heat Shock 70 kDa protein OS=homo sapiens GN=HSPA1A PE=1 SV=5	HSPA1A	70	13
Receptor Interacting Serine/Threonine Kinase 1 OS=homo sapiens GN=RIPK1 PE=1 SV=3	RIPK1	76	36
78kDa glucose regulated protein OS=homo sapiens GN=HSPA5 PE=1 SV=2	HSPA5	72	2
Serine/Threonine kinase TBK1 OS=homo sapiens GN=TBK1 PE=1 SV=1	TBK1	84	11
Baculoviral IAP repeat-containing protein 2 OS=homo sapiens GN=BIRC2 PE=1 SV=2	BIRC2	70	15
TNFR-associated factor 2 OS=homo sapiens GN=TRAF2 PE=1 SV=2	TRAF2	56	19
Heat shock cognate 71 OS=homo sapiens GN=HSPA8 PE=1 SV=1	HSPA8	71	5
Inhibitor of nuclear factor kappa-B kinase subunit epsilon OS=homo sapiens GN=IKBEK PE=1 SV=1	IKKE	80	10

Interestingly, TBK1 and IKK-ε were highly phosphorylated at Serine 172 when RIP1 levels were increased. The addition of Nec-1 inhibited the phosphorylation in line with the complex formation, arguing for a kinase- or complex-dependent activation of TBK1 and IKK-ε. Additionally, the phosphorylated state of both proteins was highly enriched in the precipitated complex fraction (Figure 11, Caspase-8 IP). Summarized, these findings clearly identified the non-canonical IKKs, TBK1 and IKK-ε, as well as the ubiquitin-ligase TRAF2 as novel components of the RIP1-induced Ripoptosome. Moreover, the kinases TBK1 and IKK-ε were substantially phosphorylated at Serine 172 when RIP1 level were increased, indicating the activation of both proteins. Furthermore, the activated state of TBK1 and IKK-ε was enriched in the caspase-8-bound IP samples.

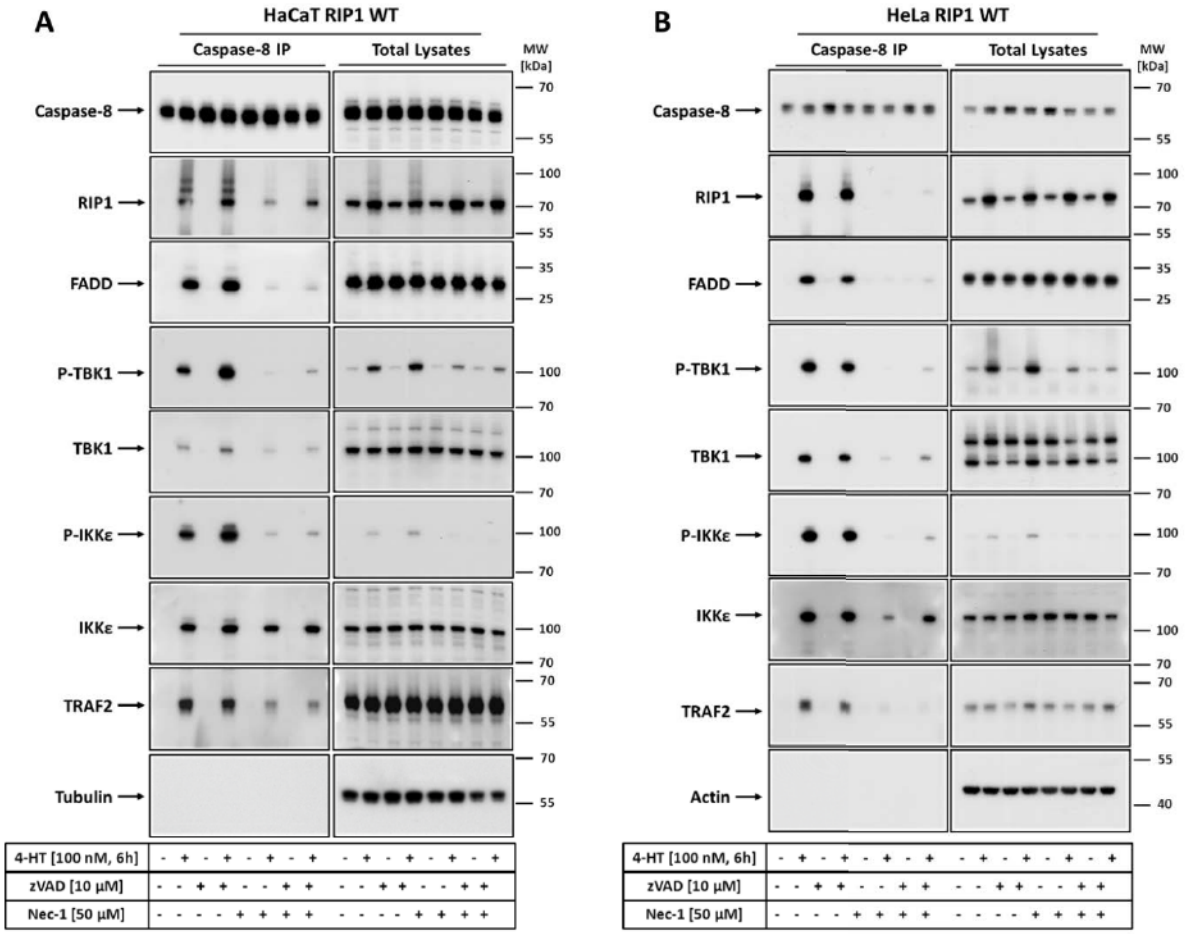

Figure 11 TBK, IKK-ε and TRAF2 are novel components of the RIP1-induced Ripoptosome.
HaCaT and HeLa RIP1 WT cells were prestimulated with 10 µM zVAD-fmk and 50 µM Nec-1 for 1h, followed by the induced expression of RIP1 with 100 nM 4-HT for 6 h. Cells were lysed in DISC-lysis buffer and caspase-8 was precipitated from 2 mg of total cellular lysates. The total lysates and the caspase-8-bound proteins were separated via SDS-PAGE. The association of TBK1, IKK-ε and TRAF2 with caspase-8 and other Ripoptosome components was visualized via Western Blot analysis.

VIII.3. The TNF complex II and the TLR3-associated Ripoptosome display physiological signaling complexes harboring TBK1, IKK-ε and TRAF2

In order to generalize the above-described findings, association of TBK1, IKK-ε and TRAF2 with TNF complex II and the TLR3-induced Ripoptosome-like complex will be analyzed in the following section. As shown above, changes in the cellular RIP1 level could lead to dramatic effects, especially cellular execution. The overexpression of RIP1 represents an extreme and quite unphysiological condition. Therefore, the observed interaction between TBK1, IKK-ε, TRAF2 and caspase-8 could very likely be an artifact of the artificial RIP1 overexpression. In contrast, the stimulation of the TLR3 receptor and formation of the TLR3-associated

Ripoptosome displays rather physiological processes during pathogen infections. Therefore, the TLR3-dependent cell death responses as well as the formation properties of the TLR3-associated complex were analyzed and compared to the formation of the TNF complex II.

VIII.3.1. Stimulation of the TLR3 receptor with poly (I:C) leads to cell death when cIAPs are depleted

As mentioned above, it was shown that stimulation of the endosomal TLR3 receptor via poly (I:C) can also induce cell death and promote the recruitment of the Ripoptosome, when cIAPs are depleted[100]. At first, cell death responses underlying TLR3 stimulation in HaCaT and HeLa cells should be analyzed to confirm the published data in the used cellular system. Moreover, the appropriate concentration of poly (I:C) for the following complex analysis should be determined.

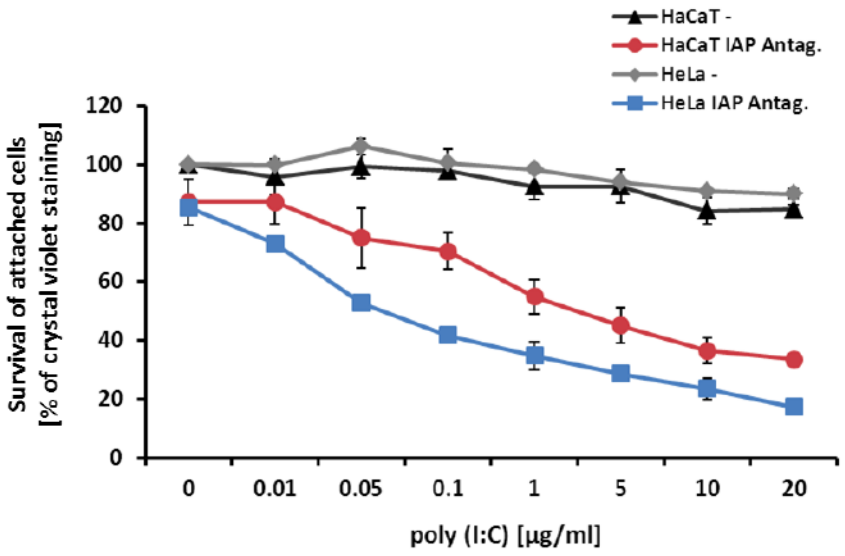

Figure 12 Combined treatment of IAP antagonist and poly (I:C) sensitizes HaCaT and HeLa cells to cell death. Parental HaCaT and HeLa cells were stimulated with 100 nM IAP antagonist (Compound A) for 1 h, followed by the addition of different concentrations of poly (I:C). After 20 h of incubation, cell detachment was visualized by crystal violet staining. The shown data display the mean values ± SEM of three independent experiments.

Therefore, parental HaCaT and HeLa cells were stimulated with IAP antagonist (Compound A), followed by the stimulation with different concentrations of poly (I:C). HaCaT and HeLa cells both showed no cell detachment, meaning no cell death when treated with poly (I:C) alone (Figure 12). In the absence of IAP function, poly (I:C)-induced a concentration-dependent killing of both cell lines. HeLa cells showed roughly 40% attached cells after

treatment with 1 µg/ml poly (I:C). In contrast, HaCaT cells had to be treated with 10 µg/ml in order to reach roughly the same amount of attached cells. That means that HeLa cells were about ten times more sensitive to the treatment than HaCaT cells (Figure 12). Taken together, these results confirmed the published data and showed that HaCaT and HeLa cells could be sensitized to cell death with the combined treatment of IAP antagonist and poly (I:C). Moreover, HaCaT cell showed a roughly ten times higher resistance to the treatment when compared to HeLa cells. For the following complex analysis, HaCaT cells were treated with 20 µg/ml and HeLa cells with 2 µg/ml poly (I:C). Both concentrations resulted in substantial cell death induction comparable to 10 µg/ml and 1 µg/ml as seen in the functional analysis (Figure 12).

VIII.3.2. TBK1, IKK-ε and TRAF2 are part of the highly dynamic TLR3-associated Ripoptosome

As a next step, the formation and recruitment of a Ripoptosome, which could explain the seen cell death response after IAP antagonist, should be analyzed. Moreover, the time-dependent formation of the complex was dissected in order to clarify the optimal stimulation time for the TLR3-associated Ripoptosome formation. Hence, parental HaCaT and HeLa cells were prestimulated for one hour with IAP antagonist (Compound A). Additionally, zVAD-fmk was added, as this stabilizes the formation of caspase-8 containing complexes[100,144]. Thereafter, both cell lines (HeLa Figure 13A, HaCaT Figure 13B) were treated with the appropriate amount of poly (I:C). The cells were incubated for different periods of time followed by the precipitation of caspase-8 in order to monitor the time-dependent formation of the poly (I:C)-induced recruited Ripoptosome (Figure 13). Increased association of RIP1 and FADD with caspase-8 was found in a time-dependent manner in both cell lines. Additionally, RIP1 showed increasing phosphorylation at Serine 166 (S166), which is most probably due to clustering and autophosphorylation[152]. Interestingly, the newly identified components, TBK1, IKK-ε and TRAF2 were also part of the TLR3-associated Ripoptosome. Moreover, phosphorylated TBK1 and IKK-ε as well as TRAF2 (especially in HaCaT) cells, seem to reach their maximum of association with the complex at an earlier point of time between two and four hours (Figure 13A and 13B). These findings indicate that the formation and function of the TLR3-associated complex is rather dynamic and is changing over time. Especially the novel identified components; TBK1, IKK-ε and TRAF2 are associated at an earlier stage in complex formation and start to dissociate from the Ripoptosome four to six hours after the beginning of the poly (I:C) treatment. Altogether, these findings validate TBK1, IKK-ε and TRAF2 as novel Ripoptosome components. Furthermore, these findings indicate, that the above-described association of these proteins with caspase-8 complexes is a related

process and not an overexpression artifact of RIP1. Additionally, the formation of the TLR3-associated complex is not a linear process as some components reach their maximum of association at different points of time.

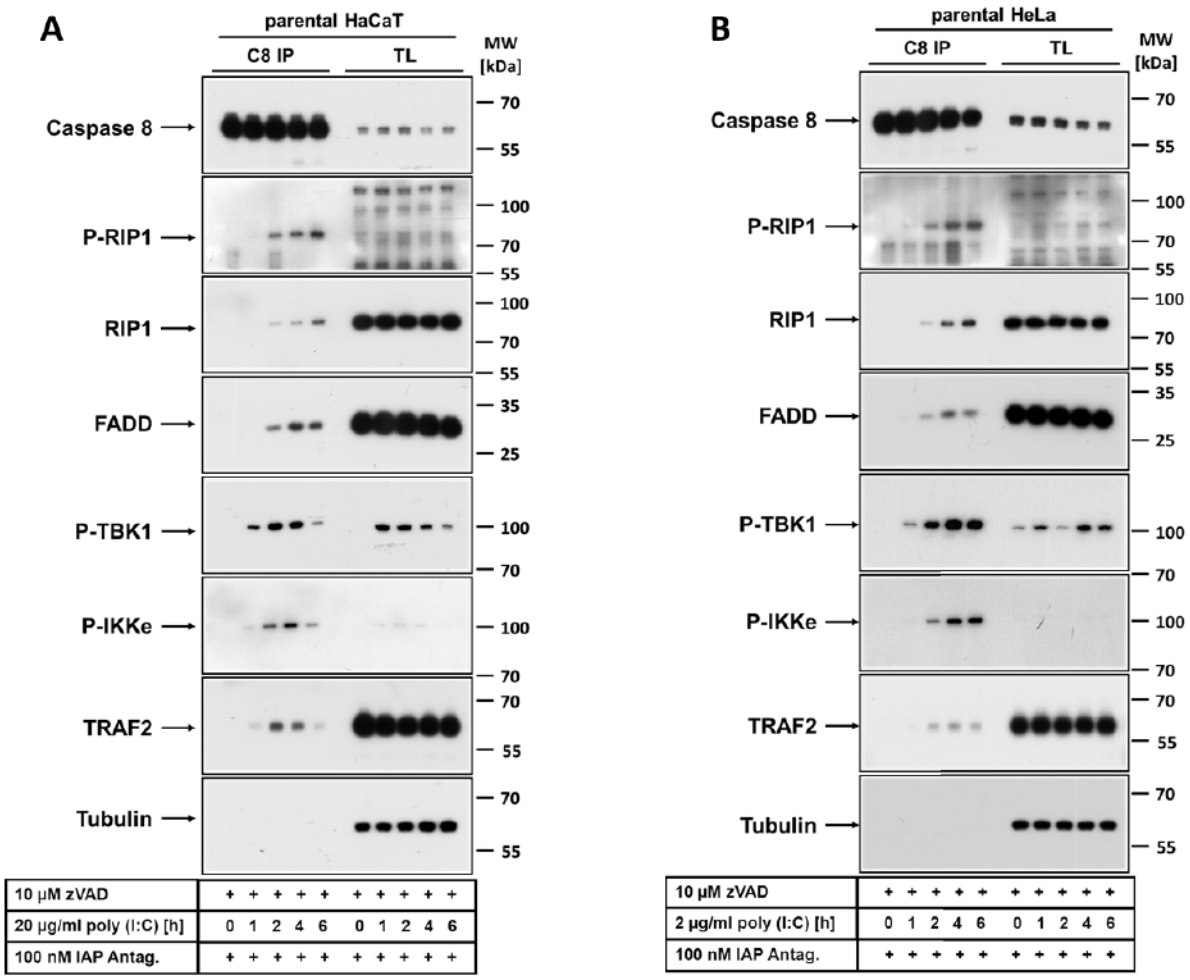

Figure 13 TBK1, IKK-ε and TRAF2 are part of the TLR3-associated complex in HaCaT and HeLa.
Parental HaCaT (A) and HeLa (B) cells were treated with 10 µM zVAD-fmk in combination with 100 nM IAP antagonist (Compound A) for 1 h, followed by incubation with respective amounts of poly (I:C) for the indicated points of time. Cellular lysates were generated using DISC-lysis buffer and caspase-8 and caspase-8-associated complexes were precipitated from 2 mg total cellular lysates. Bound proteins and total lysates were separated via SDS-PAGE. Finally, samples were analyzed via Western Blot analysis for expression of TBK1, IKK-ε, TRAF2 and other Ripoptosome-associated proteins.

In order to further validate the observed association of TBK1, IKK-ε and TRAF2 with caspase-8, Jurkat cells, representing a suspension T-lymphocyte cell line, were analyzed for their ability to form a TLR3 complex in comparison with HeLa cells. Therefore, the Jurkat cells were stimulated in line with the control HeLa cells with IAP antagonist (Compound A) followed by incubation with poly (I:C). The formed Ripoptosome was in general weaker than the complex detected in HeLa cells. The newly identified components were all precipitated

together with caspase-8 (Figure 14). Especially TBK1 was highly phosphorylated in the Jurkat cell line after the poly (I:C) stimulation. Furthermore, RIP3 was found to be part of the precipitated complex in Jurkat cells. In summary, HaCaT, HeLa and Jurkat cells, were all able to form a TLR3-associated Ripoptosome upon the combined treatment with poly (I:C) and IAP antagonist. In line with the RIP1-induced Ripoptosome, the TLR3-associated complex revealed TBK1, IKK-ε and TRAF2 as novel components of the Ripoptosome.

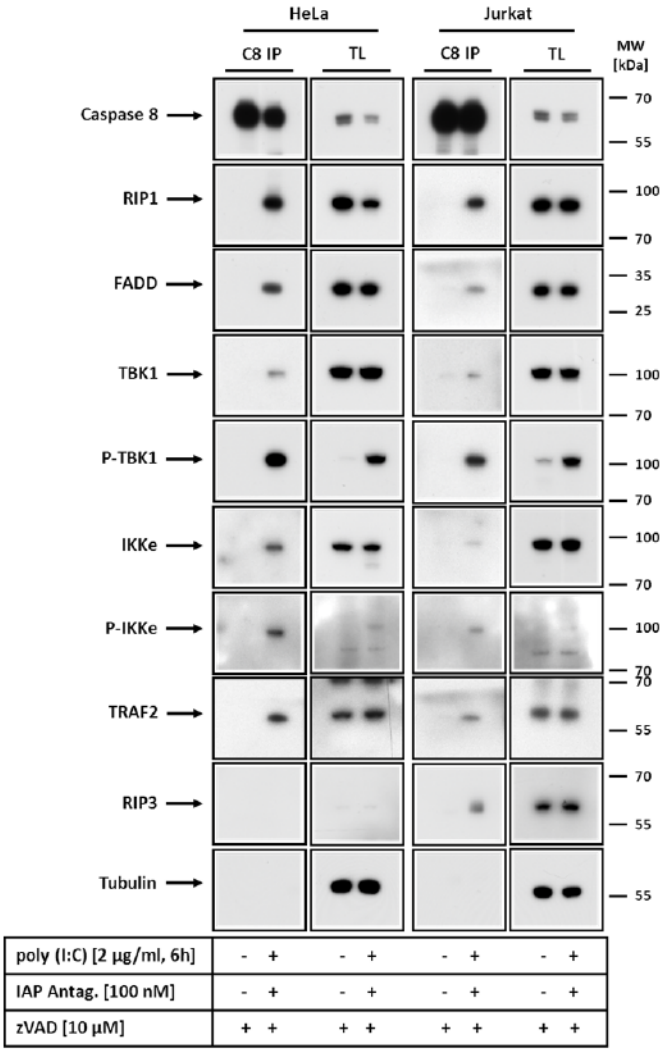

Figure 14 TBK1, IKK-ε and TRAF2 are part of the TLR3 complex in Jurkat cells.
Parental HeLa and Jurkat cells were prestimulated for 1 h with 100 nM IAP antagonist (Compound A) plus 10 µM zVAD-fmk or with zVAD alone. 2 µg/ml poly (I:C) was added to the cells for another 6 h, followed by lysis of the respective cell lines in DISC-lysis buffer. Caspase-8 and caspase-8-containing complexes were precipitated from 2 mg of total cellular lysates. The bound proteins were separated via SDS-PAGE and Ripoptosome components were visualized by Western Blot analysis.

VIII.3.3. TLR3-associated Ripoptosome formation is RIP1-dependent

As previously described, RIP1 is the central component of the Ripoptosome and RIP1-induced complex formation was highly dependent on the kinase activity. For the TLR3-associated complex, RIP1 was shown to act upstream of FADD[163]. After TLR3 stimulation, the adaptor molecule TRIF is recruited to the receptor. Thereafter, RIP1 can bind to TRIF via its RHIM domain. RIP1 can now act as an adaptor for the recruitment of FADD and caspase-8, thereby enabling Ripoptosome formation and linking this complex to the TLR3 receptor[164]. In order to clarify whether RIP1 is crucial for TLR3-related cell death, Ripoptosome formation as well as activation of TBK1 and IKK-ε, HeLa knockout cell lines were generated. Therefore, parental HeLa cells were transfected with the CRISPR/Cas9 system containing a gRNA targeting RIP1 as described in the material and method section. After single cell selection, two clones were identified and used for further experiments.

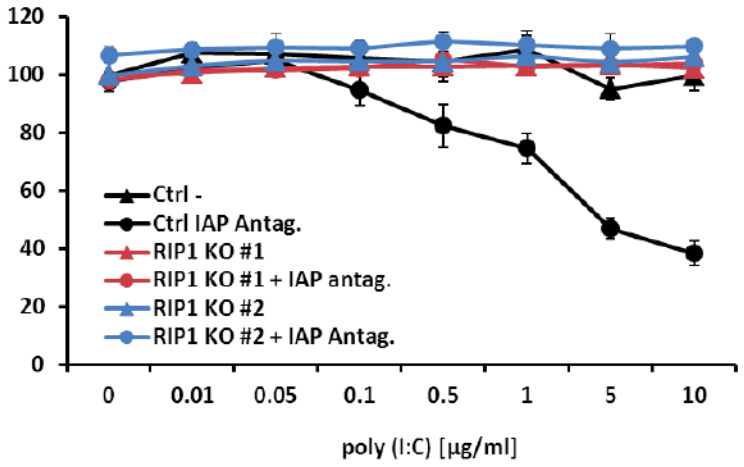

Figure 15 Loss of RIP1 blocks poly (I:C)-induced cell death in the absence of cIAPs.
RIP1 deficient and control HeLa cells were incubated with 100 nM IAP antagonist (Compound A) followed by incubation with different concentrations of poly (I:C) for 20 h. Cell attachment was analyzed by crystal violet staining. The shown data display the mean values ± SEM of three independent experiments.

When treated with IAP antagonist and poly (I:C), both cell lines showed a complete inhibition of cell death, whereas the control cells died with increasing concentrations of poly (I:C) (Figure 15). When the association of complex components with caspase-8 was analyzed, the RIP1 deficient cells showed a total inhibition of complex formation (Figure 16). Moreover, caspase-8 and cFLIP cleavage was only observed when RIP1 was present. Surprisingly, phosphorylation of IKK-ε was massively decreased when RIP1 was absent, whereas the phosphorylation of TBK1 seemed to be unaffected.

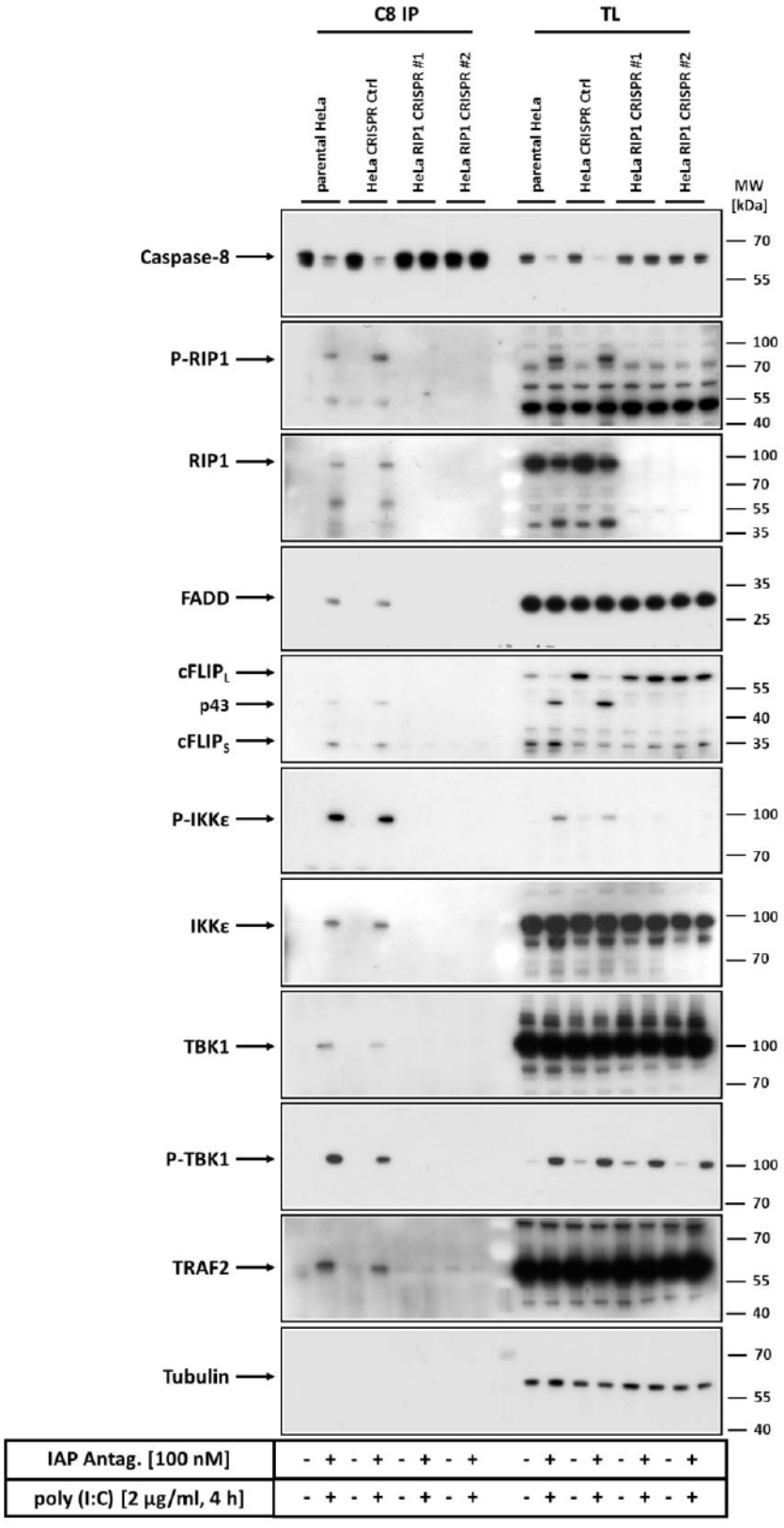

Figure 16 RIP1 knockout blocks TLR3-associated Ripoptosome formation.
RIP1 deficient, control and parental HeLa cells were prestimulated with 100 nM IAP antagonist, followed by a 4 h incubation with 2 µg/ml poly (I:C). Cells were lysed in DISC-lysis buffer and caspase-8 was precipitated from 2 mg total cellular lysates. Bound proteins and total lysates were separated via SDS-PAGE and Ripoptosome components were analyzed by Western Blotting.

That was rather unexpected, as TBK1 and IKK-ε were reported to be activated by the direct binding to TRIF upon TLR3 stimulation, meaning that RIP1 is not necessary for the phosphorylation of the non-canonical IKKs[105]. However, in the shown HeLa knockout system this was only observed for TBK1. The phosphorylation of IKK-ε is massively dependent on RIP1. Altogether, these data confirmed that RIP1 is indispensable for IAP antagonist and poly (I:C)-induced Ripoptosome formation and cell death induction. Surprisingly, loss of RIP1 showed a severe effect on the activation of IKK-ε, whereas TBK1 phosphorylation was not altered.

VIII.3.4. TBK1, IKK-ε and TRAF2 are components of the TNF complex II

As mentioned in the introduction, binding of TNF to the TNFR1 induces the intracellular formation of the TNF complex I, whose main function is the induction of inflammatory and pro-survival genes via NF-κB[54]. However, under certain cellular conditions, e.g. the depletion of cIAPs, this receptor bound complex can dissociate into the cytosol to form the TNF complex II. This complex possesses the ability to induce cell death via caspase activation or Necrosome formation[80]. Remarkably, there is still an ongoing debate whether TNF complex II, which is only observed under depleted cIAP level, is a Ripoptosome-like complex that is stabilized and increased through the additional TNF stimulation. However, in the following section the association of the newly identified proteins TBK1, IKK-ε and TRAF2 with TNF signaling complex II should be analyzed, in line with the RIP1-induced Ripoptosome and the TLR3-associated complex. Thereby the combined treatment of the poly (I:C) and IAP antagonist was used as a control for complex formation. Additionally, the impact of Etoposide treatment in respect to complex formation should be analyzed. The group of Pascal Meier showed that genotoxic stress, simulated by Etoposides, could also induce the association of caspase-8 with Ripoptosome components due to depletion of cellular cIAP level[144]. Therefore, HaCaT cells were prestimulated with IAP antagonist (Compound A) in combination with zVAD-fmk or with zVAD-fmk alone for one hour. Thereafter, cells were stimulation with TNF, poly (I:C) or Etoposides for six hours. Cells stimulated with Etoposides showed no formation of a caspase-8 associated complex (Figure 17). The group of Pascal Meier showed that substantial complex formation in line with cIAP depletion is reached after a twenty-four hour Etoposide treatment[144]. Therefore, the six-hour incubation time was most probably too short for the depletion of the cellular IAP levels. Cells treated with IAP antagonist in combination with TNF showed, in line with the data of the RIP1-induced Ripoptosome, that TBK1, IKK-ε and TRAF2 were associated with caspase-8 (Figure 17). The non-canonical IKKs again were phosphorylated and the activated state was enriched in the precipitated fractions (IP). Moreover, the precipitated proteins were analyzed for TRADD,

which is the classical adaptor for TNF complex I and is also associated with the cytosolic TNF complex II. However, some reports also highlighted a role for TRADD in TLR3 signaling, as knockout cells were resistant to TLR3-induced toxicity[165,166]. The now precipitated complexes, clearly show that TRADD is associated with the poly (I:C)-induced, TLR3 bound Ripoptosome (Figure 17, IP) and TNF complex II. Taken together, these data highlight the association of TBK1, IKK-ε and TRAF2 with TNF complex II. Moreover, TRADD is part of the TLR3-bound Ripoptosome. Based on these results, there were no observed differences in TNF complex II and the TLR3-associated Ripoptosome.

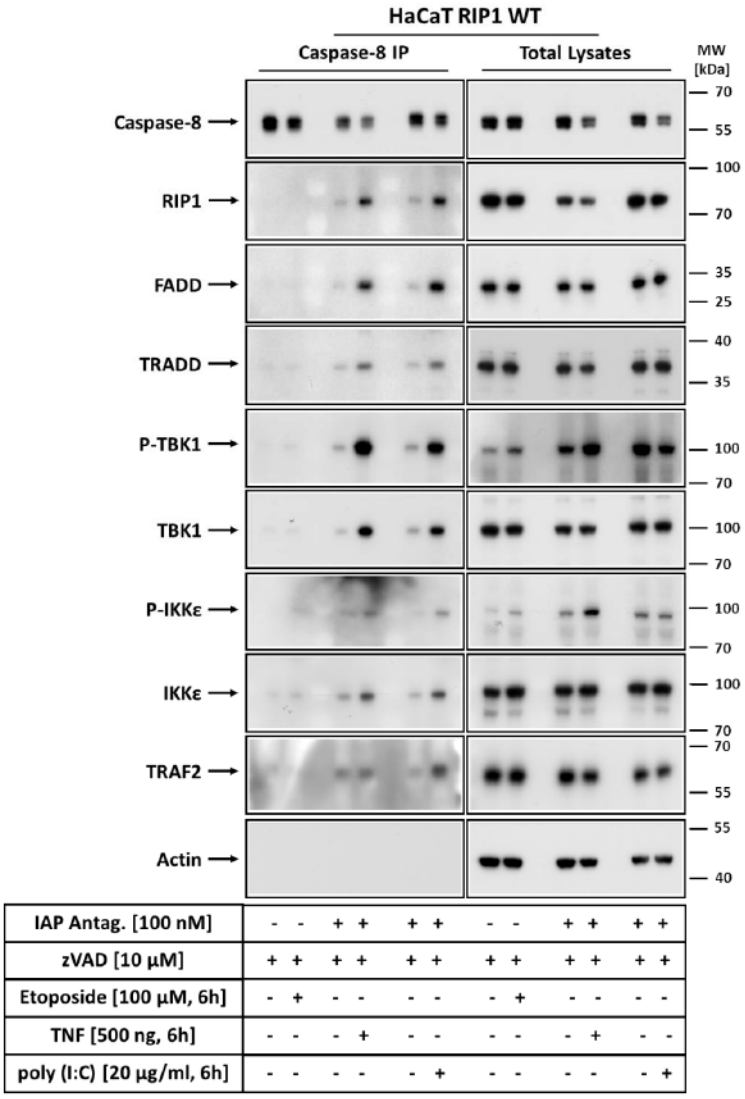

Figure 17 Comparison of TNF complex II and TLR3-associated Ripoptosome.
HaCaT RIP1 WT cells were prestimulated for 1 h with 100 nM IAP antagonist (Compound A) plus 10 µM zVAD-fmk or with zVAD-fmk alone. 500 ng TNF-HF, 100 µM Etoposides or 20 µg/ml poly (I:C) was added to the cells for another 6 h, followed by lysis of the respective cell lines. Caspase-8 and caspase-8-associated complexes were precipitated from 2 mg of total cellular lysates. Bound proteins and total lysates were separated by SDS-PAGE. Ripoptosome components were assayed by Western Blot analysis.

VIII.4. TBK1 and IKK-ε do not influence cell death but loss of TRAF2 sensitizes to PCD

The above-shown experiments clearly identified TBK, IKK-ε and TRAF2 as novel components of the Ripoptosome as well as TNF complex II. However, the tasks of these proteins in this signaling complex remained to be elusive. As the Ripoptosome is able to induce apoptosis as well as necroptosis, the impact of the novel components in respect to cell death responses were analyzed.

VIII.4.1. TRAF2 inhibits cell death upon RIP1 expression

The E3-ubiquitin ligase TRAF2 is long time known for its essential function in TNF complex I mediated NF-κB activation[77,167,168]. However, recent studies also highlighted that TRAF2 inhibits CD95L- and TNF-induced cell death[169,170]. As TRAF2 is clearly associated with the Ripoptosome, the impact of cell death was analyzed, using the RIP1 expressing HaCaT cells. In line with the above mentioned experiments, HaCaT RIP1 WT cells were transfected with different siRNAs targeting TRAF2 (Figure 18A). The siRNAs 4, 6 and 7 showed a substantial reduction in the TRAF2 protein level (Figure 18A) when compared to the scrambled control siRNA (Ctrl siRNA). The best working siRNAs (TRAF2 siRNA 4, 6, 7) were pooled for further experiments in order to reduce the off-target effect of single siRNAs. HaCaT cells transfected with the TRAF2 siRNA pool showed substantial knockdown of the target protein, comparable to the TBK1 and IKK-ε siRNAs described in the next section (Figure 18B). Next, the influence of reduced TRAF2 expression on cell death responses was analyzed by crystal violet assays. Therefore, HaCaT RIP1 WT cells were transfected with control siRNA (Ctrl siRNA) and the TRAF2 siRNA pool. Three days after transfection, cells were stimulated with zVAD-fmk and Nec-1, in order to clarify whether an effect of TRAF2 reduction can be unmasked by caspase inhibition or block of RIP1 kinase function. Thereafter, cells were incubated with different concentrations of 4-HT for twenty hours. Interestingly, the TRAF2 knockdown sensitized the HaCaT RIP1 WT cells against cell death induced by low amounts (1nM) of 4-HT (Figure 18C). Surprisingly, under conditions where caspase activity was blocked by zVAD-fmk, the knockdown showed no difference in cell attachment compared to the Ctrl siRNA treated cells. These findings implicated that the observed phenotype was rather due to changes in the apoptotic signaling pathway. This was further confirmed by the fact, that the addition of Nec-1 showed again a sensitization against RIP1-induced cell death in the cells treated with TRAF2 siRNA (Figure 18C, red bars). As expected, when apoptotic and necroptotic cell death was blocked by the combination of the

caspase inhibitor zVAD-fmk and the RIP1 inhibitor Nec-1, no difference between the Ctrl sample and the TRAF2 knockdown was observed for cell death induction. Altogether, these data indicate that TRAF2 inhibits RIP1-induced apoptotic cell death. In contrast, the caspase-independent necroptotic cell death response is not influenced by the reduction of TRAF2 protein level.

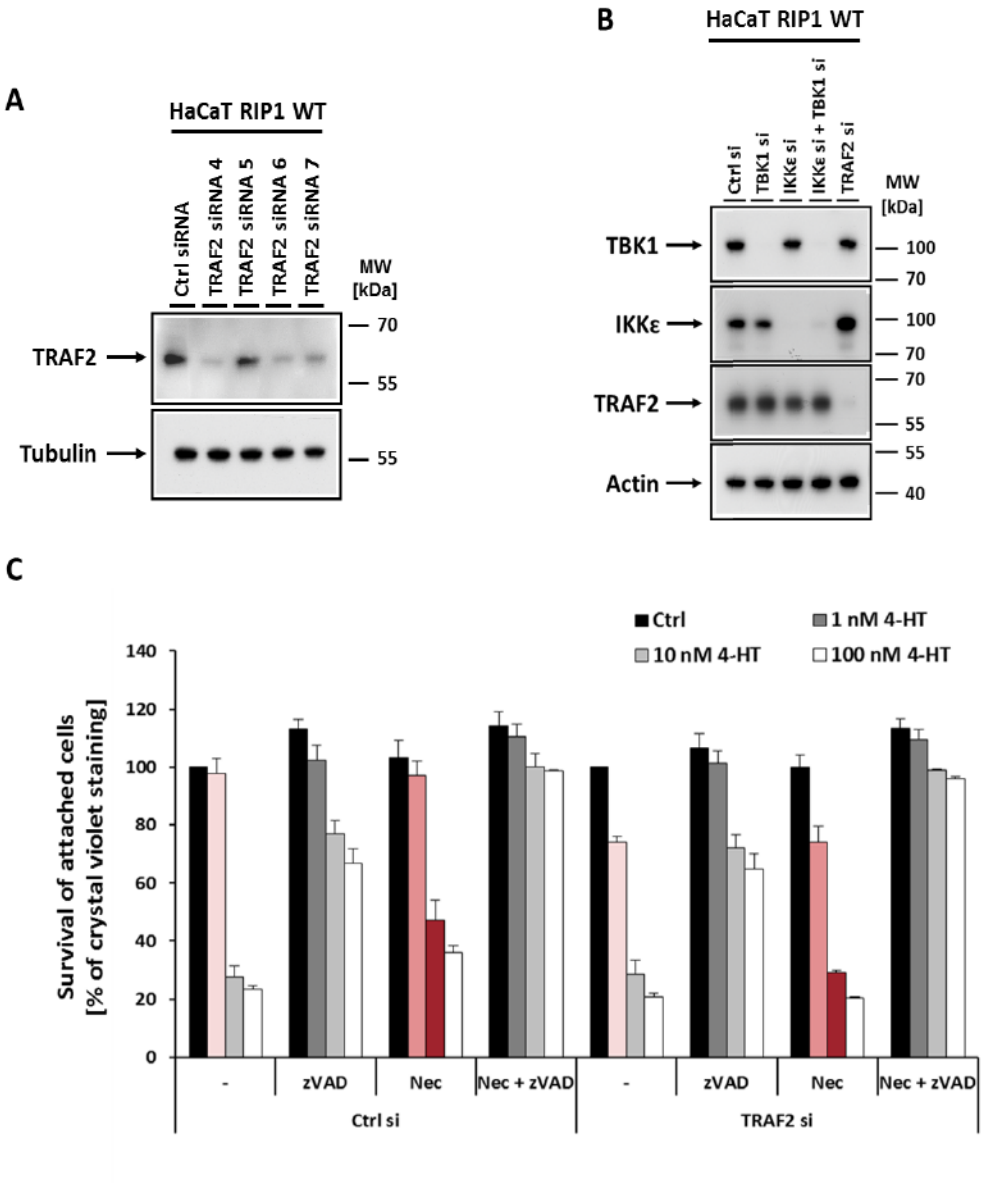

Figure 18 TRAF2 knockdown sensitizes HaCaT cells to apoptotic cell death.
HaCaT RIP1 WT cells were transfected with 5 nmol of control siRNA (Ctrl siRNA) and different TRAF2 siRNAs. (A) Knockdown efficiency was monitored 72 h after transfection via Western Blot analysis. (B) HaCaT RIP1 WT cells were transfected with Ctrl siRNA and the respective siRNA pools for TBK1, IKK-ε and TRAF2 (siRNA 4, 6, 7). Cellular lysates were analyzed for expression of the indicated proteins via Western Blot, 72 h after transfection. (C) Cell death responses were analyzed by addition of 1 nM, 10 nM and 100 nM 4-HT in the presence of zVAD-fmk (10 µM) and Nec-1 (50 µM), 72 h after transfection. After 20 h of stimulation cell attachment was analyzed by crystal violet staining. The shown bars display the mean values ± SEM of three independent experiments.

VIII.4.2. TBK1 and IKK-ε do not influence cell death signaling in RIP1 overexpressing cells

After the encouraging finding that TRAF2 knockdown sensitized against RIP1-induced apoptosis, the influence of TBK1 and IKK-ε on PCD was assessed. Therefore, different siRNAs were tested for the ability to deplete TBK1 and IKK-ε protein levels in HaCaT RIP1 WT cells. Three days after the transfection, knockdown efficiency was monitored by Western Blot analysis. Cells treated with the TBK1 siRNAs A, B, D and the IKK-ε siRNAs B, C, D showed a substantial decrease of the target protein level (Figure 19A and 19B). In line with the TRAF2 siRNAs, a pool of the best working siRNAs (namely TBK1 A, B, D and IKK-ε B, C, D) was generated to reduce off-target effects of single siRNAs.

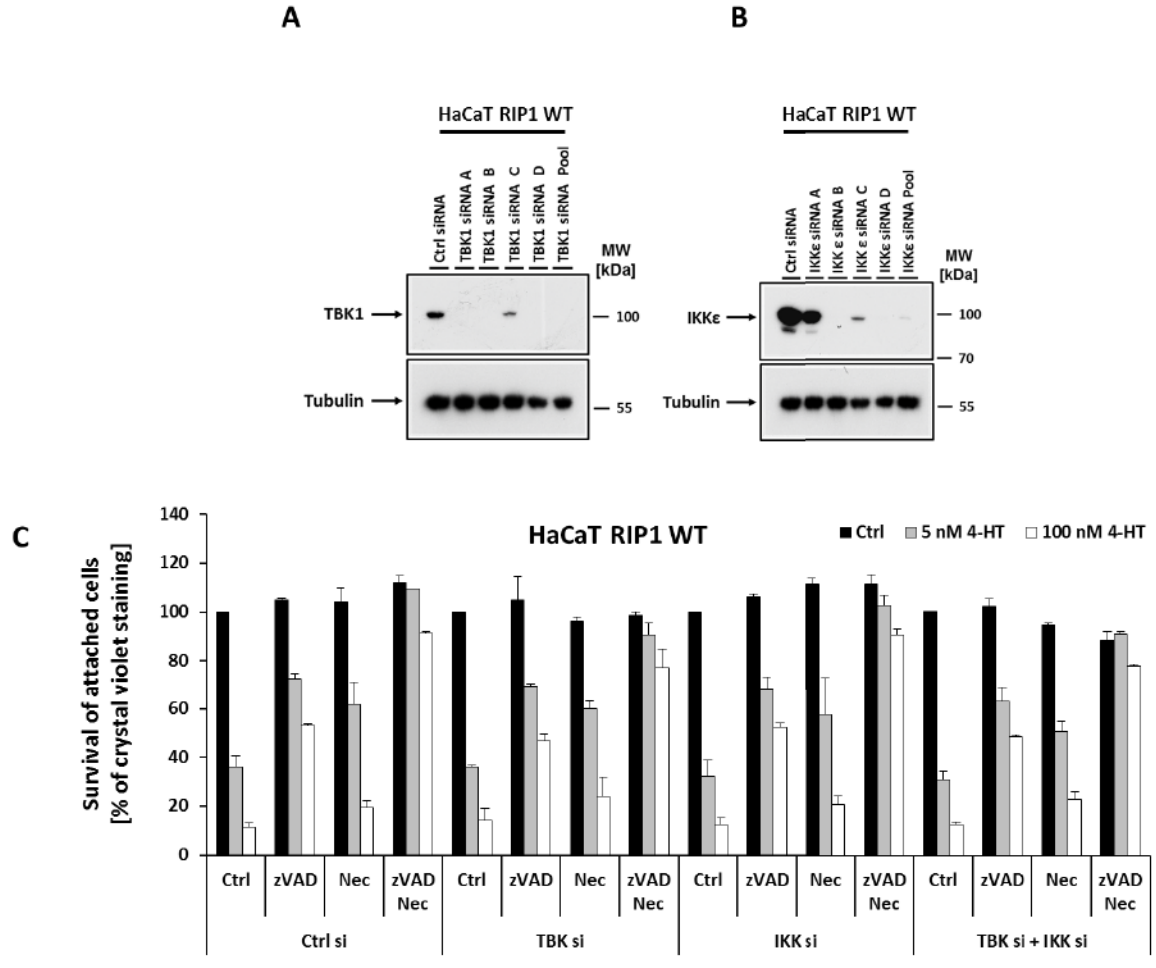

Figure 19 TBK1 and IKK-ε are not of relevance for RIP1-mediated cell death responses in HaCaT cells.
HaCaT RIP1 WT cells were transfected with 5 nmol Ctrl, TBK1 (A) and IKK-ε (B) siRNAs. Cellular lysates were analyzed 72 h after transfection via Western Blot analysis for the knockdown of the target proteins. (C) At the same time, cells were prestimulated with zVAD-fmk and Nec-1 for 1 h, followed by cell death induction via RIP1 expression with the addition of 5 nM and 100 nM 4-HT. After 20 h cell attachment was assayed by crystal violet staining. The bars represent the mean values ± SEM of three independent experiments.

Cells treated with TBK1 and IKK-ε or the combined siRNAs, showed significant reduction in the TBK1 and IKK-ε protein level (Figure 19B). In order to analyze the cell death dependency of TBK1 and IKK-ε, HaCaT RIP1 WT cells were transfected with the above mentioned siRNA pools. As previously described, the non-canonical IKKs can substitute for each other in respect of IRF3 phosphorylation. Hence, an additional, simultaneous knockdown of both kinases was performed. Therefore, siRNAs for TBK1 were also pooled with IKK-ε siRNAs in order to generate a double knockdown (Figure 19B). Finally, cellular execution was induced with the expression of RIP1, by the addition of different concentrations of 4-HT for twenty hours. Cell viability was visualized by crystal violet assay.

The Ctrl siRNA treated cells showed substantial cell death with increasing concentrations of 4-HT, equaling increasing RIP1 expression. The addition of the caspase inhibitor zVAD-fmk could rescue up to 50% of the cells. The remaining cell death was observed, because HaCaT cells are able to undergo necroptosis. In contrast, the RIP1 inhibitor Nec-1 had only a minor effect, especially on high concentrations of 4-HT (100 nM). As expected, the combination of both inhibitors blocked cell death completely. However, when compared to the control siRNA treated cells, TBK1, IKK-ε or the combined knockdown had no effect on the cell death response due to the expression of RIP1 (Figure 19C).

In summary, substantial reduction in TBK1 and IKK-ε protein level had no influence on the cell death responses carried out by the overexpression of RIP1.

VIII.5. The loss of TBK1, IKK-ε or TRAF2 does not influence Ripoptosome formation

As shown for RIP1 in TLR3 signaling, the loss of single components can suppress the formation of the Ripoptosome and, therefore, RIP1-dependent cell death responses. To analyze the impact of the newly identified components on complex formation, HeLa cell lines deficient for TRAF2, TBK1, IKK-ε and the combination of both IKKs were generated using the CRISPR/Cas9 technology as described in the material and methods section. Two clones, positive for the knockout of the target gene were analyzed in the following experiments. The protein level of the integral Ripoptosome components; caspase-8, FADD, RIP1, cFLIP, TBK1, IKK-ε and TRAF2, as well as the necroptotic relevant pseudokinase MLKL were not altered by the knockout of TBK1, IKK-ε or TRAF2 (Figure 20).

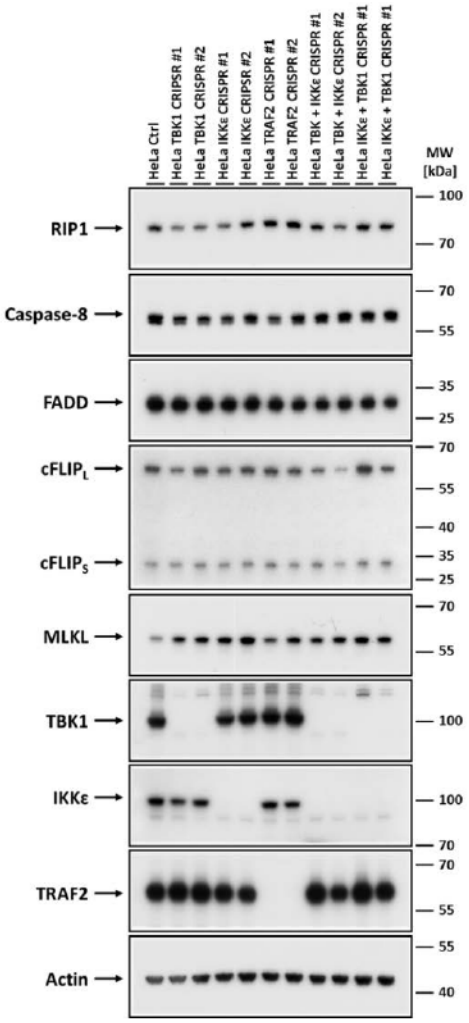

Figure 20 Expression of PCD involved proteins in TBK1, IKK-ε and TRAF2 knockout HeLa cell lines.
Parental HeLa cells were transfected with CRISPR/Cas9 plasmids containing TBK1, IKK-ε and TRAF2 specific gRNAs. Selected single cell knockout clones were lysed in DISC-lysis buffer and PCD involved proteins were visualized by Western Blot analysis.

When the cells were treated with IAP antagonist plus TNF or poly (I:C), the TBK1/IKK-ε double knockout cell line showed no significant alteration in their cell death response when compared to the control cell line (Figure 21). The TRAF2 knockout clones, showed a clear sensitization against the combined treatment of IAP antagonist plus TNF or poly (I:C). This again shows that TRAF2 inhibits cell death induction (Figure 21).

Ripoptosome formation in these cell lines was induced with the combined treatment of IAP antagonist and poly (I:C). For the TBK1/IKK-ε double knockout, two additional clones were analyzed. These additional clones (IKK-ε/TBK KO) were generated vice versa, meaning that IKK-ε knockout cells were transfected with a TBK1 CRISPR construct, in order to rule out clonal selection effects. All knockout cell lines showed substantial formation of the Ripoptosome (Figure 22A).

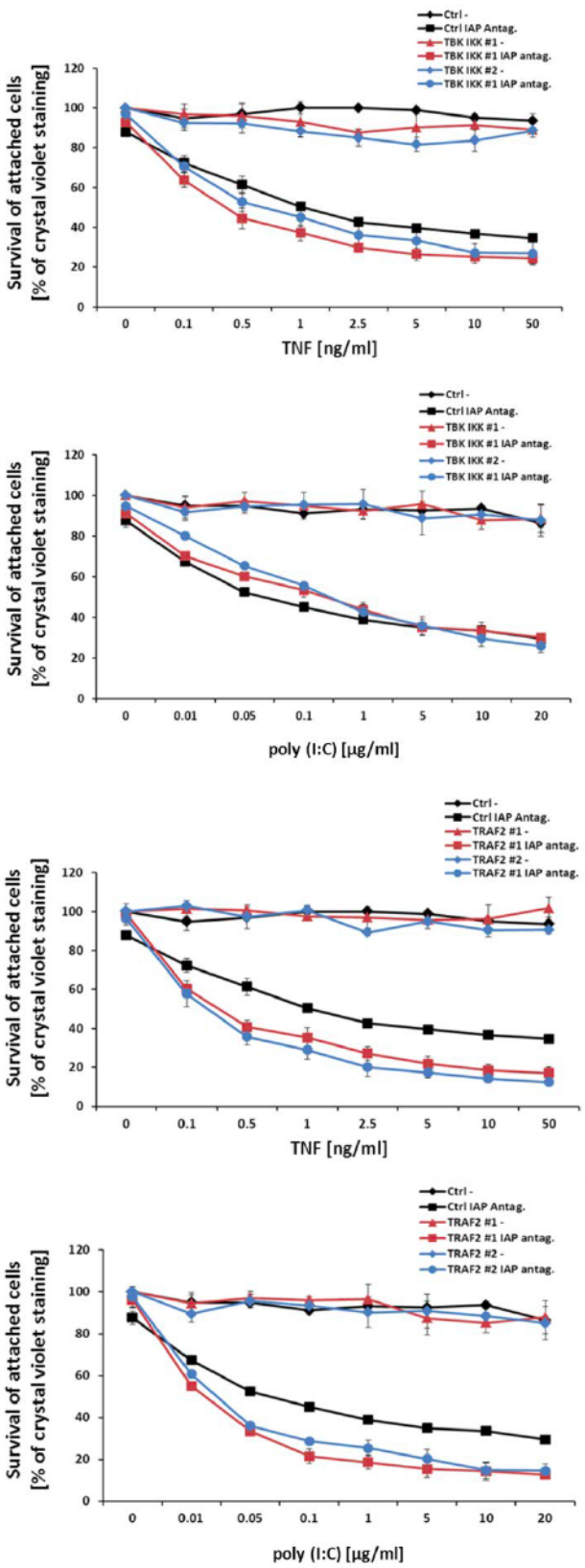

Figure 21 Characterization of TBK1, IKK-ε and TRAF2 CRISPR/Cas9 knockout HeLa cell lines in respect to TNF- or poly (I:C)-induced cell death.

Selected knockout clones were prestimulated with 100 nM IAP antagonist (Compound A), followed by stimulation with different concentrations of TNF-HF or poly (I:C) for 20 h. Cell attachment was monitored by crystal violet staining. The shown graphs display the mean values ± SEM of three independent experiments.

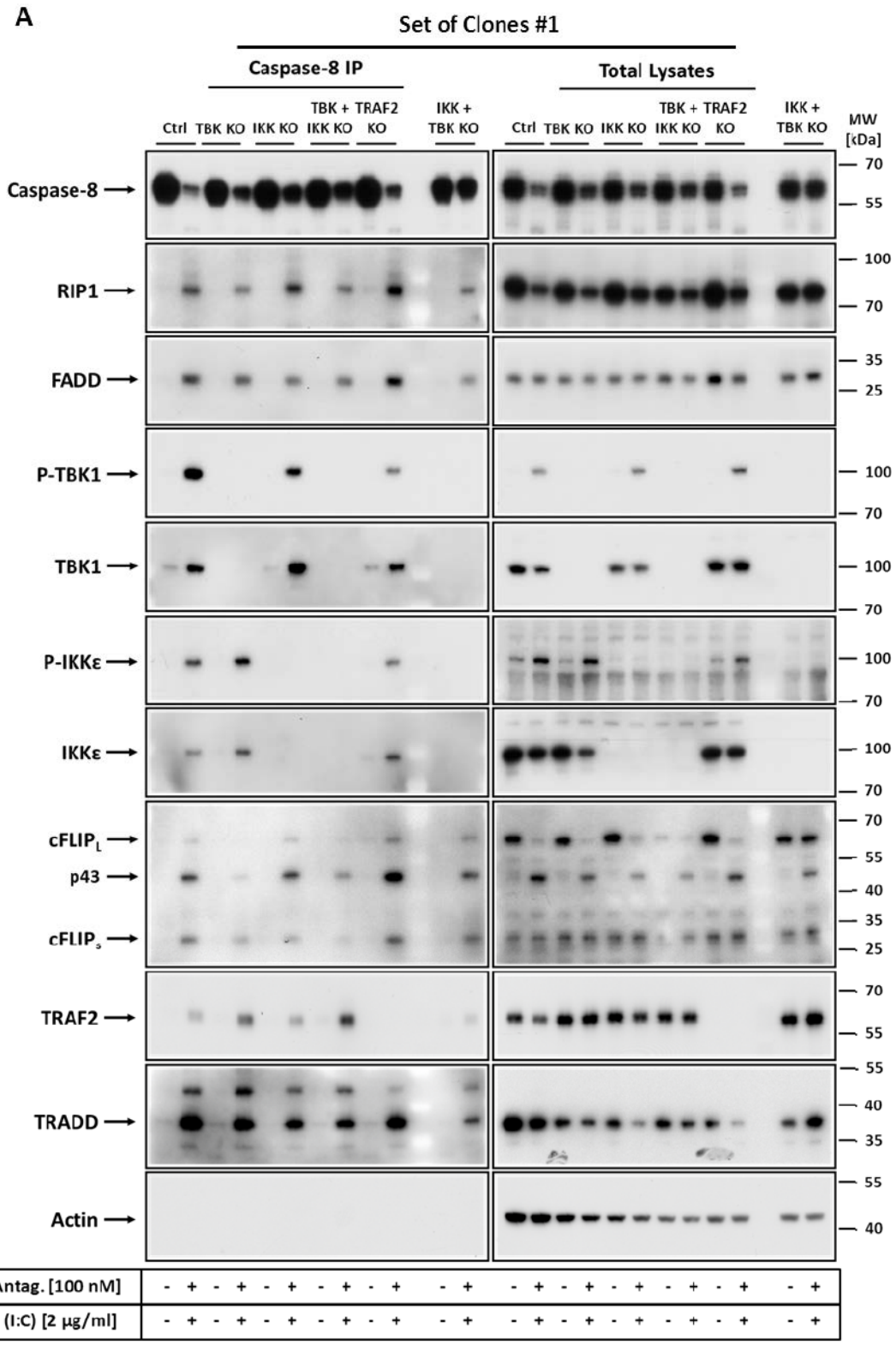

Figure 22A TBK1, IKK-ε and TRAF2 are not required for poly (I:C)-induced Ripoptosome formation.
HeLa knockout cell lines were prestimulated for 1 h with 100 nM IAP antagonist (Compound A), followed by addition of 2 µg/ml poly (I:C) for another 6 h. Caspase-8 and caspase-8-associated complexes were precipitated from 2 mg of total cellular lysates. Bound proteins and total lysates were analyzed by SDS-PAGE and Ripoptosome components were visualized by Western Blot analysis.

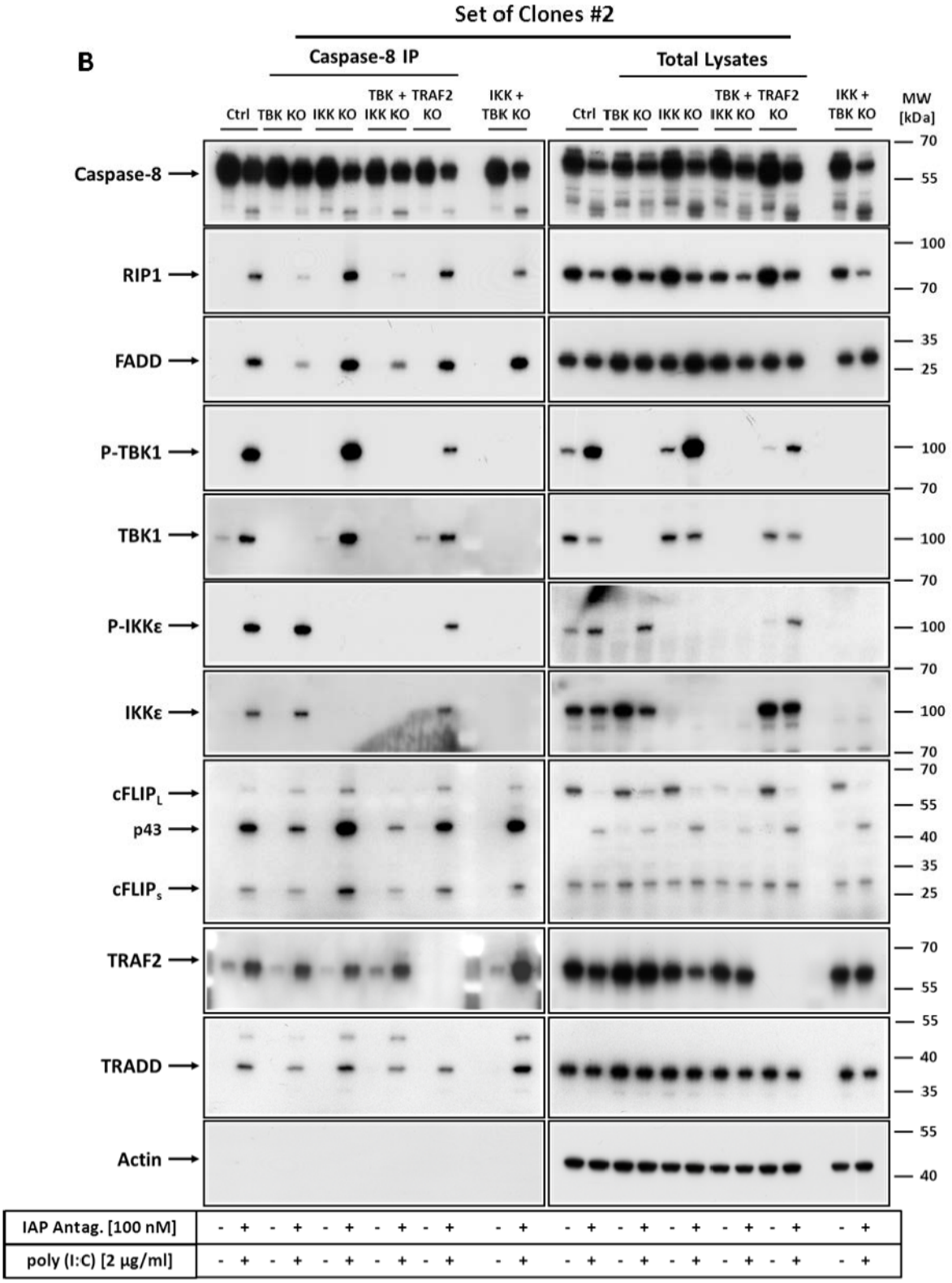

Figure 22B TBK1, IKK-ε and TRAF2 are not required for poly (I:C)-induced Ripoptosome formation.
The shown figure displays the result of the analysis of the second set of the respective TBK1, IKK-e and TRAF2 knockout clones. Cells were treated and analyzed as described in Figure 22A.

The adaptor molecule TRADD was precipitated in all knockout cells together with caspase-8 upon IAP antagonist and poly (I:C) treatment. Surprisingly, loss of TBK1, seemed to result in a lesser recruitment of components like cFLIP or RIP1 to the complex, when compared to the control or other knockout cells (Figure 22A). Interestingly, TRAF2 seems to behave the other way around. When TBK1 is lacking, TRAF2 is enriched in the precipitated complex. However, in the second set of clones, this was not true for the IKK-ε/TBK1 KO cell line (Figure 22B), which might be explained by clonal selection processes. Summarized, these data again highlight that TRADD is also part of the TLR3-associated Ripoptosome. Although, loss of the newly identified components TBK1, IKK-ε or TRAF2 did not inhibit Ripoptosome formation, lack of TBK1 seemed to change the stoichiometric composition of the complex. Both, cFLIP and RIP1 are recruited to a lesser extent, whereas TRAF2 is enriched in the caspase-8 precipitated fractions. These findings indicate that TBK1 might stabilize the binding of cFLIP and RIP1 with caspase-8, thereby competing with TRAF2 association.

VIII.6. Ripoptosome formation induces expression of NF-κB target genes

TRAF2 was already known to be involved in the cell death execution induced by CD95L or TNF[169,170]. Additionally, the above shown results highlight the role of TRAF2 in inhibiting poly (I:C)- and RIP1-induced apoptotic cell death responses. However, the role of TBK1 and IKK-ε in Ripoptosome-mediated signaling still remained to be elusive. As both proteins are known to interact and activate proteins of the NF-κB pathway, the gene inductive properties of the Ripoptosome were analyzed. Hence, RIP1 expressing HaCaT cells were stimulated with 4-HT and poly (I:C) in combination with IAP antagonist for several points of time (Figure 23).

When Ripoptosome formation was induced with 4-HT-mediated RIP1 expression, TBK1 and IKK-ε became phosphorylated five hours after stimulation, in line with the expression of the kinase RIP1 (Figure 23A). Moreover, a phosphorylation of MLKL was observed, indicating the induction of necroptosis. Interestingly, the phosphorylation of IκB-α as well as p65 became visible at the same points of time (Figure 23A). The protein levels of the non-canonical p100/p52 NF-κB proteins were not altered. Additionally, the transcription factor IRF3 was not activated after RIP1 expression (Figure 23A). In total, these data show that the expression of RIP1 induces the activation of the canonical NF-κB pathway, but interferon responses carried out by the transcription factor IRF3 are not observed upon RIP1-induced Ripoptosome formation.

When stimulated with the TLR3 antagonist poly (I:C), TBK1 and IKK-ε were subsequently activated after one hour and remained their phosphorylation status over time (Figure 23B). The phosphorylation of IκB-α started also one hour after stimulation and increased with the time of poly (I:C) treatment. In contrast, the activation of p65 reached a maximum between one and three hours after the start of the stimulation (Figure 23A). Furthermore, the non-canonical NF-κB p100 was cleaved into its functional p52 fragment. This effect was expected, as the depletion of cIAP level by IAP antagonists is known to stabilize NIK and thereby activates the non-canonical NF-κB pathway[171].

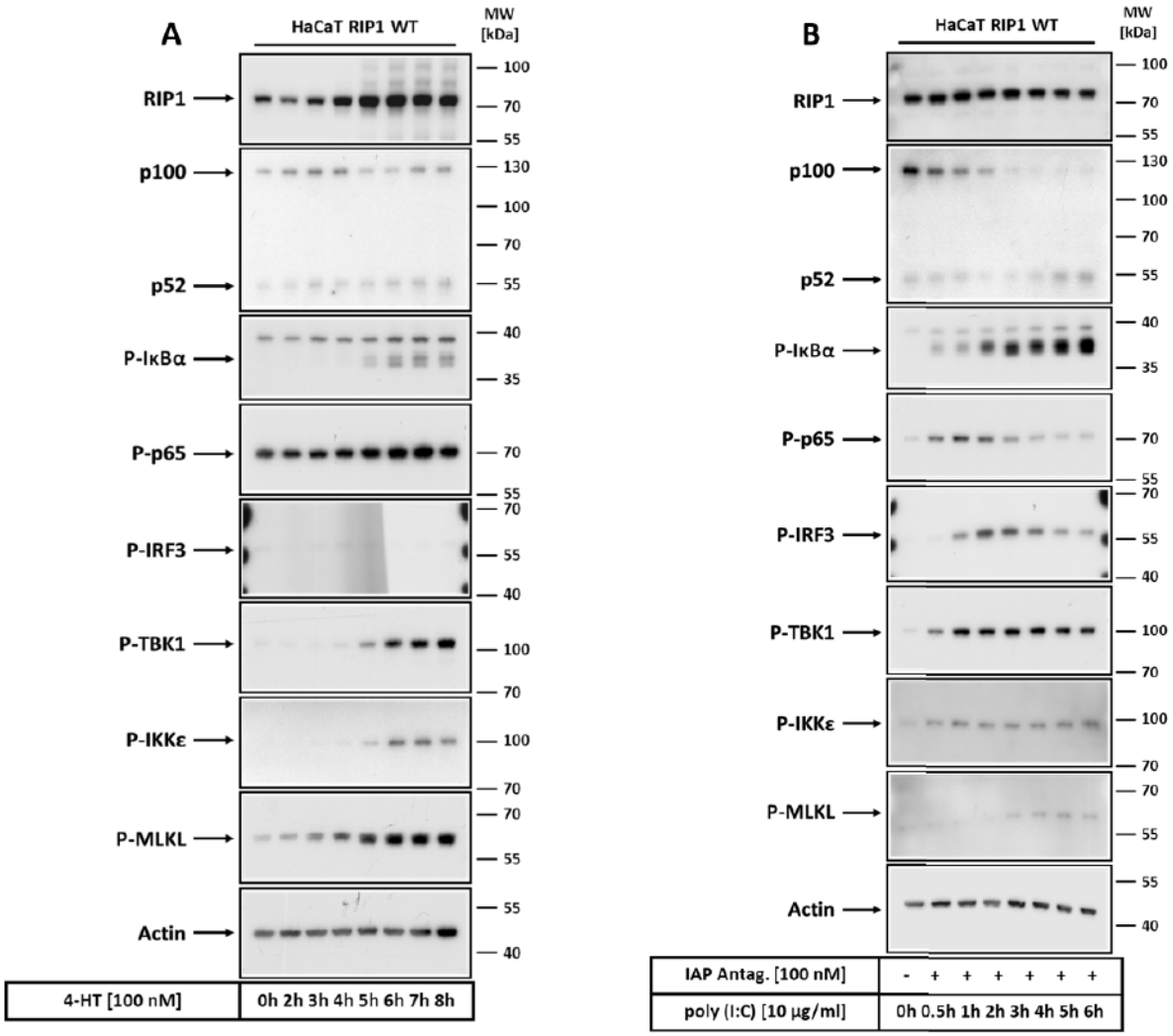

Figure 23 Ripoptosome activity induces the activation of NF-κB.
HaCaT RIP1 WT cells were starved 3 h in DMEM medium without FCS in order to reduce basal NF-κB activation through components of the FCS. (A) For the induction of RIP1, the cells were then stimulated with 100 nM 4-HT for the indicated time. (B) Additionally, HaCaT RIP1 WT cells were prestimulated 1 h with 100 nM IAP antagonist (Compound A), followed by stimulation with 10 µg/ml poly (I:C) for the indicated points of time. Cellular lysates were analyzed via SDS-PAGE and Western Blotting. Lysates were assessed for protein components of the Ripoptosome, the NF-κB signaling pathway as well as the transcription factor IRF3.

Additionally, the IRF3 transcription factor became highly phosphorylated two to three hours after the start of the treatment, showing the TLR3-dependent production of Type I interferons[106,172] (Figure 23B). In summary, the poly (I:C) data showed, that there is an early, Ripoptosome-independent NF-κB response between one and three hours, in line with the activation of IRF3. However, a secondary, canonical NF-κB response is shown by the increasing phosphorylation of IκB-α.

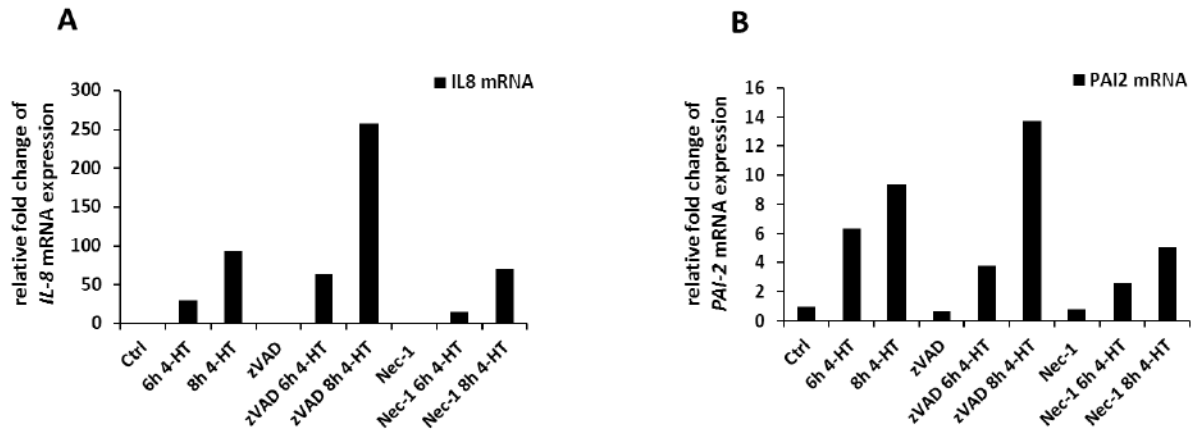

Figure 24 mRNA expression of *IL-8* and *PAI-2* are upregulated after RIP1 overexpression.
HaCaT RIP1 WT cells were starved 3 h in DMEM medium without FCS, in order to reduce the FCS induced NF-κB activation. Cells were prestimulated 1 h with 10 µM zVAD-fmk or 50 µM Nec-1 followed by addition of 100 nM 4-HT for 6 or 8 hrs. The isolated mRNA from each sample was probed for *IL-8* (**A**) and *PAI-2* (**B**) by qPCR. *GAPDH* was used as a housekeeping control gene.

To clarify whether the observed NF-κB induction results in the upregulation of specific target genes, mRNA level were analyzed over time via qPCR. Therefore, HaCaT RIP1 WT cells were stimulated with Nec-1 and zVAD-fmk, as the impact of RIP1 kinase activity on mRNA regulation should be analyzed and the caspase inhibitor is known to further increase complex-mediated gene induction[117]. After an one hour incubation with the respective inhibitor, RIP1 expression was induced by the addition of 4-HT for the indicated points of time. After the incubation, cellular RNA was isolated and probed for the NF-κB target genes *IL-8* (Interleukin-8, also CXCL8) and *PAI-2* (the plasminogen activator inhibitor-2, also *SERPINB2*) (Figure 24). *IL-8* is one of the classical NF-κB targets[138,173,174]. The upregulation and secretion of the IL-8 protein is often seen during stress responses, leading to the induction of inflammatory processes[173]. Additionally, the regulation of *PAI-2* was analyzed, as the upregulation of this protein was shown to play a major role in inhibiting TNF-induced apoptosis. This is carried out by the stabilization of transglutaminase 2 (TG2), which limits procaspase-3 activation[175]. Moreover, the induction of *PAI-2* was shown to be dependent on

TBK1 when stimulated with TNF[175]. Interestingly, both mRNA level were upregulated over time in line with the expression of RIP1. As expected, the addition of zVAD-fmk, further increased the upregulation of the target genes. In contrast, the stimulation with Nec-1 reduced NF-κB-dependent gene induction (Figure 24). This shows, in line with the biochemical complex analysis, that RIP1 kinase activity is necessary for RIP1-induced Ripoptosome formation and thereby NF-κB activation.

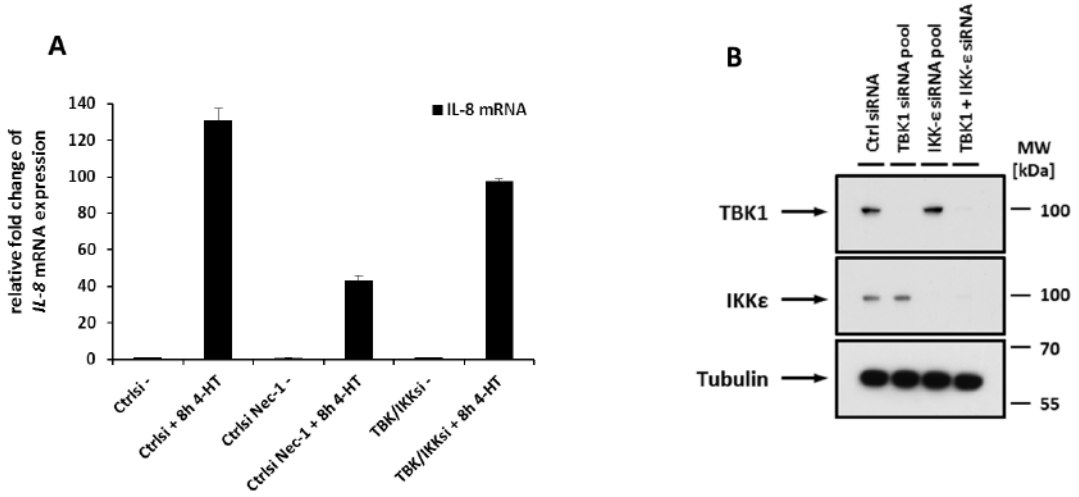

Figure 25 TBK1 and IKK-ε are required for *IL-8* mRNA induction upon RIP1 expression.
HaCaT RIP1 WT cells were transfected with 5 nmol control siRNA or 5 nmol of the combination of TBK1 and IKK-ε siRNA pools. After 72 h cells were starved 3 h in DMEM medium without FCS, to reduce basal NF-κB activation through FCS components. After the prestimulation with 10 µM zVAD-fmk or 50 µM Nec-1 for 1 h, 100 nM 4-HT was added. (**A**) 8 h after the stimulation RNA was isolated and analyzed via qPCR for *IL-8* and *PAI-2 mRNA* expression. *GAPDH* was used as a housekeeping control gene. The shown bars display the mean ± SEM of three independent experiments. (**B**) Knockdown of TBK1, IKK-ε and the combination was monitored through SDS-PAGE and via Western Blotting.

To analyze a broader subset of genes as well as to elucidate the impact of TBK1 and IKK-ε on the gene inductive properties of the Ripoptosome, micro array analyses of HaCaT RIP1 WT cells were performed. Therefore, cells were transfected with control siRNA or the combination of TBK1 and IKK-ε siRNAs in three independent experiments. Additionally, control siRNA treated cells were stimulated with the RIP1 inhibitor Nec-1, as kinase inhibition should result in a decrease of Ripoptosome-mediated gene expression as shown in Figure 24. Three days after transfection, cells were stimulated with 4-HT for eight hours to induce complex formation. Successful knockdown of the target proteins was monitored by Western Blot analysis and showed a substantial reduction of the target protein level (Figure 25B). Additionally, RNA was isolated and probed for *IL-8* induction by qPCR as a control. After RIP1 induction, *IL-8* was massively upregulated. The addition of Nec-1 could again reduce

the gene induction. The combined knockdown of TBK1 and IKK-ε was also able to decrease the *IL-8* induction about 25% (Figure 25A). In order to further evaluate these findings, mRNA expression of the three independent experiments was compared by micro array analysis for the whole genome RNA. Therefore, RNA expression was compared between the respective unstimulated control and 4-HT stimulated samples. The array analysis was kindly performed by the lab of Dr. Martin Sprick from Hi-STEM at the DKFZ and by the DKFZ genomics and proteomics core facility.

Table 12 Micro Array analysis of RIP1 expression-dependent gene induction

Ctrl vs. Ctrl + 4-HT

Gene	Fold change	P value
IL8	25.35	3.02E-29
IL8	17.28	5.38E-18
HES5	8.76	1.77E-52
CXCL1	7.25	5.94E-14
TMEM2	6.51	4.38E-59
SIAH2	6.44	4.41E-47
TNFAIP3	5.91	1.40E-25
BMP2	5.85	1.58E-40
JUN	5.23	1.83E-43
SLC16A3	4.83	2.73E-48
CCL20	4.47	6.64E-19
NFKBIZ	4.33	1.24E-40
ATF3	4.24	5.04E-29
IRF1	4.06	4.70E-44
DUSP1	3.81	2.65E-41
BCOR	3.67	1.33E-35
NFKBIA	3.58	2.23E-29
TP53INP1	3.53	1.93E-42
SERPINB2	3.51	6.39E-33
RTN4R	3.47	4.73E-37
C17ORF96	3.43	3.01E-35
EGR1	3.33	1.12E-26
SERPINB2	3.30	1.19E-29
SLC25A24	3.28	1.19E-15
CBX4	3.27	1.86E-20
TP53INP1	3.25	7.88E-39
TNF	3.20	2.82E-28
FAM46C	3,18	8,28E-33
LOC65075	3,11	1,05E-37
FOSL1	3,09	2,58E-46

Nec-1 vs. Nec-1 + 4-HT

Gene	Fold change	P value
IL8	17,43	4,07E-19
HES5	8,97	3,79E-38
IL8	8,54	2,96E-14
SIAH2	8,53	6,64E-51
TMEM2	7,21	1,53E-36
SLC16A3	5,07	1,69E-62
JUN	4,65	1,32E-53
BMP2	4,60	6,43E-40
TP53INP1	4,15	3,51E-43
CXCL1	4,06	1,06E-12
IRF1	3,66	1,90E-41
TP53INP1	3,594	4,94E-35
BCOR	3,55	4,53E-44
CCL20	3,50	9,70E-23
RTN4R	3,47	3,16E-32
ODC1	3,47	2,68E-38
CASP7	3,41	2,39E-34
CBX4	3,28	2,49E-25
FAM46C	3,18	1,09E-21
CAT	3,02	1,16E-23
LOC65075	2,96	4,05E-38
FAM117B	2,93	5,83E-35
TNFAIP3	2,84	2,27E-22
C17ORF96	2,83	6,29E-45
NFKBIZ	2,83	3,32E-47
FOXC1	2,81	1,74E-27
FOSL1	2,77	1,11E-44
ATF3	2,73	2,56E-20
CAT	2,63	2,64E-36
SERPINB2	2,57	3,21E-39

TBK1/IKK-ε KD vs. TBK/IKK-ε + 4-HT

Gene	Fold change	P value
IL8	21,50	7,11E-13
IL8	12,87	5,57E-14
HES5	8,95	2,20E-39
TMEM2	6,84	1,12E-44
JUN	6,40	1,10E-37
SIAH2	5,84	2,64E-37
CXCL1	5,61	1,00E-13
TNFAIP3	5,40	2,44E-23
SLC16A3	5,27	5,29E-43
SERPINB2	4,43	5,13E-15
BMP2	4,34	8,40E-35
LOC650757	4,04	1,66E-45
IRF1	3,97	3,01E-42
HBEGF	3,91	5,43E-19
DUSP1	3,87	6,60E-27
NFKBIZ	3,84	6,41E-27
SERPINB2	3,82	6,04E-22
BCOR	3,81	2,24E-38
CCL20	3,78	2,12E-16
C17ORF96	3,63	2,62E-24
FOSL1	3,61	1,59E-47
NFKBIA	3,51	2,68E-24
ATF3	3,16	4,47E-44
CLCF1	3,15	1,20E-19
IL1A	3,09	8,12E-20
CASP7	2,99	9,96E-32
KLF6	2,90	4,43E-25
EGR1	2,86	3,53E-30
ZFP36	2,84	1,08E-23
FAM46C	2,77	1,17E-26

The 30 most regulated genes of the comparison are shown in Table 12. The upregulated genes represent typical NF-κB-related targets and genes involved in activation of cytokines like TNF and chemokines like CXCL1 or CCL20. The top regulated gene is *IL-8*, which was also observed by the qPCR experiments. In line with the biochemical and qPCR data, the gene induction could be reduced by the addition of Nec-1. The absolute fold change of the *IL-8* mRNA was decreased from roughly 25 to 17, which displays a reduction of ~30%. The combined knockdown of TBK1 and IKK-ε decreased the *IL-8* induction from 25 to 21 (~ 15%). This was also true for other inflammatory genes like *CXCL1* (roughly 7 to 5; ~ 25%) or *CCL20* (roughly 4.5 to 3.8; ~ 20%). Interestingly, the *SERPINB2* gene was also upregulated after RIP1 induction. In line with the *IL-8* results, Nec-1 reduced the induction substantially from 3.5 to 2.5, meaning again a reduction of ~ 30%. However, the induction of *SERPINB2* was not reduced when TBK1 and IKK-ε were knocked down by siRNA.

Summarized, these data clearly show the gene inductive properties of the Ripoptosome, which are highly dependent on the kinase activity of RIP1. Moreover, the upregulation of the shown mRNAs displays the induction of an inflammatory response carried out by NF-κB with *IL-8* as the most dominant regulated gene. The reduction of TBK1 and IKK-ε protein level could reduce the RIP1-induced proinflammatory gene expression, shown by *IL-8*, *CXCL1* or *CCL20*. These results indicate that TBK1 and IKK-ε support Ripoptosome-mediated proinflammatory responses. However, the influence of TBK1 and IKK-ε in respect to *PAI-2*[175] induction, could not be verified in terms of the RIP1-induced Ripoptosome, indicating that a subset of upregulated genes is not regulated by TBK1 or IKK-ε.

VIII.7. TBK1 and IKK-ε induce phosphorylation of autophagy receptors after Ripoptosome formation

As mentioned in the introduction, the non-canonical IKKs are involved in many different cellular signaling pathways. Some recent studies also connected TBK1 to the phosphorylation of autophagic receptors like optineurin (OPTN) and sequestosome-1 (SQSTM1 or p62), which are sensing damaged mitochondria or microbial infections, finally inducing autophagic removal[141–143]. To assess whether Ripoptosome formation results also in the TBK1- and IKK-ε-mediated activation of autophagic receptors, SILAC (stable isotope labeling with amino acids in cell culture) labeling and mass spectrometric analysis of the phosphosites were analyzed in HeLa RIP1 WT TBK1/IKK-ε deficient cells. Therefore, HeLa Ctrl and TBK1/IKK-ε knockout cells with inducible RIP1 expression were established.

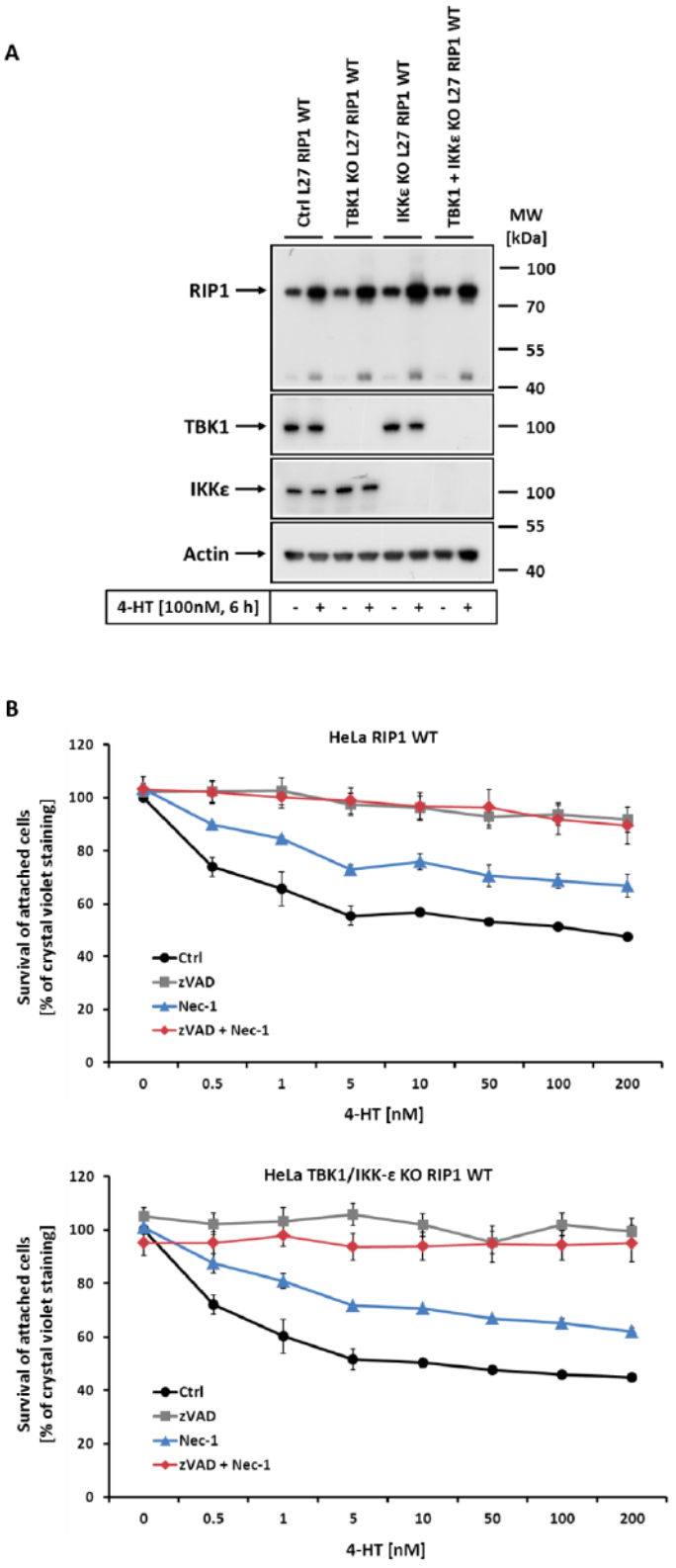

Figure 26 RIP1 expression and cell death responses in HeLa TBK/IKK-ε KO RIP1 WT cells.
HeLa CIRSPR cell lines were lentivirally transduced with pF Super PGK Hygro (Gev16) and pF 5x UAC MCS W SV40 containing RIP1 WT cDNA. (A) RIP1 expression was induced with 100 nM 4-HT for 6 h. Cellular lysates were analyzed by SDS-PAGE and Western Blotting for RIP1 expression and knockout of the target genes. (B) Cells were prestimulated with 10 µM zVAD-fmk and 50 µM Nec-1, followed by stimulation with different concentrations of 4-HT for 20 h. Cell attachment was monitored by crystal violet staining. The graphs display the mean values ± SEM of three independent experiments.

In order to rule out functional changes due to clonal selection, RIP1 expression as well as cell death responses were analyzed in the newly established cell lines. Therefore, expression of RIP1 was induced by 4-HT for six hours and RIP1 expression was monitored by Western Blot analysis (Figure 26A). All cell lines showed comparable expression of RIP1 after the 4-HT treatment. Cell death induction was visualized by crystal violet staining after stimulation with different concentrations of 4-HT in combination with zVAD-fmk and Nec-1 for twenty hours, as described above. The control cell line as well as the double knockout showed significant reduction in cell attachment with increasing concentrations of 4-HT. As seen before, the addition of the caspase inhibitor zVAD-fmk could completely block cell death, whereas treatment with the RIP1 kinase inhibitor Nec-1 could only partially block cellular execution (Figure 26B). These results rule out possible changes in the expected functionality in terms of RIP1 expressing, due to clonal selection. Hence, the generated cells could then be used in the mentioned phosphosite analysis.

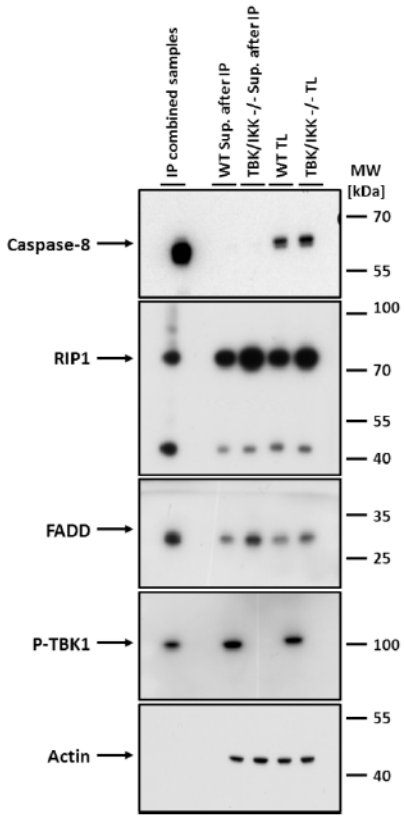

Figure 27 RIP1-induced Ripoptosome formation in SILAC labeled HeLa TBK1/IKK-ε KO RIP1 WT cells.
HeLa TBK1/IKK-ε KO RIP1 WT and HeLa RIP1 WT control cells were grown in medium containing heavy (WT) and light (TBK1/IKK-ε KO) labeled amino acids (done by the lab of Ivan Dikic). RIP1 expression was induced with 100 nM 4-HT for 6 h. Caspase-8 was precipitated from 2 mg of cellular lysates. Precipitated proteins of the WT and TBK1/IKK-ε KO cells were fused (IP combined samples). Finally, bound proteins, total lysates (TL) and fractions from the non-bound proteins after the IP (Sup. after IP) were separated by SDS-PAGE and analyzed for Ripoptosome components via Western Blotting.

The SILAC labeling and mass spectrometric analyses described in the following section were kindly done by the lab of Ivan Dikic from the Institute of Biochemistry II, Goethe University Medical School in Frankfurt. In brief, HeLa RIP1 WT and TBK/IKK-ε KO RIP1 WT cells were grown in medium containing heavy (HeLa WT) or light (TBK/IKK-ε KO) isotope labeled amino acids. When the labeled cells reached a certain confluence, RIP1 expression was induced with 4-HT and Ripoptosome formation was assayed by caspase-8 IP as seen in Figure 27. Caspase-8 was completely depleted from the protein lysates after the IP (Figure 27 Sup. after IP). As the only purpose of this experiment was to verify the ability of the generated cell lines to form a Ripoptosome, bound proteins of the WT and TBK/IKK-ε knockout cells were pooled after the caspase-8 precipitation. The combined samples of the Ctrl and knockout cells showed a substantial co-precipitation of RIP1, FADD and phospho-TBK together with caspase-8. Additionally TBK1 was phosphorylated in the WT cells upon RIP1 expression. For phosphosite analysis, both cell lines were again grown in medium containing labeled amino acids. Total cellular lysates were generated after RIP1 induction and mixed in a 1:1 ratio. The combined samples were finally analyzed for differences in the phosphorylation status by mass spectrometry.

Table 13 Selected phosphoproteome analysis in HeLa TBK1/IKK-ε knockout cells

Name	Gene	Position	H/L Ratio
Sequestosome-1	SQSTM1	277;361	13,186
Receptor-interacting serine/threonine-protein kinase 1	RIPK1	25;25	11,664
Sequestosome-1	SQSTM1	282;366	9,617
TNF receptor-associated factor 2	TRAF2	7;7;7;7;7;7;7	5,5734
E3 ubiquitin-protein ligase XIAP	XIAP	5;5;5	5,5438
TNF receptor-associated factor 2	TRAF2	11;11;11;11	4,5564
Transcription factor AP-1	JUN	243	3,6255
Optineurin	OPTN	120;177;177;120	3,3097
TGF-beta-activated kinase 1 and MAP3K7-binding protein 2	TAB2	582	2,704
Receptor-interacting serine/threonine-protein kinase 1	RIPK1	320;274	2,1382

Shown in Table 13 are selected results from the phosphosite analysis. The autophagy cargo adaptor sequestosome-1 is roughly thirteen times more phosphorylated at Serine 277 and Serine 361 and roughly ten times more phosphorylated at Serine 282 and Serine 366 when TBK1 and IKK-ε were present (Table 13 marked in red). Additionally, the mitophagy adaptor optineurin is phosphorylated at Serine 120 and Serine 177 in a TBK1/IKK-ε-dependent manner. Interestingly, RIP1 was also eleven times more phosphorylated at S25 and two times more phosphorylated at Serine 320 and Serine 274 when the non-canonical IKKs were

present. Additionally, the phosphorylation status of TRAF2 was changed at two sites (Serine 7 and Serine 11) in the knockout cell line. The NF-κB linker TAB2 was also influenced by the loss of TBK1 and IKK-ε, supporting the above-shown involvement of TBK1 and IKK-ε in Ripoptosome mediated NF-κB induction. Moreover, the anti-apoptotic XIAP protein is phosphorylated in a TBK1-dependent manner. In line with this, the transcription factor AP-1 (JUN) is phosphorylated, indicating the induction of anti-apoptotic pro-survival responses.

In summary, these data show that autophagy adaptors like sequestosome-1 or optineurin were phosphorylated after RIP1 expression in a TBK1- and IKK-ε-dependent manner. These findings might implicate that TBK1 and IKK-ε are responsible for the activation of autophagy during RIP1-induced Ripoptosome formation. However, this has to be validated through further experiments. The NF-κB activator TAB2 was also phosphorylated in a TBK1/IKK-ε-dependent manner. This might explain the above described decrease in NF-κB target gene expression after TBK1/IKK-ε knockdown. Furthermore, the phosphorylation state of Ripoptosome components (RIP1, TRAF2) as well as anti-apoptotic proteins (XIAP, TRAF2, JUN) were influenced by TBK1 and IKK-ε. Altogether both kinases influence the phosphorylation of different proteins, which are known to be involved in Ripoptosome, cell death and NF-κB signaling as well as the autophagic pathway. However, for a final clarification of the role of TBK1 and IKK-ε function within the Ripoptosome for the regulation of autophagic and non-cell death signaling pathways further experiments are needed.

Altogether, the results in this thesis clearly identified TBK1, IKK-ε and TRAF2 as novel Ripoptosome components. Moreover, TRAF2 could be verified as a potent apoptosis inhibitor, whereas TBK1 and IKK-ε had no influence on Ripoptosome-mediated cell death signaling. Interestingly, it could be also shown that complex formation was not only inducing cell death but also holds the possibility of gene induction via NF-κB. These gene inductive properties were dependent on the kinases TBK1 and IKK-ε. Last, but not least, Ripoptosome induction was inducing the phosphorylation of autophagy receptors in a TBK1- and IKK-ε-dependent manner. Hence, it can be speculated that complex formation possibly activated the autophagic machinery. Altogether, the generated results shed new light into Ripoptosome composition and signaling and are, therefore, of great interest for the understanding of this cellular stress sensor.

IX. Discussion

The decision between cellular execution and cell survival is a tightly regulated mechanism in the life cycle of multicellular organisms. Deregulations in these processes can have severe consequences[176] including the appearance of several diseases like *multiple sclerosis* [177,178] or *lupus erythematosus*[179] or the development of cancer[180]. The Ripoptosome, a 2 MDa intracellular signaling complex, was identified as one of the key cellular stress sensors, regulating cell death and survival[181]. Genotoxic stress as well as the depletion of cellular inhibitors of apoptosis proteins (cIAPs) can trigger the formation of this multiprotein complex, which contains the name-giving RIP1 and associated proteins such as FADD, caspase-8, RIP3 and cFLIP. Based on the stoichiometric composition and the activity of the respective associated proteins, the Ripoptosome can support apoptosis, necroptosis or cell survival[95,144]. In this study, novel components of the Ripoptosome were identified and their role in cell death regulation as well as in the propagation of non-cell death signaling was investigated.

IX.1. Spontaneous Ripoptosome formation and cell death induction depends on intracellular RIP1 level

RIP1 is one of the key regulators on the crossroad in intracellular cell death and pro-survival signaling. Thereby, the dual function of RIP1 is not only carried out during cell homeostasis but also during fetal parturition[182]. RIP1 knockout mice displayed perinatal lethality due to increased apoptosis and necroptosis induced by the innate immune system[182]. The observed phenotype highlighted the indispensable function of RIP1 for the suppression of cell death by the activation of pro-survival genes through NF-κB, as exemplified during TNF signalling[54,151,183]. In contrast, RIP1 activity can also lead to necroptotic cell execution via Necrosome formation and RIP3 activation[97]. Furthermore, RIP1 is the central component of the above described apoptotic and necroptotic potent Ripoptosome, whose formation is highly dependent on the intracellular RIP1 level, which are guarded by cIAPs[100,144,184].

Based on these intriguing findings, cell death responses and conditions for Ripoptosome formation through RIP1 expression were investigated in HaCaT and HeLa cells. In line with previously published data[95,100], dramatic changes in intracellular RIP1 level resulted in the induction of cell death in both cell lines (Figure 7). HaCaT cells showed cell execution mainly through apoptosis, since the cell death response was only partially affected under inhibition

of RIP1 kinase activity by Nec-1. Additionally, necroptosis could be unmasked by the caspase inhibitor zVAD-fmk (Figure 7B). In contrast, HeLa cells were unable to undergo necroptosis, as zVAD-fmk alone was able to block cell death completely (Figure 7D). The phenotype observed in RIP3 deficient HeLa cells was rather expected as recently published data showed that lack of RIP3 suppressed necroptosis induction in melanoma and other cancer identities[160,185]. Therefore, the general decreased sensitivity to RIP1-induced apoptosis observed in HeLa cells when compared to HaCaT (Figure 7B and 7D) can be explained with the absence of RIP3, as recent publications highlighted that methylation-dependent loss of RIP3 is a common cause for the repression of necroptotic cell death in many cancer identities[160,185,186]. Another reason for the decreased sensitivity of HeLa cells in respect to apoptosis induced by RIP1 overexpression could be the presence of cFLIP isoforms (Figure 7C), which in turn can inhibit caspase-8 activation and activity. cFLIP isoforms were shown to regulate Ripoptosome function and thereby the mode of cell death induced by this complex[95,100]. Heterodimers of the long isoform ($cFLIP_L$) and caspase-8 were identified to promote RIP1 cleavage and cell survival[95,100]. In contrast, caspase-8 and $cFLIP_S$ dimers favor RIP1 stabilization, resulting in RIP3 activation and thereby necroptotic execution[95,100]. Absences of cFLIP encourages caspase-8 homodimerization, thereby promoting caspase activation and apoptosis[95,100]. Summarized, cFLIP is long time known to be a potent caspase inhibitor[93,117,187], thereby explaining the observed discrepancy in the cell death responses seen in HaCaT and HeLa cells (Figure 7B and 7D). On the molecular level, uncontrolled and increased RIP1 expression or inhibition of the direct negative regulator of RIP1 (cIAPs) by IAP antagonists induced the formation of the Ripoptosome. This could be shown by the complex association of RIP1, FADD, cFLIP (HeLa) and RIP3 (HaCaT) with caspase-8 (Figure 8). In line with former publications, the addition of zVAD-fmk increased the formation of the caspase-8 containing complex[144]. Inhibition of the RIP1 kinase activity by Nec-1 largely suppressed Ripoptosome formation. Tenev and co-workers observed a similar effect when they induced complex formation via the depletion of cIAP level by Etoposide treatment [188]. Inhibition of RIP1 kinase activity by Nec-1 or by overexpression of a kinase mutant ($RIP1^{K137A}$) resulted in suppression of Ripoptosome formation. Moreover, Geserick and co-workers highlighted that RIP1 kinase activity is important for the transition of the receptor-bound CD95 DISC to a cytosolic Ripoptosome-like complex II under conditions where cIAPs were depleted[87]. Taken together, these findings highlight the essential role of RIP1 kinase activity and increased intracellular RIP1 kinase level for Ripoptosome formation. It can be speculated that autophosphorylation of RIP1 or the phosphorylation of other complex components by RIP1, is important for Ripoptosome stability.

Interestingly, the caspase inhibitor cFLIP seemed to be not required for RIP1 induced complex formation (Figure 8). When HaCaT cells, which harbor very low level of cFLIP, were

analyzed after RIP1 overexpression, no changes in Ripoptosome formation were observed compared to HeLa cells. Therefore, cFLIP might, as mentioned above, play an essential role in the regulation of cell death responses carried out by the Ripoptosome, however, it is not required for Ripoptosome formation and association of the other complex components (Figure 8).

In contrast to the inhibitory effect on RIP1-induced complexes, the above-mentioned cell death responses could only partially been blocked by the addition of Nec-1 (Figure 7B and 7D). On the contrary, Tenev and co-workers observed largely reduced caspase activation upon Nec-1 treatment in respect to Etoposide-mediated cell death induction[144]. This could not be seen in the here described model system (Figure 7B and 7D). However, both findings indicate that RIP1 kinase activity is required for Ripoptosome formation. As mentioned above, phosphorylation events through RIP1 might be required for complex stability. Moreover, the decreased amounts of remaining complexes are still sufficient to induce cell death (Figure 7B and 7D). Additionally, cIAP depletion and thereby the Ripoptosome-forming potential of Etoposides where analyzed for a short period time (Figure 17). In contrast to studies from Tenev[188] and colleagues, treatment with Etoposides showed no significant induction of the Ripoptosome after six hours (Figure 17). This discrepancy might be reasoned by the short incubation (six hours), leading to insufficient depletion of cIAP by the Etoposide treatment[188]. Therefore, longer exposure times, up to twenty-four hours, have to be used in order to observe substantial Ripoptosome formation due to absence of cIAPs after Etoposide treatment.

Nec-1 was shown to exhibit some off-target effects, influencing other cellular pathways, for example proliferation of T-cells by interfering with TCR (T-cell receptor) signaling[189] or the suppression of the immunomodulatory enzyme indoleamine 2,3-dioxygenase (IDO)[158,190]. Therefore, the observed Nec-1-dependent effects on Ripoptosome formation could likely be due to other cellular changes despite the inhibition of the RIP1 kinase activity. However, this was mainly ruled out by the usage of the specific RIP1 kinase inhibitor GSK'481[160], which further validated the above-mentioned findings. Ripoptosome formation induced through RIP1 expression was largely suppressed by GSK'481 (Figure 9). In contrast, downstream inhibition of the necroptotic signaling pathway by the RIP3 inhibitor GSK'840[160] had no effect on complex assembly. These data support indeed a model were RIP1 kinase activity is required for substantial Ripoptosome formation.

IX.2. TBK1, IKK-ε and TRAF2 are novel components of the RIP1-induced and TLR3-associated Ripoptosome as well as TNF complex II

As mentioned above, many recent studies highlighted the important role of Ripoptosome for regulation of apoptotic and necroptotic cell death pathways[95,99,144,191]. However, complex composition and downstream signaling was thus far only dissected in terms of already known components of PCD pathways, namely RIP1, caspase-8, FADD, cFLIP and RIP3. The appearance of gene regulation, resulting in the production of interferons or inflammatory cytokines[106,107,192] is a very common concept after formation of multiprotein complexes. Therefore, it is very likely that the Ripoptosome exhibits, besides the regulation of cell death programs, similar functional properties. The focus of this study was, therefore, based on the identification of novel components involved in Ripoptosome-mediated signaling. When cellular lysates from RIP1 expressing HaCaT cells were size-specific separated on sucrose gradients[148], the appearance of a high molecular weight complex containing caspase-8 and RIP1 was observed (Figure 10A). These data confirmed that the overexpression of RIP1 leads to formation of the 2 MDa sized Ripoptosome. When this complex was analyzed by mass spectrometry, RIP1 and caspase-8 related peptides were found in large quantities (Table 11). As stated above, FADD has never been recognized in these experiments. This could for example be due to the stoichiometric composition of the Ripoptosome. As shown for the CD95 DISC signaling, one FADD molecule can bind to several caspase-8 proteins via its DED domain[193,194]. Therefore, one can speculate that one FADD molecule is also able to bind several portions of RIP1 via DD interactions. Furthermore, RIP1 could assemble in amyloid structures, thereby leading to a huge underrepresentation of FADD when compared to RIP1 or caspase-8, although FADD is of enormous relevance for the complex formation. In contrast, FADD was easily detected in the biochemical complex analysis seen in Figure 8 and Figure 9. Another reason could be the experimental limitations of the used mass spectrometric settings. FADD is a rather small protein of 28 kDA[195,196] and depending on the used protease for peptide digestion, the generated peptides could be just too small for detection[197]. Most probably a combination of different reasons was leading to the absence of FADD in the mass spectrometric analysis.

However, the analysis revealed the rather unexpected association of TBK1, IKK-ε, as well as TRAF2 (Table 11) with the caspase-8-associated RIP1 complexes. This was further verified by the biochemical analysis of the Ripoptosome (Figure 11), where all three components could be co-precipitated with caspase-8. Interestingly, the non-canonical IKKs were found to be highly phosphorylated and the phosphorylated state was highly enriched in the caspase-8-associated fractions (displaying the Ripoptosome). The phosphorylation of Serine 172

displays the classical activation side of the non-canonical IKKs[198]. Experimentally, it is very difficult to dissect, if the observed phosphorylation occurred in the cytosol and the phosphorylated protein is recruited to the complex or if the two kinases are phosphorylated after complex binding. The ability of both kinases for auto- and transphosphorylation due to local clustering, would argue for the latter point[136,198,199]. As shown in Figure 27, a high quantity of phosphorylated TBK1 is found in the unbound fraction after immunoprecipitation although caspase-8 is completely depleted. These findings indicate that there is a free pool of phosphorylated TBK1, which is not bound to the caspase-8 containing complex. This argues for the release of phosphorylated TBK1 from the Ripoptosome or for the phosphorylation of a free cytosolic TBK1 pool through other factors. Moreover, the decreased phosphorylation of the non-canonical IKKs correlates with the decreased complex formation through the addition of Nec-1. These results clearly link RIP1-induced Ripoptosome formation to the phosphorylation of TBK1 and IKK-ε.

The activation of TLR receptor signaling pathways, in response to pathogen infections, displays a quite common event in the life cycle of multicellular organisms[200]. During the last years, TLR3 receptor stimulation could be linked to cellular execution through the association of a Ripoptosome-like complex when cIAPs were depleted[100,191,200]. As described by Feoktistova and co-workers, the combined stimulation with IAP antagonist and poly (I:C)-induced cell death in HaCaT and HeLa cells[100] (Figure 12). Moreover, the observed phenotype was explained by the formation of a TLR3-associated Ripoptosome, as described before[100]. Of note, stimulation with IAP antagonist (data not shown) or poly (I:C) alone was not sufficient to induce cell death[100]. In line with TNF receptor signaling and complex II formation, stimulation of the TL3 receptor by poly (I:C) is primary leading to gene induction via NF-κB or IRF3[80,201]. First the recruitment of the IAP antagonist-induced Ripoptosome to the TLR3 receptor enables for cell death induction, as observed for TNF complex II[80,100,188]. In summary, that means that the receptor-associated Ripoptosome converts pro-inflammatory cytokines into prodeath signals[188]. This could have important impact on the design of anticancer therapies, utilizing cancer-related inflammation. Given that Ripoptosome formation sensitizes cells to cytokines such as TNF and poly (I:C), it seems likely that therapeutic strategies designed to boost Ripoptosome assembly will help to convert cancer-related proinflammatory signals into pro-death stimuli[188].

Interestingly, when the TLR3-bound complexes were analyzed for the newly identified components, the three novel proteins; TBK1, IKK-ε and TRAF2 were all coprecipitated with caspase-8 (Figure 13). This was also true when Jurkat cells were tested for IAP antagonist together with poly (I:C)-induced complex formation (Figure 14). These findings argue for a general integration of the three proteins into Ripoptosome-like complexes. The stoichiometric

composition of the TLR3-associated complex undergoes time-dependent changes (Figure 13). The three novel components reach their maximum of complex association at a rather early point of time and become released over time. This data could explain why the above-mentioned free pool of phospho-TBK1 was observed in the unbound fraction (Figure 27).

It is long time known that RIP1-association with the TLR3 adaptor TRIF via RHIM domain interactions is required for TLR3-dependent NF-κB activation[202,203]. During the last years, the impact of RIP1 in TLR3-associated Ripoptosome formation and cell death induction was highlighted[100]. The partial elimination of RIP1 by siRNA or shRNA mediated knockdown, was able to block cell death and decrease IAP antagonist and poly (I:C)-induced complex formation. In order to further clarify the role of RIP1 for poly (I:C) and IAP antagonist-induced Ripoptosome signaling, HeLa RIP1 knockout cells were generated using the CRISPR/Cas9 system. The CRISPR/Cas9 technology revolutionized the scientific landscape through the last years. It provided a tool for any kind of fast and easy genetic manipulations[204], including complete genetic knockouts. However, off-target effects are a common event of the CRISPR/Cas9 system, creating unspecific genetic alterations in unexpected DNA regions[205,206]. Furthermore, selection of single cell clones in order to generate homogenic cell lines can result in the favoritisms of cells with unwanted genetic side effects[207]. In order to circumvent this problem, at last two knockout clones were used in the following analysis.

In line with the RIP1 knockdown experiments, CRISPR/Cas9 mediated RIP1 knockout resulted in total inhibition of cell death execution by poly (I:C) in the absence of cIAPs (Figure 15). Not surprising, TLR3-associated Ripoptosome formation was completely inhibited with the loss of RIP1 (Figure 16). Remarkably, the phosphorylation of TBK1 upon poly (I:C) treatment was not impaired (Figure 16, TL samples), but association with caspase-8 was fully blocked. These data support the published findings that activation of TBK1 and further propagation of the IRF3 pathway in respect to TLR3 activation is not dependent on RIP1[105,172,208]. Taken together, these data support a model where depletion of cellular IAP level leads to the association of RIP1 and FADD via their DD domains. This leads to further binding of caspase-8 to FADD via their DED domains, finally forming the Ripoptosome and enabling the complex for cell death induction. When the TLR3 receptor is in addition stimulated, the binding of TRIF to the cytosolic part of the receptor starts the recruitment of the Ripoptosome to the TLR3 receptor by RHIM interactions between RIP1 and TRIF. The novel identified proteins TBK1, IKK-ε and TRAF2 might now be recruited via other domains of RIP1, e.g. the death domain, into the Ripoptosome. Another possibility is that recruitment of FADD or caspase-8 triggers the association of these novel components into the complex. However, the exact binding sites and how these proteins are recruited to the complex remain to be elucidated.

Binding of TNF to its specific receptor is long time known to induce gene expression, leading to inflammatory responses[73,116]. Thus, deregulations in TNF receptor signaling is linked to many inflammatory diseases including Crohn's disease and rheumatoid athritis[209–211]. Furthermore, TNF plays a pivotal role in cancer development and progression. Tumor cells were found to constitutively express and secrete low levels of TNF, thereby leading to the constant NF-κB-dependent expression of anti-apoptotic and pro-survival genes[73,212]. However, many studies highlighted that cIAP depletion plus TNF stimulation can, similar to the TLR3-associated complex, lead to the formation of the so called TNF complex II, which harbors the ability to induce apoptosis and necroptosis[80,81]. Therefore, complex II formation and cell death induction could be used as a potential target for cancer therapies[213]. On the molecular level, the Ripoptosome and TNF complex II incorporate identical components and are both able to induce cell death based on the stoichiometric composition. The Ripoptosome can form independent of death receptor stimulation by TNF through the depletion of cIAPs[100,144]. In contrast, TNF complex II relies on TNF stimulation and the transition of the receptor-bound complex I to the cytosolic complex II[80]. Another difference was made by the modification status of RIP1. Ripoptosome formation incorporates unmodified RIP1 due to the lack of cIAPs[214] whereas TNF complex II harbors CYLD-modified RIP1 from complex I[215].

However, based on the findings in this study differences between TNF complex II, TLR3-associated and RIP1-induced Ripoptosome could not be identified. When HaCaT cells were stimulated with IAP antagonist and TNF-HF in the presence of zVAD-fmk for six hours, substantial association of caspase-8 with complex II components RIP1, FADD and TRADD was observed. Interestingly, presence of the TNF complex adaptor TRADD was observed in the TLR3-associated complex (Figure 17), although it is a classical compound of the TNF complex signaling pathway[165]. TRADD binds to the intracellular part of activated TNF receptor to enable the formation of the intracellular signaling complex I. Moreover, TRADD was shown to bind TRAF2 thereby promoting the association of cIAPs, which are responsible for RIP1 modifications in TNF complex I[76,77,166]. However, TRADD was also reported to play a role in TLR3 mediated gene induction as well as poly (I:C)-mediated toxicity in MEFs[165,166]. With the above-mentioned findings, one can now speculate that influence of TRADD on TLR3-mediated signaling is due to the association with the TLR3-bound Ripoptosome. Furthermore, the data suggest TRADD as a general member of Ripoptosome-like signaling complexes. Interestingly, in addition to TRADD, the novel identified components; TBK1, IKK-ε and TRAF2 were also found to be part of the precipitated TNF complex II. These findings additionally confirm that Ripoptosome-like complexes harbor the integral components TBK1, IKK-ε, TRAF2 and TRADD.

IX.3. TRAF2 but not TBK1 and IKK-ε inhibits apoptotic cells death upon RIP1 overexpression

The E3 ubiquitin-ligase TRAF2 is long known as an important member of the TNF complex I signaling complex and an important apoptosis inhibitor in TNF signaling[80,168,216]. TRAF2 is also responsible for the association of cIAPs in order to modify RIP1, thereby enabling NF-κB activation and finally expression of anti-apoptotic proteins[217,218]. Moreover, recent reports highlighted the additional inhibitory effect of TRAF2 in TNF-, CD95L- and TRAIL-mediated necroptosis[169,170]. However, TRAF2 has thus far not been linked to Ripoptosome formation. In this study siRNA mediated knockdown of TRAF2 (Figure 18A and 18B) resulted in increased apoptotic cell death, unmasked by Nec-1 treatment after RIP1 overexpression (Figure 18C), supporting the anti-apoptotic effect of TRAF2. It is very intuitive that TRAF2 might, similar to the function in TNF complex I signaling, induce the binding of cIAPs to the Ripoptosome. This would enable the cIAPs to modify RIP1, thereby leading either to disassembly of the complex by the degradation of RIP1 or the induction of other signaling pathways like NF-κB and the expression of anti-apoptotic factors. In contrast, the reported inhibitory effect of TRAF2 on necroptosis[169,170] was not observed. When cells were treated with the caspase inhibitor zVAD-fmk, followed by overexpression of RIP1, no differences in necroptotic cell death responses were observed between the control cell line and the TRAF2 knockdown (Figure 18C). It might be that the necroptotic responses due to RIP1-induced Ripoptosome formation behave differently when compared to the reported effects after death receptor stimulation through TNF, CD95L or TRAIL.

The surprising finding of the non-canonical IKKs (TBK1 and IKK-ε) as novel components of the Ripoptosome encouraged the examination of both kinases in respect to cell death induction. TBK1 and IKK-ε are very well established key regulators of the innate immune system[133,198]. Moreover, recent reports highlighted TBK1 as an inhibitor of TNF-induced apoptosis by the induction of anti-apoptotic gene products[175]. In this study, we therefore tested the influence of TBK1 and IKK-ε on cell death responses induced by the expression of RIP1. When both kinases were knocked down by siRNA (Figure 18B, 19A and 19B), no significant changes in PCD responses were observed (Figure 19C). Therefore, the anti-apoptotic effect could not be verified in respect to RIP1 expression. However, here, as described above for TRAF2, the formation of the RIP1-induced Ripoptosome could display a total different scenario than TNF stimulation. In the reported setting, TBK1 could very well exhibit gene inductive properties in TNF complex I, thereby leading to the expression of anti-apoptotic proteins, whereas in the RIP1-induced situation there is no gene induction carried out by complex I. Summarized, our analysis identified an inhibitory function for TRAF2 on

RIP1-induced apoptosis whereas the necroptotic response was unaltered. TBK1 and IKK-ε seemed to have no obvious influence on PCD signaling in the RIP1 overexpression system.

IX.4. Ripoptosome formation in TLR3-signaling is IKK-ε- and TRAF2-independent, but TBK1 modulates complex stoichiometry

Many proteins including FADD and caspase-8 can fulfill scaffolding functions in specific signaling complexes or pathways[196,219,220]. Ripoptosome composition or stoichiometry or activity of other complex-associated proteins might, therefore, be influenced by the lack of TBK1, IKK-ε and TRAF2. Genetic knockouts of all three components in HeLa cells, including the TBK1/IKK-ε double knockout, were generated and analyzed for changes in complex composition. Therefore, the double knockout of TBK1 and IKK-ε was generated in both directions to rule out off-target effects (TBK1 knockout cell line transfected with the IKK-ε CRISPR and vice versa). When analyzed for the expression of PCD involved proteins, no effects on complex-related protein expression was observed (Figure 20). Cell death caused by the combined treatment of IAP antagonist and poly (I:C) was not altered by the double knockout of TBK1 and IKK-ε. These data confirmed the above-mentioned knockdown experiments, again showing that TBK1 and IKK-ε have no direct influence on Ripoptosome-mediated cell death signaling. In contrast, the TRAF2 knockout showed in line with the above described data for RIP1 expression, a sensitization against IAP antagonist plus poly (I:C) treatment (Figure 21). Therefore, TRAF2 could be identified as an inhibitor of programmed cell death through RIP1- or IAP antagonist plus poly (I:C)-induced Ripoptosome formation. The inhibitory function might most probably be carried out by suppression of anti-apoptotic gene expression, which was already reported for TNF, CD95 and TRAIL treatment[169,170,216].

When complex formation was analyzed in the knockout cells, TLR3-associated Ripoptosome formation could be observed in all cell lines. Loss of IKK-ε and TRAF2 did not alter the complex formation when compared to the control cells (Figure 22A and 22B). Interestingly, the lack of TBK1 resulted in a changed stoichiometry of the Ripoptosome. RIP1, FADD and cFLIP showed a decreased association with caspase-8-associated RIP1 complexes, whereas levels of IKK-ε or TRADD were not affected. In turn, TRAF2 seemed to be increased in the formed Ripoptosome when TBK1 was not present. Interestingly, TRAF2 was shown to form a complex with TANK (TRAF family member-associated NF-kappa-B activator) and TBK1, resulting in TBK1 activation and finally NF-κB induction[221–223]. One can now speculate that both proteins carry out a similar function in Ripoptosome signaling. Complex formation could bring TRAF2 and TBK1 into close proximity, which enabled the

TRAF2-dependent activation of TBK1, resulting in the final activation of NF-κB. The observed enrichment of TRAF2 in the Ripoptosome (formed in the TBK1 knockout cell lines) could display a compensatory mechanism, as the postulated TBK1/TRAF2 pathway was abolished. TBK1 activation by TRAF2 could result in the release of TRAF2 from the complex, therefore, explaining the increased TRFA2 level in the TBK1 knockout cells. An interesting further question in this respect would be if TANK could also be found associated with the Ripoptosome. However, lack of TBK1 seemed to influence caspase-8 association of many different complex components (RIP1, FADD, cFLIP). Therefore, it might also be possible that TBK1 exhibits a scaffolding function for regulated complex assembly. The knockout situation might now result in unregulated or unstable association of the Ripoptosome components thereby explaining the seen differences in single factors. Of note, cell death responses were unaltered after the TBK1 knockout (Figure 21), meaning that the changes in complex composition do not affect the Ripoptosome-mediated cell death responses. However, further analyses have to be made to clarify the role of TBK1 in respect to Ripoptosome formation.

As stated above, the CRISPR/Cas9 system as well as the single cell selection process could result in different genetic alterations. This could be seen, as the described TBK1-dependent effect on complex composition was not observed in the IKK-ε/TBK1 double knockout in the second set of clones (Figure 22B, IKK/TBK KO), although the knockout and basal protein expression showed no differences. The mentioned clone could have alterations in other proteins (not analyzed in these experiments) that act downstream of the Ripoptosome/TBK1 axis, thereby enabling the compensation of the TBK1 loss. Altogether, the results created with CRISPR/Cas9 mediated knockout cells should be interpreted very critically and validated through additional methods, as the role of TBK1 for TLR3-associated Ripoptosome formation could not conclusively be verified from the observed data. However, as three out of four clones showed similar alterations after TBK1 loss, it is rather likely that the observed changes where due to the absence of TBK1.

IX.5. Ripoptosome formation induces phosphorylation of NF-κB inhibitors, resulting in TBK1- and IKK-ε-dependent target gene expression

From the generated data, TBK1 and IKK-ε could be identified as Ripoptosome components not involved in complex-dependent cell death signaling pathways. As mentioned-above and further encouraged by the enriched association of TRAF2 in the complex when TBK1 is absent, Ripoptosome formation might very likely induce gene expression. This might be

carried out by the activation of the NF-κB pathway or other transcriptional activators in a TBK1- and IKK-ε-dependent manner. Time-dependent kinetics of RIP1 expression or IAP antagonist plus poly (I:C) treatment indeed showed stimulation-dependent phosphorylation of the NF-κB inhibitor IκB-α (Figure 23A and 23B), which is a long known indicator for canonical NF-κB activation[112,224]. In contrast, phosphorylation of the NF-κB protein p65 (RelA) at Serine 536 was differentially regulated during RIP1 expression and IAP antagonist plus poly (I:C) treatment. Interestingly, it was shown that this regulatory NF-κB subunit can be activated independently of IκB-α degradation and induce a specific subset of target genes, including the inflammatory cytokine *interleukin-8* (*IL-8*)[225–227]. Furthermore, IKK-ε was shown to directly target p65 for phosphorylation after TNF stimulation[228]. Under expression of RIP1, phosphorylation of p65 was increased over time in line with the increasing phosphorylation of the non-canonical IKKs as well as MLKL, indicating Ripoptosome formation and necroptosis induction (Figure 23A). One may now envision that the RIP1-induced complex formation could lead to the phosphorylation of p65 in an IKK-ε-dependent manner. Moreover, IκB-α was phosphorylated over time, in line with increasing RIP1 level. In total, the data clearly show that increased RIP1 expression leads to the activation of the NF-κB pathways. In contrast, treatment with IAP antagonist and poly (I:C) resulted in early p65 phosphorylation, which was lost over time (Figure 23B). Additionally, phosphorylation state of TBK1 and IKK-ε was increased at early points of time, but did not change with increasing incubation time. It is known that poly (I:C) binding to the TLR3 receptor induces NF-κB responses, which are propagated via TRAF6 and a TAK/TAB complex[107,201], explaining the early seen activation of p65 and phosphorylation of IκB-α. Additionally, poly (I:C) stimulation is known to result in the activation of the transcription factor IRF3[105,136,138]. This was also observed in our experiments (Figure 22B), giving the reason for the rapid phosphorylation of TBK1 and IKK-ε. Furthermore, the non-canonical NF-κB pathway was activated after IAP antagonist and poly (I:C) treatment, as shown by the cleavage of NF-κB p100 precursor into the active p52 fragment. This activation was rather expected as depletion of cIAPs is known to stabilize the NF-κB inducing kinase NIK, thereby activating the non-canonical NF-κB pathway[123,125]. Taken together, IAP antagonist and poly (I:C) treatment display a rather complicated system to study NF-κB activation in respect to Ripoptosome formation. Treatment with poly (I:C) alone is sufficient to induce NF-κB after the recruitment of a TRAF6/TAK/TAB complex to the receptor-bound TRIF (Figure 5)[107,201]. This complex can then target the IKK complex, finally leading to IκB-α degradation. In parallel, TBK1/IKK-ε are recruited to TRIF to activate IRF3 [105,106,229]. Moreover, depletion of cIAPs by IAP antagonists result in the activation of the non-canonical NF-κB pathway by stabilization of NIK[123,125]. Finally, poly (I:C) and IAP antagonist treatment results in the recruitment of the Ripoptosome to the TLR3 receptor, further increasing the NF-κB response as seen through the RIP1 induction (Figure 5). Therefore,

many different independent pathways are switched on by poly (I:C) and the depletion of cIAPs, making it difficult to discriminate between TLR3-dependent and Ripoptosome-induced signaling. The overexpression of RIP1 also resulted in the induction of NF-κB (Figure 23), although the expression of RIP1 kinase displayed a single trigger for the observed modifications of NF-κB components and activators. Therefore, gene expression analyses in this study, were based on the expression of RIP1, as NF-κB induction was clearly visible in this system in line with increasing RIP1 level.

As mentioned above, p65 phosphorylation is an indication for induction of inflammatory genes especially *IL-8*[226,230]. Gene expression analysis after RIP1 induction indeed revealed an up to 100 fold induction of *IL-8* mRNA (Figure 24A). As described by Kavuri and colleagues[117], the addition of the caspase inhibitor zVAD-fmk further increased this mRNA expression. Interestingly, inhibition of the kinase activity of RIP1 by Nec-1 decreased *IL-8* expression, especially seen for the six-hour incubation time (Figure 24A). As shown by the previous data (Figure 8) Nec-1 inhibits RIP1-induced Ripoptosome formation, arguing for complex dependency of the observed gene induction. The described results were also true for the anti-apoptotic gene *SERPINB2* (Figure 24B). Expression of *SERPINB2* was shown to be dependent on TBK1-mediated phosphorylation of p65 after TNF stimulation[175], displaying expression of specific activation of a subset of NF-κB target genes. These data might link Ripoptosome-mediated gene induction to the observed association and activation of TBK1 with the complex. This hypothesis was further verified when TBK1/IKK-ε double knockdown was assessed for *IL-8* mRNA expression. Compared to the control cells, the absence of TBK-1 and IKK-ε reduced *IL-8* expression of about 25%, indicating a direct influence of both proteins for complex mediated gene expression. Micro Array analysis of the whole mRNA expression identified that increased RIP1 levels influenced not only *IL-8*, but also altered the expression of different chemokines involved inflammatory responses (Table 12). Especially the expression of *CXCL-1* and *CCL-20*, two NF-κB target genes, were induced upon increased RIP1 expression. Both cytokines were shown to be classically upregulated in inflammatory diseases[231,232]. Furthermore, the expression of *CXCL-1* and *CCL-20* was found after cytokine stimulation, including CD95L treatment and pathogen infection[91,231–234]. In line with the *IL-8* data, the reduction of TBK1 and IKK-ε protein level resulted in the suppression of both cytokines. In contrast, the expression of *SERPINB2* was not substantially changed under TBK1 and IKK-ε knockdown conditions. This might argue for a different regulation of this particular anti-apoptotic gene during Ripoptosome formation when compared to TNF stimulation. The use of siRNA-mediated knockdown could also explain the absent effect on *SERPINB2*, as little amounts of TBK1 could still be sufficient to fulfill the p65 phosphorylation needed for *SERPINB2* induction. Altogether, the observed pattern of regulated genes after

RIP1 overexpression displayed a common NF-κB signature, finally resulting in inflammatory and pro-survival responses, which are often seen after cellular stress stimuli.

Altogether, these data linked Ripoptosome formation to NF-κB-mediated gene expression involved in inflammatory responses. Similar results were reported for other RIP1 containing complexes, like TNF complex I or CD95 DISC complex II[54,116,233]. Altogether, RIP1 complex association, especially in the Ripoptosome seems to interconnect cell death-inducing signaling complexes to NF-κB-dependent gene induction. Furthermore, gene expression of several inflammatory genes was decreased by the reduction of TBK1 and IKK-ε protein level, supporting the idea that complex-associated TBK1 and IKK-ε function as regulators for a subset of NF-κB target genes. However, downstream targets of both kinases remain to be elusive, although p65 was shown to be phosphorylated by both kinases[175,225,226] and therefore, displays a promising target.

IX.6. Overexpression of RIP1 induces TBK1- and IKK-ε-dependent phosphorylation of autophagy receptors

Recent studies highlighted the pivotal role of TBK1 for autophagic or especially mitophagic clearance during stress signaling[141,143]. As stated above, Ripoptosome formation displays a cellular stress response due to changes in RIP1 level. Therefore, one can speculate that there is a crosstalk between Ripoptosome formation and autophagy induction. HeLa TBK1/IKK-ε double knockout cells showed, in line with the above described poly (I:C) treatment, no alteration in their cell death response induced by RIP1 expression when compared to control cells (Figure 26B). Ripoptosome formation was also unaltered by the loss of TBK1 and IKK-ε (Figure 27). However, when phosphorylation sites of the whole cellular extracts after RIP1 expression were compared to control cells, significant changes in the phosphorylation status of different proteins were observed (Table 13).

Interestingly, the autophagy inducing proteins optineurin and sequestosome-1 were phosphorylated upon RIP1 expression in a TBK1- and IKK-ε-dependent manner. Of note, both proteins were shown to physically interact with TBK1 for example during the clearance of damaged mitochondria[143]. Optineurin modification on Serine 177 was shown to be TBK1-dependent and responsible for the recruitment of ATG8 (autophagy related protein-8), which is required for autophagosome formation[62,143,235]. In contrast, Serine 120 phosphorylation is thus far not described for optineurin, displaying a possible novel target site for autophagy induction. One can also speculate that this specific site is targeted by IKK-ε for

complementary autophagic activation in line with TBK1 Serine 177 phosphorylation. Additionally, the autophagy cargo protein sequestosome-1 was found to be phosphorylated at Serine 282 and 366 in a TBK1- and IKK-ε-dependent manner[141,198]. Sequestosome-1 classically recognizes toxic cellular waste and targets it for autophagic clearance[236]. Pilli and colleagues identified TBK1 as the kinase that targets sequestosome-1 on Serine 403 during microbial infections, thereby enabling autophagosome maturation[141]. In contrast, the identified TBK1- and IKK-ε-dependent phosphorylation sites were not characterized thus far. Moreover, sequestosome-1 was shown to interact with RIP1 for the activation of NF-κB[237]. Therefore, sequestosome-1 might also bind to Ripoptosome-bound RIP1 and might then be targeted by TBK1 or IKK-ε to induce NF-κB. Interestingly, the activation of autophagy was shown to exhibit dual functions in respect to tumor progression and cell death resistance in cancer cells. The tumor suppressor function is mainly linked to the ability to prevent the accumulation of toxic oxygen radicals by scavenging damaged oxidative organelles[238,239]. In contrast, autophagy was shown to be upregulated in many cancer identities, where it promotes cell survival and cell death resistances[240]. The tumor promotor function of autophagy was proposed to be one critical reason for the development of secondary resistances after modern drug based cancer therapies like RAF (rapidly accelerated fibrosarcoma) inhibition in melanoma treatment[241]. Drug based inhibition of cellular pathways, like treatment with PI3K (Phosphoinositid-3-Kinasen) inhibitors, can mimic starvation conditions, thereby promoting the autophagic recycling of intracellular components and finally cell survival[242]. It can be hypothesized that the observed phosphorylation of autophagy receptors after Ripoptosome formation could be a similar survival mechanism. As mentioned above, formation of the Ripoptosome is a cellular stress sensor to different extrinsic and intrinsic stimuli, which harbors the ability to induce programmed cell death. The parallel induction of autophagy could now act as a surveillance system, trying to maintain cell viability. However, further analyses have to be made and mutations of the single phosphorylation sites are required to finally clarify their role and impact of autophagy induction in Ripoptosome-mediated signaling.

Additionally, the phosphorylation status of Ripoptosome components RIP1 and TRAF2 were altered in a TBK1- and IKK-ε-dependent manner. The identified RIP1 phosphorylation sites were thus far not identified as functional RIP1 modifications[243,244]. However, these sites could very well display novel regulatory elements involved in Ripoptosome-mediated RIP1 signaling. In the case of TRAF2, phosphorylation at Serine 11 is a well described modification, which is responsible for the anti-apoptotic function and gene inductive properties of TRAF2[245,246]. In contrast, phosphorylation on Serine 7 is thus far not described. These data support the above-mentioned idea that TRAF2 association and apoptosis inhibition during Ripoptosome formation is most likely carried out by the induction of anti-

apoptotic genes. Interestingly, the therefore necessary phosphorylation seems to be carried out by the associated kinases TBK1 and IKK-ε. Moreover, the phosphorylation status of the NF-κB inducing protein TAB2[247] was changed by loss of the non-canonical IKKs. Altogether these results might explain how and why the loss of TBK1 and IKK-ε result in reduced expression of NF-κB target genes, although further studies will be needed to validate and dissect the function of both kinases in this respect.

Summarized, the data presented in this study promote the in Figure 28 described Ripoptosome model. Genotoxic stress or chemical compound-mediated depletion of the cellular IAP level results in a changed balance of the cellular RIP1 equilibrium. The increasing pool of active and free RIP1 promotes the formation of the Ripoptosome, containing the proteins RIP1, caspase-8, FADD, cFLIP and the novel identified proteins TRADD, TRAF2, TBK1 and IKK-ε. Furthermore, the combination of cIAP depletion together with death receptor activation or stimulation of the TLR3 receptor can promote recruitment and accumulation of the Ripoptosome to the respective receptors. Based on the complex stoichiometry, especially the portion of associated cFLIP, formation of this signaling platform can lead to apoptotic cell execution by caspase-8 activation or necroptotic cell death through activation of the RIP1/RIP3 axis. In this study, TRAF2 was identified as a novel complex component, influencing the apoptotic cell death response upon Ripoptosome formation. The anti-apoptotic function of TRAF2 might very well be carried out, similar to the TNF complex, through activation of anti-apoptotic gene expression[167,218,221]. The binding of TRAF2 to the Ripoptosome might be dependent on TRADD, which was also found to be a part of the Ripoptosome-like complexes in this study. TRADD was shown to directly interact with TRAF2[76,168] in order to facilitate RIP1 modifications through cIAPs in TNF complex signaling. Therefore, both proteins might execute similar functions in the Ripoptosome as in TNF signaling. However, further studies have to be made in order to dissect whether TRAF2 really bind via TRADD to the complex and if loss of TRAF2 inhibits induction of anti-apoptotic gene products after Ripoptosome formation. In addition, the non-canonical IKKs, TBK1 and IKK-ε were found to be integral parts of TNF complex II and the RIP1- and poly (I:C)-induced Ripoptosome. However, loss of both proteins had no effect on Ripoptosome-mediated PCD execution. In parallel to cell death induction, gene expression of inflammatory cytokines was increased via the activation of NF-κB after complex formation. As previously described, the induction of a subset of inflammatory NF-κB target genes was dependent on the kinases TBK1 and IKK-ε. The phosphorylation of p65 might be a possible target of both kinases, as similar functions were reported before in case of TNF receptor signalling[175]. However, if NF-κB activation after Ripoptosome is differentially regulated by both kinases or if they complement each other, still has to be clarified.

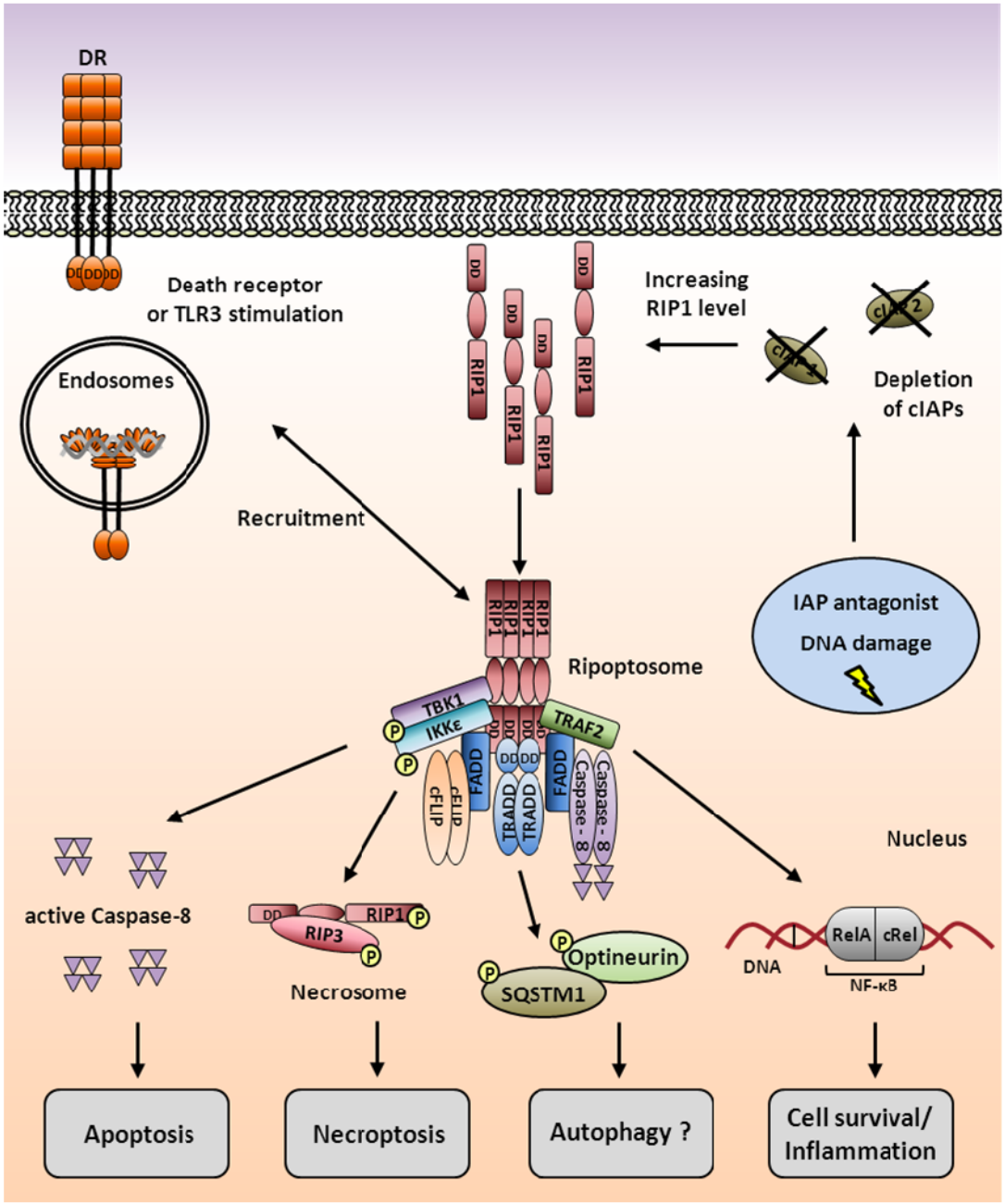

Figure 28 Potential role of the Ripoptosome for regulation of apoptotic, necroptotic, autophagic and cell death-independent signaling pathways.

Cellular stress signals and chemical compounds promote the depletion of cIAPs, thereby stabilizing and increasing the active RIP1 pool. Accelerated RIP1 level induce the association of RIP1 with caspase-8, FADD, TRADD, cFLIP, TRAF2, TBK1 and IKK-ε into the Ripoptosome. Functions carried out by this complex are dependent on the activity of single components as well as on the stoichiometric composition. The simultaneous stimulation of death receptors or the TLR3 receptor in absence of functional cIAPs can target the cytosolic complex to these receptors and further accelerate the formation of the complex. Activation of caspase-8 within the Ripoptosome or the activation of RIP3 can induce cell death through apoptosis and necroptosis. In parallel, Ripoptosome formation results in the induction of NF-κB target genes, leading to inflammatory responses, which are dependent on TBK1 and IKK-ε. Furthermore, phosphorylation of the autophagy receptors optineurin and sequestosome-1 is induced due to changes in RIP1 level in a TBK1- and IKK-ε-dependent manner.

Additionally, phosphorylation state of different proteins was dramatically changed depending on TBK1 and IKK-ε after the expression of RIP1. Interestingly, autophagic receptors optineurin and sequestosome-1 were differentially modified at several sites after the lack of TBK1 and IKK-ε. These findings might link Ripoptosome formation and the activity of the different molecules within this complex to autophagy regulation, displaying a novel pathway that is regulated by this signaling complex. However, the physiological appearance of autophagy still needs to be tested. Additionally, the function of the newly identified phosphosites needs to be elucidated in order to clarify their role for cell death regulation or non-cell death linked pathways. Altogether, this study highlighted novel components and signaling pathways that are influenced after Ripoptosome formation. The better understanding of Ripoptosome-mediated signaling might offer novel ideas for target tumor therapies, as the complex is predominantly formed in cancer cells but not in primary cells[100,188,248]. A combined treatment of tumor patients with Smac mimetics and chemotherapy is currently under clinical trials, as many cancer identities including ALL (acute lymphoblastic leukemia) can be sensitized to cellular execution by promoting Ripoptosome assembly[249,250]. In contrast, chronic lymphocytic leukemia (CLL) was shown to be resistant to Smac mimetic treatment as these cells were unable to form a Ripoptosome[147]. It can be speculated that targeted suppression of the here identified Ripoptosome-mediated non-cell death signaling pathways (NF-κB and autophagy), could display novel mechanisms further accelerating Ripoptosome-induced cell death. As mentioned above, autophagy inhibition might display a novel strategy to overcome secondary resistances in tumor growth. Therefore, Smac mimetic treatment combined with autophagy inhibition could sensitize resistant tumor cells to cell death. Furthermore, direct modulation of the newly identified components TBK1, IKK-ε or TRAF2 might provide novel Ripoptosome signaling-mediated therapy approaches. Especially, the inhibition of TRAF2 could favor cellular execution in resistant cancer cells, as decreased TRAF2 level were sensitizing to death receptor and TLR3-mediated PCD[169,170]. Hence, the better understanding and characterization of these novel components and signaling pathways might be important for the development and improvement of specialized, targeted cancer therapies or disease treatments.

X. References

1. Vogt, C. Untersuchungen über die Entwicklungsgeschichte der Geburtshelferkroete (Alytes obstetricans). 130 (1842).

2. Kerr, J. F. A histochemical study of hypertrophy and ischaemic injury of rat liver with special reference to changes in lysosomes. *J. Pathol. Bacteriol.* **90,** 419–435 (1965).

3. Kerr, J. F., Wyllie, a H. & Currie, a R. Apoptotsis: a basic biological phenomenon with wide ranging implications in tissue kinetics. *Br J Cancer* **26,** 239–247 (1972).

4. Kerr J. F. R., Wyllie A. H., C. a. R. Apoptosis : a Basic Biological Phenomenon With Wide-. *Br. J. Cancer* **26,** 239–257 (1972).

5. Kuan, C. Y. *et al.* The Jnk1 and Jnk2 protein kinases are required for regional specific apoptosis during early brain development. *Neuron* **22,** 667–676 (1999).

6. Mori, C. *et al.* Programmed cell death in the interdigital tissue of the fetal mouse limb is apoptosis with DNA fragmentation. *Anat. Rec.* **242,** 103–110 (1995).

7. James, T. N., Terasaki, F., Pavlovich, E. R. & Vikhert, A. M. Apoptosis and pleomorphic micromitochondriosis in the sinus nodes surgically excised from five patients with the long QT syndrome. *J. Lab. Clin. Med.* **122,** 309–323 (1993).

8. Lazebnik, Y. A., Cole, S., Cooke, C. A., Nelson, W. G. & Earnshaw, W. C. Nuclear events of apoptosis in vitro in cell-free mitotic extracts: A model system for analysis of the active phase of apoptosis. *J. Cell Biol.* **123,** 7–22 (1993).

9. Coleman, M. L. *et al.* Membrane blebbing during apoptosis results from caspase-mediated activation of ROCK I. *Nat. Cell Biol.* **3,** 339–345 (2001).

10. Jiang, J. X., Mikami, K., Shah, V. H. & Torok, N. J. Leptin induces phagocytosis of apoptotic bodies by hepatic stellate cells via a rho guanosine triphosphatase-dependent mechanism. *Hepatology* **48,** 1497–1505 (2008).

11. Erwig, L.-P. & Henson, P. M. Clearance of apoptotic cells by phagocytes. *Cell Death Differ.* **15,** 243–50 (2008).

12. Taylor, R. C., Cullen, S. P. & Martin, S. J. Apoptosis: controlled demolition at the cellular level. *Nature reviews. Molecular cell biology* **9,** 231–241 (2008).

13. Cohen, G. M. Caspases: the executioners of apoptosis. *Biochem. J.* **326 (Pt 1,** 1–16 (1997).

14. Fulda, S. & Debatin, K.-M. Extrinsic versus intrinsic apoptosis pathways in anticancer chemotherapy. *Oncogene* **25,** 4798–4811 (2006).

15. Portt, L., Norman, G., Clapp, C., Greenwood, M. & Greenwood, M. T. Anti-apoptosis and cell survival: A review. *Biochimica et Biophysica Acta - Molecular Cell Research* **1813,** 238–259 (2011).

16. Bouillet, P. & Strasser, A. BH3-only proteins - evolutionarily conserved proapoptotic Bcl-2 family members essential for initiating programmed cell death. *J. Cell Sci.* **115,** 1567–1574 (2002).

17. Strasser, a *et al.* The role of bim, a proapoptotic BH3-only member of the Bcl-2 family in cell-death control. *Ann. N. Y. Acad. Sci.* **917,** 541–8 (2000).

18. Bleicken, S., Landeta, O., Landajuela, A., Basa??ez, G. & Garc??a-S??ez, A. J. Proapoptotic Bax and Bak proteins form stable protein-permeable pores of tunable size. *J. Biol. Chem.* **288,** 33241–33252 (2013).

19. Li, H., Zhu, H., Xu, C. J. & Yuan, J. Cleavage of BID by caspase 8 mediates the mitochondrial damage in the Fas pathway of apoptosis. *Cell* **94,** 491–501 (1998).

20. Zou, H., Henzel, W. J., Liu, X., Lutschg, A. & Wang, X. Apaf-1, a human protein homologous to C. elegans CED-4, participates in cytochrome c-dependent activation of caspase-3. *Cell* **90,** 405–413 (1997).

21. Li, P. *et al.* Cytochrome c and dATP-dependent formation of Apaf-1/caspase-9 complex initiates an apoptotic protease cascade. *Cell* **91,** 479–89 (1997).

22. Acehan, D. *et al.* Three-dimensional structure of the apoptosome: Implications for assembly, procaspase-9 binding, and activation. *Mol. Cell* **9,** 423–432 (2002).

23. Slee, E. A., Adrain, C. & Martin, S. J. Executioner Caspase-3, -6, and -7 Perform Distinct, Non-redundant Roles during the Demolition Phase of Apoptosis. *J. Biol. Chem.* **276,** 7320–7326 (2001).

24. Enari, M. *et al.* A caspase-activated DNase that degrades DNA during apoptosis, and its inhibitor ICAD. *Nature* **391,** 43–50 (1998).

25. Holcik, M. & Korneluk, R. G. XIAP, the guardian angel. *Nat. Rev. Mol. Cell Biol.* **2,** 550–556 (2001).

26. Scott, F. L. *et al.* XIAP inhibits caspase-3 and -7 using two binding sites: evolutionarily conserved mechanism of IAPs. *EMBO J.* **24,** 645–655 (2005).

27. Liu, Z. *et al.* Structural basis for binding of Smac/DIABLO to the XIAP BIR3 domain. *Nature* **408,** 1004–1008 (2000).

28. Srinivasula, S. *et al.* A conserved XIAP-interaction motif in caspase-9 and Smac/DIABLO regulates caspase activity and apoptosis. *Nature* **410,** 112–116 (2001).

29. Wang, L. *et al.* The Fas-FADD death domain complex structure reveals the basis of DISC assembly and disease mutations. *Nat. Struct. Mol. Biol.* **17,** 1324–1329 (2010).

30. Thomas, L. R., Henson, A., Reed, J. C., Salsbury, F. R. & Thorburn, A. Direct binding of Fas-associated death domain (FADD) to the tumor necrosis factor-related apoptosis-inducing ligand receptor DR5 is regulated by the death effector domain of FADD. *J. Biol. Chem.* **279,** 32780–32785 (2004).

31. Sprick, M. R. *et al.* FADD/MORT1 and caspase-8 are recruited to TRAIL receptors 1 and 2 and are essential for apoptosis mediated by TRAIL receptor 2. *Immunity* **12,** 599–609 (2000).

32. Pezzulo, A. a *et al.* Caspases 3 and 7: Key Mediators of Mitochondrial Events of Apoptosis. *Science (80-.).* **487,** 109–113 (2013).

33. McDonnell, T. J. *et al.* bcl-2-Immunoglobulin transgenic mice demonstrate extended B cell survival and follicular lymphoproliferation. *Cell* **57,** 79–88 (1989).

34. Hockenbery, D., Nuñez, G., Milliman, C., Schreiber, R. D. & Korsmeyer, S. J. Bcl-2 is an inner mitochondrial membrane protein that blocks programmed cell death. *Nature* **348,** 334–336 (1990).

35. Schug, Z. T., Gonzalvez, F., Houtkooper, R. H., Vaz, F. M. & Gottlieb, E. BID is cleaved by caspase-8 within a native complex on the mitochondrial membrane. *Cell Death Differ.* **18,** 538–548 (2011).

36. Jiang, X. & Wang, X. Cytochrome c promotes caspase-9 activation by inducing nucleotide binding to Apaf-1. *J. Biol. Chem.* **275,** 31199–31203 (2000).

37. Cowling, V. & Downward, J. Caspase-6 is the direct activator of caspase-8 in the cytochrome c-induced apoptosis pathway: absolute requirement for removal of caspase-6 prodomain. *Cell Death Differ.* **9,** 1046–1056 (2002).

38. Hitomi, J. *et al.* Identification of a Molecular Signaling Network that Regulates a Cellular Necrotic Cell Death Pathway. *Cell* **135,** 1311–1323 (2008).

39. Chautan, M., Chazal, G., Cecconi, F., Gruss, P. & Golstein, P. Interdigital cell death can occur through a necrotic and caspase-independent pathway. *Curr. Biol.* **9,** 967–970 (1999).

40. Vandenabeele, P., Galluzzi, L., Vanden Berghe, T. & Kroemer, G. Molecular mechanisms of necroptosis: an ordered cellular explosion. *Nat. Rev. Mol. Cell Biol.* **11,** 700–14 (2010).

41. Berghe, T. Vanden *et al.* Necroptosis, necrosis and secondary necrosis converge on similar cellular disintegration features. *Cell Death Differ.* **17,** 922–930 (2010).

42. Galluzzi, L. & Kroemer, G. Necroptosis: A Specialized Pathway of Programmed Necrosis. *Cell* **135,** 1161–1163 (2008).

43. Lin, Y., Devin, A., Rodriguez, Y. & Liu, Z. G. Cleavage of the death domain kinase RIP by Caspase-8 prompts TNF-induced apoptosis. *Genes Dev.* **13,** 2514–2526 (1999).

44. Feng, S. *et al.* Cleavage of RIP3 inactivates its caspase-independent apoptosis pathway by removal of kinase domain. *Cell. Signal.* **19,** 2056–2067 (2007).

45. Deveraux, Q. L. & Reed, J. C. IAP family proteins--suppressors of apoptosis. *Genes Dev.* **13,** 239–252 (1999).

46. Bertrand, M. J. M. *et al.* cIAP1 and cIAP2 Facilitate Cancer Cell Survival by Functioning as E3 Ligases that Promote RIP1 Ubiquitination. *Mol. Cell* **30,** 689–700 (2008).

47. Declercq, W., Vanden Berghe, T. & Vandenabeele, P. RIP Kinases at the Crossroads of Cell Death and Survival. *Cell* **138,** 229–232 (2009).

48. Cho, Y. *et al.* Phosphorylation-Driven Assembly of the RIP1-RIP3 Complex Regulates Programmed Necrosis and Virus-Induced Inflammation. *Cell* **137,** 1112–1123 (2016).

49. Sun, L. *et al.* Mixed lineage kinase domain-like protein mediates necrosis signaling downstream of RIP3 kinase. *Cell* **148,** 213–227 (2012).

50. Wang, H. *et al.* Mixed Lineage Kinase Domain-like Protein MLKL Causes Necrotic Membrane Disruption upon Phosphorylation by RIP3. *Mol. Cell* **54,** 133–146 (2014).

51. Cai, Z. *et al.* Plasma membrane translocation of trimerized MLKL protein is required for TNF-induced necroptosis. *Nat. Cell Biol.* **16,** 55–65 (2014).

52. Dondelinger, Y. *et al.* MLKL Compromises Plasma Membrane Integrity by Binding to Phosphatidylinositol Phosphates. *Cell Rep.* **7,** 971–981 (2014).

53. Cai, Z. *et al.* Plasma membrane translocation of trimerized MLKL protein is required for TNF-induced necroptosis. *Nat. Cell Biol.* **16,** 55–65 (2014).

54. Kelliher, M. A. *et al.* The death domain kinase RIP mediates the TNF-induced NF-κB signal. *Immunity* **8,** 297–303 (1998).

55. Wang, X. *et al.* RNA viruses promote activation of the NLRP3 inflammasome through a RIP1-RIP3-DRP1 signaling pathway. *Nat. Immunol.* **15,** 1126–1133 (2014).

56. Pasparakis, M. & Vandenabeele, P. Necroptosis and its role in inflammation. *Nature* **517,** 311–320 (2015).

57. Choi, A. M. K., Ryter, S. W. & Levine, B. Autophagy in human health and disease. *N. Engl. J. Med.* **368,** 651–62 (2013).

58. Wong, Y. C. & Holzbaur, E. L. Optineurin is an autophagy receptor for damaged mitochondria in parkin-mediated mitophagy that is disrupted by an ALS-linked mutation. *Proc Natl Acad Sci U S A* **111,** E4439–48 (2014).

59. Bj??rk??y, G. *et al.* Chapter 12 Monitoring Autophagic Degradation of p62/SQSTM1. *Methods in Enzymology* **451,** 181–197 (2009).

60. Gordon, P. B., Kovacs, A. L. & Seglen, P. O. Temperature dependence of protein degradation, autophagic sequestration and mitochondrial sugar uptake in rat hepatocytes. *BBA - Mol. Cell Res.* **929,** 128–133 (1987).

61. Gutierrez, M. G. *et al.* Autophagy is a defense mechanism inhibiting BCG and Mycobacterium tuberculosis survival in infected macrophages. *Cell* **119,** 753–766 (2004).

62. Nakatogawa, H., Ichimura, Y. & Ohsumi, Y. Atg8, a Ubiquitin-like Protein Required for Autophagosome Formation, Mediates Membrane Tethering and Hemifusion. *Cell* **130,** 165–178 (2007).

63. He, C. *et al.* Exercise-induced BCL2-regulated autophagy is required for muscle glucose homeostasis. *Nature* **481,** 511–515 (2012).

64. Kroemer, G. & Levine, B. Autophagic cell death: the story of a misnomer. *Nat. Rev. Mol. Cell Biol.* **9,** 1004–10 (2008).

65. Shimizu, S. *et al.* Role of Bcl-2 family proteins in a non-apoptotic programmed cell death dependent on autophagy genes. *Nat. Cell Biol.* **6,** 1221–1228 (2004).

66. Pattingre, S. *et al.* Bcl-2 antiapoptotic proteins inhibit Beclin 1-dependent autophagy. *Cell* **122,** 927–939 (2005).

67. Yu, L. *et al.* Regulation of an ATG7-beclin 1 program of autophagic cell death by caspase-8. *Science (80-.).* **304,** 1500–1502 (2004).

68. Tsujimoto, Y. & Shimizu, S. Another way to die: autophagic programmed cell death. *Cell Death {&} Differ.* **12 Suppl 2,** 1528–1534 (2005).

69. Kolb, B. Y. W. P. & Grangert, G. A. LYMPHOCYTE IN VITRO CYTOTOXICITY: CHARACTERIZATION OF HUMAN LYMPHOTOXIN. *Microbiology* 1250–1255 (1968).

70. Carswell, E. A. *et al.* An endotoxin-induced serum factor that causes necrosis of tumors. *Proc. Natl. Acad. Sci. U. S. A.* **72,** 3666–70 (1975).

71. Thoma, B., Grell, M., Pfizenmaier, K. & Scheurich, P. Identification of a 60-kD tumor necrosis factor (TNF) receptor as the major signal transducing component in TNF responses. *J. Exp. Med.* **172,** 1019–23 (1990).

72. Grell, M., Wajant, H., Zimmermann, G. & Scheurich, P. The type 1 receptor (CD120a) is the high-affinity receptor for soluble tumor necrosis factor. *Proc. Natl. Acad. Sci. U. S. A.* **95,** 570–575 (1998).

73. Idriss, H. T. & Naismith, J. H. TNF alpha and the TNF receptor superfamily: structure-function relationship(s). *Microsc. Res. Tech.* **50,** 184–195 (2000).

74. Vanlangenakker, N., Bertrand, M. J. M., Bogaert, P., Vandenabeele, P. & Vanden Berghe, T. TNF-induced necroptosis in L929 cells is tightly regulated by multiple TNFR1 complex I and II members. *Cell Death Dis.* **2,** e230 (2011).

75. Sawai, H. Characterization of TNF-induced caspase-independent necroptosis. *Leuk. Res.* **38,** 706–713 (2014).

76. Hsu, H., Shu, H. B., Pan, M. G. & Goeddel, D. V. TRADD-TRAF2 and TRADD-FADD interactions define two distinct TNF receptor 1 signal transduction pathways. *Cell* **84,** 299–308 (1996).

77. Haas, T. L. *et al.* Recruitment of the Linear Ubiquitin Chain Assembly Complex Stabilizes the TNF-R1 Signaling Complex and Is Required for TNF-Mediated Gene Induction. *Mol. Cell* **36,** 831–844 (2009).

78. Dynek, J. N. *et al.* c-IAP1 and UbcH5 promote K11-linked polyubiquitination of RIP1 in TNF signalling. *EMBO J.* **29,** 4198–4209 (2010).

79. Draber, P. *et al.* LUBAC-Recruited CYLD and A20 Regulate Gene Activation and Cell Death by Exerting Opposing Effects on Linear Ubiquitin in Signaling Complexes. *Cell Rep.* **13,** 2258–2272 (2015).

80. Micheau, O. & Tschopp, J. Induction of TNF receptor I-mediated apoptosis via two sequential signaling complexes. *Cell* **114,** 181–190 (2003).

81. Han, J., Zhong, C.-Q. & Zhang, D.-W. Programmed necrosis: backup to and competitor with apoptosis in the immune system. *Nat. Immunol.* **12,** 1143–9 (2011).

82. Wajant, H. Death receptors. *Essays Biochem* **39,** 53–71 (2003).

83. Stanger, B. Z., Leder, P., Lee, T. H., Kim, E. & Seed, B. RIP: A novel protein containing a death domain that interacts with Fas/APO-1 (CD95) in yeast and causes cell death. *Cell* **81,** 513–523 (1995).

84. Muzio, M. *et al.* FLICE, a novel FADD-homologous ICE/CED-3-like protease, is recruited to the CD95 (Fas/APO-1) death-inducing signaling complex. *Cell* **85,** 817–827 (1996).

85. Kischkel, F. C. *et al.* Cytotoxicity-dependent APO-1 (Fas/CD95)-associated proteins form a death-inducing signaling complex (DISC) with the receptor. *EMBO J.* **14,** 5579–88 (1995).

86. Juo, P., Kuo, C. J., Yuan, J. & Blenis, J. Essential requirement for caspase-8/FLICE in the initiation of the Fas-induced apoptotic cascade. *Curr. Biol.* **8,** 1001–8 (1998).

87. Geserick, P. *et al.* Cellular IAPs inhibit a cryptic CD95-induced cell death by limiting RIP1 kinase recruitment. *J. Cell Biol.* **187,** 1037–1054 (2009).

88. Legembre, P. *et al.* Induction of apoptosis and activation of NF-kappaB by CD95 require different signalling thresholds. *EMBO Rep.* **5,** 1084–9 (2004).

89. Farley, S. M. *et al.* Fas ligand-induced proinflammatory transcriptional responses in reconstructed human epidermis: Recruitment of the epidermal growth factor receptor and activation of MAP kinases. *J. Biol. Chem.* **283,** 919–928 (2008).

90. Park, D. R. *et al.* Fas (CD95) induces proinflammatory cytokine responses by human monocytes and monocyte-derived macrophages. *J. Immunol.* **170,** 6209–6216 (2003).

91. Farley, S. M. *et al.* Fas ligand elicits a caspase-independent proinflammatory response in human keratinocytes: implications for dermatitis. *J. Invest. Dermatol.* **126,** 2438–2451 (2006).

92. Bagnoli, M., Canevari, S. & Mezzanzanica, D. Cellular FLICE-inhibitory protein (c-FLIP) signalling: A key regulator of receptor-mediated apoptosis in physiologic context and in cancer. *International Journal of Biochemistry and Cell Biology* **42,** 210–213 (2010).

93. Siegmund, D., Hadwiger, P., Pfizenmaier, K., Vornlocher, H.-P. & Wajant, H. Selective inhibition of FLICE-like inhibitory protein expression with small interfering RNA oligonucleotides is sufficient to sensitize tumor cells for TRAIL-induced apoptosis. *Mol. Med.* **8,** 725–732 (2002).

94. Leverkus, M. *et al.* Regulation of tumor necrosis factor-related apoptosis-inducing ligand sensitivity in primary and transformed human keratinocytes. *Cancer Res.* **60,** 553–559 (2000).

95. Feoktistova, M., Geserick, P., Panayotova-Dimitrova, D. & Leverkus, M. Pick your poison: The Ripoptosome, a cell death platform regulating apoptosis and necroptosis. *Cell Cycle* **11,** 460–467 (2012).

96. Vanden Berghe, T. *et al.* Regulated necrosis: the expanding network of non-apoptotic cell death pathways. *Nat. Rev. Mol. Cell Biol.* **15,** 135–47 (2014).

97. Li, J. *et al.* The RIP1/RIP3 necrosome forms a functional amyloid signaling complex required for programmed necrosis. *Cell* **150,** 339–350 (2012).

98. Greenwald, J. & Riek, R. Biology of amyloid: Structure, function, and regulation. *Structure* **18,** 1244–1260 (2010).

99. Imre, G., Larisch, S. & Rajalingam, K. Ripoptosome: A novel IAP-regulated cell death-signalling platform. *J. Mol. Cell Biol.* **3,** 324–326 (2011).

100. Feoktistova, M. *et al.* cIAPs block Ripoptosome formation, a RIP1/caspase-8 containing intracellular cell death complex differentially regulated by cFLIP isoforms. *Mol. Cell* **43,** 449–63 (2011).

101. Bowie, a & O'Neill, L. a. The interleukin-1 receptor/Toll-like receptor superfamily: signal generators for pro-inflammatory interleukins and microbial products. *J. Leukoc. Biol.* **67,** 508–514 (2000).

102. Li, C., Zienkiewicz, J. & Hawiger, J. Interactive sites in the MyD88 Toll/interleukin (IL) 1 receptor domain responsible for coupling to the IL1?? signaling pathway. *J. Biol. Chem.* **280,** 26152–26159 (2005).

103. Slack, J. L. *et al.* Identification of two major sites in the type I interleukin-1 receptor cytoplasmic region responsible for coupling to pro-inflammatory signaling pathways. *J. Biol. Chem.* **275,** 4670–4678 (2000).

104. Alexopoulou, L., Holt, a C., Medzhitov, R. & Flavell, R. a. Recognition of double-stranded RNA and activation of NF-kappaB by Toll-like receptor 3. *Nature* **413,** 732–738 (2001).

105. Liu, S. *et al.* Phosphorylation of innate immune adaptor proteins MAVS, STING, and TRIF induces IRF3 activation. *Science* **347,** aaa2630 (2015).

106. Doyle, S. E. *et al.* IRF3 Mediates a TLR3/TLR4-Specific Antiviral Gene Program. *Immunity* **17,** 251–263 (2002).

107. Jiang, Z. *et al.* Poly I:C-induced TLR3-mediated activation of NFkB and MAP kinases is through and IRAK-independent pathway employing signaling components TLR§-TRAF6-TAK1-TAB2-PKR. *JBC* (2003).

108. Sen, R. & Baltimore, D. Inducibility of kappa immunoglobulin enhancer-binding protein Nf-kappa B by a posttranslational mechanism. *Cell* **47,** 921–8 (1986).

109. Ghosh, S. *et al.* Cloning of the p50 DNA binding subunit of NF-??B: Homology to rel and dorsal. *Cell* **62,** 1019–1029 (1990).

110. Ghosh, S., May, M. J. & Kopp, E. B. NF- κ B AND REL PROTEINS : Evolutionarily Conserved Mediators of Immune Responses. *Annu. Rev. iImunology* **16,** 225–260 (1998).

111. Rushlow, C. & Warrior, R. The rel family of proteins. *Bioessays* **14,** 89–95 (1992).

112. Baldwin, A. S. THE NF-κB AND IκB PROTEINS: New Discoveries and Insights. *Annu. Rev. Immunol* **14,** 649–81 (1996).

113. Mercurio, F., DiDonato, J. A., Rosette, C. & Karin, M. p105 and p98 precursor proteins play an active role in NF-kappa B-mediated signal transduction. *Genes Dev.* **7,** 705–718 (1993).

114. Rice, N. R., MacKichan, M. L. & Israël, A. The precursor of NF-kappa B p50 has I kappa B-like functions. *Cell* **71,** 243–53 (1992).

115. Naumann, M., Wulczyn, F. G. & Scheidereit, C. The NF-kappa B precursor p105 and the proto-oncogene product Bcl-3 are I kappa B molecules and control nuclear translocation of NF-kappa B. *EMBO J.* **12,** 213–22 (1993).

116. Diessenbacher, P. *et al.* NF-kappaB inhibition reveals differential mechanisms of TNF versus TRAIL-induced apoptosis upstream or at the level of caspase-8 activation independent of cIAP2. *J. Invest. Dermatol.* **128,** 1134–47 (2008).

117. Kavuri, S. M. *et al.* Cellular FLICE-inhibitory Protein (cFLIP) isoforms block CD95- and TRAIL death receptor-induced gene induction irrespective of processing of caspase-8 or cFLIP in the death-inducing signaling complex. *J. Biol. Chem.* **286,** 16631–16646 (2011).

118. Oeckinghaus, A., Hayden, M. S. & Ghosh, S. Crosstalk in NF-κB signaling pathways. *Nat. Immunol.* **12,** 695–708 (2011).

119. Zandi, E., Rothwarf-D, Delhase, M., Hayakawa, M. & Karin ReprintAuthor), M. The i kappa b kinase complex (ikk) contains two kinase subunits, ikk alpha and ikk beta, necessary for i kappa b phosphorylation and nf kappa b activation. *Cell* **91,** 243–252 (1997).

120. Yamaoka, S. *et al.* Complementation cloning of NEMO, a component of the IκB kinase complex essential for NF-κB activation. *Cell* **93,** 1231–1240 (1998).

121. Chen, Z. *et al.* Signal-induced site-specific phosphorylation targets I kappa B alpha to the ubiquitin-proteasome pathway. *Genes Dev* **9,** 1586–1597 (1995).

122. Chen, F. E. & Ghosh, G. Regulation of DNA binding by Rel/NF-kappaB transcription factors: structural views. *Oncogene* **18,** 6845–6852 (1999).

123. Zarnegar, B. J. *et al.* Noncanonical NF-kappaB activation requires coordinated assembly of a regulatory complex of the adaptors cIAP1, cIAP2, TRAF2 and TRAF3 and the kinase NIK. *Nat. Immunol.* **9,** 1371–8 (2008).

124. Ling, L., Cao, Z. & Goeddel, D. V. NF-kappaB-inducing kinase activates IKK-alpha by phosphorylation of Ser-176. *Proc. Natl. Acad. Sci. U. S. A.* **95,** 3792–3797 (1998).

125. Sun, S.-C. Non-canonical NF-κB signaling pathway. *Cell Res.* **21177,** 71–8571 (2011).

126. Xiao, G., Harhaj, E. W. & Sun, S. C. NF-kappaB-inducing kinase regulates the processing of NF-kappaB2 p100. *Mol. Cell* **7,** 401–409 (2001).

127. Coope, H. J. *et al.* CD40 regulates the processing of NF-??B2 p100 to p52. *EMBO J.* **21,** 5375–5385 (2002).

128. Yoneyama, M. *et al.* The RNA helicase RIG-I has an essential function in double-stranded RNA-induced innate antiviral responses. *Nat. Immunol.* **5,** 730–737 (2004).

129. Oshiumi, H., Matsumoto, M., Funami, K., Akazawa, T. & Seya, T. TICAM-1, an adaptor molecule that participates in Toll-like receptor 3-mediated interferon-beta induction. *Nat. Immunol.* **4,** 161–167 (2003).

130. Yamamoto, M. *et al.* Cutting Edge: A Novel Toll/IL-1 Receptor Domain- Containing Adapter That Preferentially Activates the IFN-B Promoter in the Toll-Like Receptor Signaling. *J. Immunol.* **169,** 6668–6672 (2002).

131. Tojima, Y. *et al.* NAK is an IkappaB kinase-activating kinase. *Nature* **404,** 778–782 (2000).

132. Peters, R. T., Liao, S. M. & Maniatis, T. IKKepsilon is part of a novel PMA-inducible IkappaB kinase complex. *Mol. Cell* **5,** 513–522 (2000).

133. Sharma, S. *et al.* Triggering the interferon antiviral response through an IKK-related pathway. *Science (80-.).* **300,** 1148–1151 (2003).

134. Yu, T. *et al.* The pivotal role of TBK1 in inflammatory responses mediated by macrophages. *Mediators of Inflammation* **2012,** (2012).

135. Helgason, E., Phung, Q. T. & Dueber, E. C. Recent insights into the complexity of Tank-binding kinase 1 signaling networks: The emerging role of cellular localization in the activation and substrate specificity of TBK1. *FEBS Lett.* **587,** 1230–1237 (2013).

136. Tanaka, Y. & Chen, Z. J. STING specifies IRF3 phosphorylation by TBK1 in the cytosolic DNA signaling pathway. *Sci. Signal.* **5,** ra20 (2012).

137. Bonnard, M. *et al.* Deficiency of T2K leads to apoptotic liver degeneration and impaired NF-kappaB-dependent gene transcription. *EMBO J.* **19,** 4976–85 (2000).

138. Verhelst, K., Verstrepen, L., Carpentier, I. & Beyaert, R. I??B kinase ?? (IKK??): A therapeutic target in inflammation and cancer. *Biochemical Pharmacology* **85,** 873–880 (2013).

139. Hemmi, H. *et al.* The roles of two IkappaB kinase-related kinases in lipopolysaccharide and double stranded RNA signaling and viral infection. *J. Exp. Med.* **199,** 1641–50 (2004).

140. Clément, J.-F., Meloche, S. & Servant, M. J. The IKK-related kinases: from innate immunity to oncogenesis. *Cell Res.* **18,** 889–899 (2008).

141. Pilli, M. *et al.* TBK-1 Promotes Autophagy-Mediated Antimicrobial Defense by Controlling Autophagosome Maturation. *Immunity* **37,** 223–234 (2012).

142. Lazarou, M. *et al.* The ubiquitin kinase PINK1 recruits autophagy receptors to induce mitophagy. *Nature* **524,** 309–14 (2015).

143. Heo, J. M., Ordureau, A., Paulo, J. A., Rinehart, J. & Harper, J. W. The PINK1-PARKIN Mitochondrial Ubiquitylation Pathway Drives a Program of OPTN/NDP52 Recruitment and TBK1 Activation to Promote Mitophagy. *Mol. Cell* **60,** 7–20 (2015).

144. Tenev, T. *et al.* The Ripoptosome, a Signaling Platform that Assembles in Response to Genotoxic Stress and Loss of IAPs. *Mol. Cell* **43,** 432–448 (2011).

145. Selmi, T. *et al.* ZFP36 stabilizes RIP1 via degradation of XIAP and cIAP2 thereby promoting ripoptosome assembly. *BMC Cancer* **15,** 357 (2015).

146. Shi, S. *et al.* Synergistic anticancer effect of cisplatin and Chal-24 combination through IAP and c-FLIPL degradation, Ripoptosome formation and autophagy-mediated apoptosis. *Oncotarget* **6,** 1640–51 (2015).

147. Maas, C. *et al.* CLL cells are resistant to smac mimetics because of an inability to form a ripoptosome complex. *Cell Death Dis.* **4,** e782 (2013).

148. Hughes, M. A., Langlais, C., Cain, K. & MacFarlane, M. Isolation, characterisation and reconstitution of cell death signalling complexes. *Methods* **61,** 98–104 (2013).

149. Noll, E. M. *et al.* CYP3A5 mediates basal and acquired therapy resistance in different subtypes of pancreatic ductal adenocarcinoma. *Nat. Med.* **22,** (2016).

150. Richter, B. *et al.* Phosphorylation of OPTN by TBK1 enhances its binding to Ub chains and promotes selective autophagy of damaged mitochondria. *Proc. Natl. Acad. Sci.* 201523926 (2016). doi:10.1073/pnas.1523926113

151. Christofferson, D. E., Li, Y. & Yuan, J. Control of life-or-death decisions by RIP1 kinase. *Annu. Rev. Physiol.* **76,** 129–50 (2014).

152. Ofengeim, D. & Yuan, J. Regulation of RIP1 kinase signalling at the crossroads of inflammation and cell death. *Nat. Rev. Mol. Cell Biol.* **14,** 727–36 (2013).

153. Festjens, N., Vanden Berghe, T., Cornelis, S. & Vandenabeele, P. RIP1, a kinase on the crossroads of a cell's decision to live or die. *Cell Death Differ.* **14,** 400–410 (2007).

154. Ofengeim, D. & Yuan, J. Regulation of RIP1 kinase signalling at the crossroads of inflammation and cell death. *Nat. Rev. Mol. Cell Biol.* **14,** 727–36 (2013).

155. Chen, J., Li, Y., Wang, L., Lu, M. & Chopp, M. Caspase inhibition by Z-VAD increases the survival of grafted bone marrow cells and improves functional outcome after MCAo in rats. *J. Neurol. Sci.* **199,** 17–24 (2002).

156. Kim, W. J., Mohan, R. R. & Wilson, S. E. Caspase inhibitor z-VAD-FMK inhibits keratocyte apoptosis, but promotes keratocyte necrosis, after corneal epithelial scrape. *Exp. Eye Res.* **71,** 225–32 (2000).

157. Lemaire, C., Andréau, K., Souvannavong, V. & Adam, A. Inhibition of caspase activity induces a switch from apoptosis to necrosis. *FEBS Lett.* **425,** 266–270 (1998).

158. Xie, T. *et al.* Structural basis of RIP1 inhibition by necrostatins. *Structure* **21,** 493–499 (2013).

159. Degterev, A., Maki, J. L. & Yuan, J. Activity and specificity of necrostatin-1, small-molecule inhibitor of RIP1 kinase. **20,** 366 (2012).

160. Geserick, P. *et al.* Absence of RIPK3 predicts necroptosis resistance in malignant melanoma. *Cell Death Dis.* **6,** e1884 (2015).

161. Bertrand, M. J. M. & Vandenabeele, P. The Ripoptosome: Death Decision in the Cytosol. *Molecular Cell* **43,** 323–325 (2011).

162. Jang, T. H. *et al.* Structural study of the RIPoptosome core reveals a helical assembly for kinase recruitment. *Biochemistry* **53,** 5424–5431 (2014).

163. Kaiser, W. J. & Offermann, M. K. Apoptosis induced by the toll-like receptor adaptor TRIF is dependent on its receptor interacting protein homotypic interaction motif. *J. Immunol.* **174,** 4942–4952 (2005).

164. Estornes, Y. *et al.* dsRNA induces apoptosis through an atypical death complex associating TLR3 to caspase-8. *Cell Death Differ.* **19,** 1482–94 (2012).

165. Pobezinskaya, Y. L. *et al.* The function of TRADD in signaling through tumor necrosis factor receptor 1 and TRIF-dependent Toll-like receptors. *Nat. Immunol.* **9,** 1047–1054 (2008).

166. Chen, N.-J. *et al.* Beyond tumor necrosis factor receptor: TRADD signaling in toll-like receptors. *Proc. Natl. Acad. Sci. U. S. A.* **105,** 12429–12434 (2008).

167. Tada, K. *et al.* Critical roles of TRAF2 and TRAF5 in tumor necrosis factor-induced NF-kappa B activation and protection from cell death. *J. Biol. Chem.* **276,** 36530–4 (2001).

168. Shu, H.-B., Takeuchi, M. & Goeddel, D. V. The tumor necrosis factor receptor 2 signal transducers TRAF2 and c-IAP1 are components of the tumor necrosis factor receptor 1 signaling complex. *Proc. Natl. Acad. Sci.* **93,** 13973–13978 (1996).

169. Karl, I. *et al.* TRAF2 inhibits TRAIL- and CD95L-induced apoptosis and necroptosis. *Cell Death Dis.* **5,** e1444 (2014).

170. Petersen, S. L. *et al.* TRAF2 is a biologically important necroptosis suppressor. *Cell Death Differ.* **1,** 1–12 (2015).

171. Varfolomeev, E. *et al.* IAP Antagonists Induce Autoubiquitination of c-IAPs, NF-??B Activation, and TNF??-Dependent Apoptosis. *Cell* **131,** 669–681 (2007).

172. Reimer, T., Brcic, M., Schweizer, M. & Jungi, T. W. poly(I:C) and LPS induce distinct IRF3 and NF-kappaB signaling during type-I IFN and TNF responses in human macrophages. *J. Leukoc. Biol.* **83,** 1249–1257 (2008).

173. Baggiolini, M. & Clark-Lewis, I. Interleukin-8, a chemotactic and inflammatory cytokine. *FEBS Letters* **307,** 97–101 (1992).

174. Kunsch, C. & Rosen, C. A. NF-kappa B subunit-specific regulation of the interleukin-8 promoter. *Mol. Cell. Biol.* **13,** 6137–46 (1993).

175. Delhase, M. *et al.* TANK-binding kinase 1 (TBK1) controls cell survival through PAI-2/serpinB2 and transglutaminase 2. *Proc. Natl. Acad. Sci. U. S. A.* **109,** E177–86 (2012).

176. Zhivotovsky, B. & Orrenius, S. Cell cycle and cell death in disease: Past, present and future. in *Journal of Internal Medicine* **268,** 395–409 (2010).

177. D'Souza, S. D. *et al.* Multiple sclerosis: Fas signaling in oligodendrocyte cell death. *J. Exp. Med.* **184,** 2361–70 (1996).

178. Wosik, K. *et al.* Oligodendrocyte injury in multiple sclerosis: a role for p53. *J. Neurochem.* **85,** 635–644 (2003).

179. Shao, W.-H. & Cohen, P. L. Disturbances of apoptotic cell clearance in systemic lupus erythematosus. *Arthritis Res. Ther.* **13,** 202 (2011).

180. Brown, J. M. & Attardi, L. D. The role of apoptosis in cancer development and treatment response. *Nat. Rev. Cancer* **5,** 231–237 (2005).

181. Mocarski, E. S., Upton, J. W. & Kaiser, W. J. Viral infection and the evolution of caspase 8-regulated apoptotic and necrotic death pathways. *Nat. Rev. Immunol.* **12,** 79–88 (2011).

182. Kaiser, W. J. *et al.* RIP1 suppresses innate immune necrotic as well as apoptotic cell death during mammalian parturition. *Proc Natl Acad Sci U S A* **111,** 7753–7758 (2014).

183. Ea, C. K., Deng, L., Xia, Z. P., Pineda, G. & Chen, Z. J. Activation of IKK by TNF?? Requires Site-Specific Ubiquitination of RIP1 and Polyubiquitin Binding by NEMO. *Mol. Cell* **22,** 245–257 (2006).

184. Darding, M. & Meier, P. IAPs: Guardians of RIPK1. *Cell Death Differ.* **19,** 58–66 (2012).

185. Koo, G.-B. *et al.* Methylation-dependent loss of RIP3 expression in cancer represses programmed necrosis in response to chemotherapeutics. *Cell Res.* **25,** 707–725 (2015).

186. Newton, K. *et al.* Activity of protein kinase RIPK3 determines whether cells die by necroptosis or apoptosis. *Science* **343,** 1357–60 (2014).

187. Wachter, T. *et al.* cFLIPL inhibits tumor necrosis factor-related apoptosis-inducing ligand-mediated NF-κB activation at the death-inducing signaling complex in human keratinocytes. *J. Biol. Chem.* **279,** 52824–52834 (2004).

188. Tenev, T. *et al.* The Ripoptosome, a Signaling Platform that Assembles in Response to Genotoxic Stress and Loss of IAPs. *Mol. Cell* **43,** 432–448 (2011).

189. Cho, Y., McQuade, T., Zhang, H., Zhang, J. & Chan, F. K. M. RIP1-dependent and independent effects of necrostatin-1 in necrosis and T cell activation. *PLoS One* **6,** (2011).

190. Takahashi, N. *et al.* Necrostatin-1 analogues: critical issues on the specificity, activity and in vivo use in experimental disease models. *Cell Death Dis.* **3,** e437–10 (2012).

191. Blander, J. M. A long-awaited merger of the pathways mediating host defence and programmed cell death. *Nat Rev Immunol* **14,** 601–618 (2014).

192. Sabio, G. & Davis, R. J. TNF and MAP kinase signalling pathways. *Seminars in Immunology* **26,** 237–245 (2014).

193. Schleich, K. *et al.* Stoichiometry of the CD95 Death-Inducing Signaling Complex: Experimental and Modeling Evidence for a Death Effector Domain Chain Model. *Mol. Cell* **47,** 306–319 (2012).

194. Dickens, L. S. *et al.* A Death Effector Domain Chain DISC Model Reveals a Crucial Role for Caspase-8 Chain Assembly in Mediating Apoptotic Cell Death. *Mol. Cell* **47,** 291–305 (2012).

195. Chinnaiyan, A. M., O'Rourke, K., Tewari, M. & Dixit, V. M. FADD, a novel death domain-containing protein, interacts with the death domain of fas and initiates apoptosis. *Cell* **81,** 505–512 (1995).

196. Tourneur, L. & Chiocchia, G. FADD: A regulator of life and death. *Trends in Immunology* **31,** 260–269 (2010).

197. Patterson, S. D. Protein identification and characterization by mass spectrometry. *Curr. Protoc. Mol. Biol.* **Chapter 10,** Unit 10.22 (2001).

198. Helgason, E., Phung, Q. T. & Dueber, E. C. Recent insights into the complexity of Tank-binding kinase 1 signaling networks: The emerging role of cellular localization in the activation and substrate specificity of TBK1. *FEBS Lett.* **587,** 1230–1237 (2013).

199. Suzuki, T. *et al.* Cell type-specific subcellular localization of phospho-TBK1 in response to cytoplasmic viral DNA. *PLoS One* **8,** e83639 (2013).

200. Mogensen, T. H. Pathogen recognition and inflammatory signaling in innate immune defenses. *Clinical Microbiology Reviews* **22,** 240–273 (2009).

201. Jiang, Z., Mak, T. W., Sen, G. & Li, X. Toll-like receptor 3-mediated activation of NF-kappaB and IRF3 diverges at Toll-IL-1 receptor domain-containing adapter inducing IFN-beta. *Proc. Natl. Acad. Sci. U. S. A.* **101,** 3533–3538 (2004).

202. Cusson-Hermance, N., Khurana, S., Lee, T. H., Fitzgerald, K. a & Kelliher, M. a. Rip1 mediates the Trif-dependent toll-like receptor 3- and 4-induced NF-{kappa}B activation but does not contribute to interferon regulatory factor 3 activation. *J. Biol. Chem.* **280,** 36560–6 (2005).

203. Meylan, E. *et al.* RIP1 is an essential mediator of Toll-like receptor 3-induced NF-kappa B activation. *Nat. Immunol.* **5,** 503–507 (2004).

204. Ran, F. A. *et al.* Genome engineering using the CRISPR-Cas9 system. *Nat. Protoc.* **8,** 2281–2308 (2013).

205. Wu, X., Kriz, A. J. & Sharp, P. A. Target specificity of the CRISPR-Cas9 system. *Quant Biol* **2,** 59–70 (2014).

206. Ran, F. A. *et al.* Genome engineering using the CRISPR-Cas9 system. *Nat. Protoc.* **8,** 2281–2308 (2013).

207. Grassian, A. R. *et al.* A Medium-Throughput Single Cell CRISPR-Cas9 Assay to Assess Gene Essentiality. *Biol. Proced. Online* **17,** 15 (2015).

208. Cusson-Hermance, N., Khurana, S., Lee, T. H., Fitzgerald, K. a & Kelliher, M. a. Rip1 mediates the Trif-dependent toll-like receptor 3- and 4-induced NF-{kappa}B activation but does not contribute to interferon regulatory factor 3 activation. *J. Biol. Chem.* **280,** 36560–6 (2005).

209. Bradley, J. R. TNF-mediated inflammatory disease. *Journal of Pathology* **214,** 149–160 (2008).

210. van Deventer, S. J. Tumour necrosis factor and Crohn's disease. *Gut* **40,** 443–448 (1997).

211. van Schouwenburg, P. a, Rispens, T. & Wolbink, G. J. Immunogenicity of anti-TNF biologic therapies for rheumatoid arthritis. *Nat. Rev. Rheumatol.* **9,** 164–72 (2013).

212. Balkwill, F. TNF-?? in promotion and progression of cancer. *Cancer and Metastasis Reviews* **25,** 409–416 (2006).

213. Walczak, H. TNF and ubiquitin at the crossroads of gene activation, cell death, inflammation, and cancer. *Immunological Reviews* **244,** 9–28 (2011).

214. Vince, J. E. *et al.* IAP Antagonists Target cIAP1 to Induce TNF??-Dependent Apoptosis. *Cell* **131,** 682–693 (2007).

215. Wang, L., Du, F. & Wang, X. TNF-?? Induces Two Distinct Caspase-8 Activation Pathways. *Cell* **133,** 693–703 (2008).

216. Tada, K. *et al.* Critical roles of TRAF2 and TRAF5 in tumor necrosis factor-induced NF-kappa B activation and protection from cell death. *J. Biol. Chem.* **276,** 36530–4 (2001).

217. Vince, J. E. *et al.* TRAF2 must bind to cellular inhibitors of apoptosis for tumor necrosis factor (TNF) to efficiently activate NF-κB and to prevent TNF-induced apoptosis. *J. Biol. Chem.* **284,** 35906–35915 (2009).

218. Lewandowski, C. M. & Co-investigator, N. TRAF2 regulates TNF and NF-κB signalling to suppress apoptosis and skin. *J. Chem. Inf. Model.* **53,** 1689–1699 (2015).

219. Dillon, C. P. *et al.* Survival Function of the FADD-CASPASE-8-cFLIPL Complex. *Cell Rep.* **1,** 401–407 (2012).

220. Zhang, H. *et al.* Functional complementation between FADD and RIP1 in embryos and lymphocytes. *Nature* **471,** 373–376 (2011).

221. Pomerantz, J. L. & Baltimore, D. NF-kappaB activation by a signaling complex containing TRAF2, TANK and TBK1, a novel IKK-related kinase. *EMBO J.* **18,** 6694–6704 (1999).

222. Chariot, A. *et al.* Association of the adaptor TANK with the IκB kinase (IKK) regulator NEMO connects IKK complexes with IKKε and TBK1 kinases. *J. Biol. Chem.* **277,** 37029–37036 (2002).

223. Clark, K., Takeuchi, O., Akira, S. & Cohen, P. The TRAF-associated protein TANK facilitates cross-talk within the IkappaB kinase family during Toll-like receptor signaling. *Proc. Natl. Acad. Sci. U. S. A.* **108,** 17093–8 (2011).

224. Karin, M. How NF-kB is activated: the role of the IkB kinase (IKK) complex. *Oncogene* **18,** 6867–6874 (1999).

225. Hochrainer, K., Racchumi, G. & Anrather, J. Site-specific phosphorylation of the p65 protein subunit mediates selective gene expression by differential NF-??B and RNA polymerase II promoter recruitment. *J. Biol. Chem.* **288,** 285–293 (2013).

226. Sasaki, C. Y., Barberi, T. J., Ghosh, P. & Longo, D. L. Phosphorylation of RelA/p65 on serine 536 defines an I{kappa}B{alpha}-independent NF-{kappa}B pathway.（标题貌似很重要，但暂时与柴胡文章无关）. *J. Biol. Chem.* **280,** 34538–47 (2005).

227. Sakurai, H. *et al.* Tumor necrosis factor-α-induced IKK phosphorylation of NF-κB p65 on serine 536 is mediated through the TRAF2, TRAF5, and TAK1 signaling pathway. *J. Biol. Chem.* **278,** 36916–36923 (2003).

228. Adli, M. & Baldwin, A. S. IKK-i/IKK?? controls constitutive, cancer cell-associated NF-??B activity via regulation of Ser-536 p65/RelA phosphorylation. *J. Biol. Chem.* **281,** 26976–26984 (2006).

229. Tanaka, Y. & Chen, Z. J. STING specifies IRF3 phosphorylation by TBK1 in the cytosolic DNA signaling pathway. *Sci. Signal.* **5,** ra20 (2012).

230. Sabatel, H. *et al.* Phosphorylation of p65(ReLA) on ser 547 by ATM represses NF-??b-dependent transcription of specific genes after genotoxic stress. *PLoS One* **7,** (2012).

231. Spandau, U. H. M., Toksoy, A., Verhaart, S., Gillitzer, R. & Kruse, F. E. High expression of chemokines Gro-alpha (CXCL-1), IL-8 (CXCL-8), and MCP-1 (CCL-2) in inflamed human corneas in vivo. *Arch. Ophthalmol.* **121,** 825–31 (2003).

232. Kaser, A. *et al.* Increased expression of CCL20 in human inflammatory bowel disease. *J. Clin. Immunol.* **24,** 74–85 (2004).

233. Cullen, S. P. *et al.* Fas/CD95-Induced Chemokines Can Serve as ' Find-Me' Signals for Apoptotic Cells. *Mol. Cell* **49,** 1034–1048 (2013).

234. Hosokawa, Y., Hosokawa, I., Ozaki, K., Nakae, H. & Matsuo, T. Increase of CCL20 expression by human gingival fibroblasts upon stimulation with cytokines and bacterial endotoxin. *Clin. Exp. Immunol.* **142,** 285–291 (2005).

235. Wild, P. *et al.* Phosphorylation of the autophagy receptor optineurin restricts Salmonella growth. *Science* **333,** 228–33 (2011).

236. Rusten, T. E. & Stenmark, H. P62, an Autophagy Hero or Culprit? *Nat. Cell Biol.* **12,** 207–209 (2010).

237. Sanz, L., Sanchez, P., Lallena, M. J., Diaz-Meco, M. T. & Moscat, J. The interaction of p62 with RIP links the atypical PKCs to NF-κB activation. *EMBO J.* **18,** 3044–3053 (1999).

238. Galluzzi, L. *et al.* Life, death and burial: multifaceted impact of autophagy. *Biochem. Soc. Trans.* **36,** 786–90 (2008).

239. Debnath, J. The multifaceted roles of autophagy in tumors-implications for breast cancer. *J. Mammary Gland Biol. Neoplasia* **16,** 173–87 (2011).

240. Janji, B., Viry, E., Moussay, E. & Paggetti, J. The multifaceted role of autophagy in tumor evasion from immune surveillance. **7,** (2016).

241. Xie, X., White, E. P. & Mehnert, J. M. Coordinate Autophagy and mTOR Pathway Inhibition Enhances Cell Death in Melanoma. *PLoS One* **8,** (2013).

242. Bray, K. *et al.* Autophagy suppresses RIP kinase-dependent necrosis enabling survival to mTOR inhibition. *PLoS One* **7,** (2012).

243. McQuade, T., Cho, Y. & Chan, F. K.-M. Positive and negative phosphorylation regulates RIP1- and RIP3-induced programmed necrosis. *Biochem. J.* **456,** 409–15 (2013).

244. Cho, Y. *et al.* Phosphorylation-Driven Assembly of the RIP1-RIP3 Complex Regulates Programmed Necrosis and Virus-Induced Inflammation. *Cell* **137,** 1112–1123 (2009).

245. Blackwell, K. *et al.* TRAF2 phosphorylation modulates tumor necrosis factor alpha-induced gene expression and cell resistance to apoptosis. *Mol. Cell. Biol.* **29,** 303–314 (2009).

246. Zhang, L., Blackwell, K., Altaeva, A., Shi, Z. & Habelhah, H. TRAF2 phosphorylation promotes NF-κB-dependent gene expression and inhibits oxidative stress-induced cell death. *Mol. Biol. Cell* **22,** 128–40 (2011).

247. Morlon, A., Munnich, A. & Smahi, A. TAB2, TRAF6 and TAK1 are involved in NF-??B activation induced by the TNF-receptor, Edar and its adaptator Edaradd. *Hum. Mol. Genet.* **14,** 3751–3757 (2005).

248. Schilling, R., Geserick, P. & Leverkus, M. Characterization of the ripoptosome and its components: Implications for anti-inflammatory and cancer therapy. *Methods Enzymol.* **545,** 83–102 (2014).

249. Chen, D. J. & Huerta, S. Smac mimetics as new cancer therapeutics. *Anticancer. Drugs* **20,** 646–658 (2009).

250. Belz, K. *et al.* Smac mimetic and glucocorticoids synergize to induce apoptosis in childhood ALL by promoting ripoptosome assembly. *Blood* **124,** 240–250 (2014).

XI. Abbreviations

%	Percent
°C	Degree Celsius
4-HT	4-Hydroxytamoxifen
AIF	Apoptosis inducing factor
Apaf-1	Apoptotic protease activation factor 1
ATG	Autophagy related protein
Bak	Bcl-2 antagonist or killer
Bax	Bcl-2-like protein 4
Bax	Bcl-2-associated X protein
Bcl-2	B-cell lymphoma 2
BH3	Bcl-2 homology 3
Bid	BH3 interacting-domain death agonist
Bid	BH3 interacting-domain death agonist
CARD	Caspase recruiting domain
caspases	Cystein-aspartatic proteases
CCL-20	Chemokine (C-C motif) ligand 20
CD95	Cluster of differentiation 95
CD95L	CD95 ligand
cFLIP	Cellular FLICE-like inhibitory protein
cIAPs	Cellular inhibitor of apoptosis proteins
Ctrl	Control
CXCL-1	chemokine (C-X-C motif) ligand 1
DD	Death domain
DED	Death effector domain
Diablo	Direct IAP binding protein with low pI
DISC	Death inducing signalling complex
DL	Death ligand
DNA	Deoxyribonucleic acid
dNTP	Deoxynucleoside triphosphate
DR	Death receptor
DTT	Dithiothreitol
EDTA	Ethylenediaminetetraacetic acid
FADD	Fas-associated protein with death domain
FCS	Fetal calf serum
FLICE	FADD-like IL-1β-converting enzyme
g	Gram
GAPDH	Glyceraldehyde 3-phosophate dehydrogenase
h	Hour

Hepes	2-[4-(2-hydroxyethyl)piperazin-1-yl]ethanesulfonic acid
HLH	Helix-loop-helix
IFN	Interferon
IKK	IκB kinase
IKK-α	Inhibitor of nuclear factor kappa-B kinase subunit alpha
IKK-β	Inhibitor of nuclear factor kappa-B kinase subunit beta
IKK-ε	Inhibitor of nuclear factor kappa-B kinase subunit epsilon
IL-8	Interleukin-8
IMS	Intermembrane space
IP	Immunoprecipitation
IRF-3	Interferon regulatory factor 3
IκB-α	Inhibitor of kappa B-alpha
KD	Kinase domain
kDa	Kilodalton
l	Liter
LB	Lysogeny broth
LUBAC	Linear ubiquitin chain assembly complex
LZ	Lysine-zipper
m	Milli
M	Molarity
min	Minute
MLKL	Mixed Lingase Kinase Ligase
n	Nano
NBD	NEMO binding domain
Nec-1	Necrostatin-1
NEMO	NF-κB-essential modulator
NF-κB	Nuclear factor kappa-light-chain-enhancer of activated B cells
NIK	NF-κB-inducing kinase
NLS	Nuclear localization singal
OPTN	Optineurin
PBS	Phosphate buffered saline
PCD	Programmed cell death
PCR	Polymerase chain reaction
PINK	PTEN-induced putative kinase 1
poly (I:C)	Polyinosinic:polycytidylic acid
PVDF	Polyvinylidene difluoride
qPCR	Quantitative real-time polymerase chain reaction
RIP1	Receptor Interacting Protein 1
RIP3	Receptor Interacting Protein 3
RNA	Ribonucleic acid
RT	Room temperature

sec	Second
shRNA	Short hairpin RNA
siRNA	Small interfering RNA
Smac	Second mitochondria-derives activator of caspases
SQSTM1	Sequestosome-1
TAB2	TAK1 binding protein 2
TAK1	Transforming growth factor β-activated kinase 1
TANK	TRAF family member-associated NF-kappa-B activator
tBid	Truncated Bid
TBK1	TANK binding kinase 1
TIR	Toll/interleukin-1 receptor
TL	Total cell lysate
TLR	Toll-like receptor
TNF	Tumor necrosis factor
TNFR	TNF receptor
TRADD	TNFR 1-associated death domain protein
TRAF2	TNF receptor-associated factor 2
TRAF6	TNF receptor-associated factor 6
TRIF	TIR-domain-containing adapter-inducing interferon-β
ULD	Ubiquitin-like domain
UV	Ultra violet
V	Volt
w/v	Weight per volume
x g	Gravitational acceleration
XIAP	X-linked inhibitor of apoptosis protein
zVAD-fmk	z-Val-Ala-DL-Asp-fluoromethylketone

XII. Acknowledgements

Although only my name is written on this dissertation, there are many people without whom I would never have come this far.

First of all I want to thank **Prof. Dr. Martin Leverkus** who sadly passed away before I could finish this thesis. Martin accepted me as a young student and gave me the opportunity to develop into a matured PhD. He always inspired me with his great optimism and catching enthusiasm, which I will never forget.

Some of the described experiments would never have been possible without the help of some cooperating groups. Therefore, I am very grateful for the collaboration with **Prof. Dr. Marion MacFarlane** and **Prof. Dr. Ivan Dikic**, who supported my work with their great techniques. Additionally, I want to thank the whole lab of **Prof. Pascal Meier**, especially **Tencho** and **Sidonie,** who gave me the possibility to learn the CRISPR/Cas9 technique directly from their hands and made my stay in London an unforgettable time.

Furthermore, I want to thank **Dr. Martin Sprick** for his valuable ideas during my TAC meetings and that he always offered his help to push my project into new directions.

A special thanks also goes to **Prof. Petra Boukamp** who brightened my TAC meetings with fruitful discussions and additionally was so kind to function as my second supervisor after Martin faded away so unexpectedly.

Special acknowledgements go to **Dr. Peter Geserick** who was so kind to prove read this thesis and supported me throughout the last four years.

Next, I want to thank **Prof. Victor Umansky** for being my first supervisor as well as **Prof. Ralf Bartenschlager** and **Dr. Björn Tews** for acting as examiners in my disputation.

The PhD time would never have been such a great experience without the people around me. Therefore, I want to thank **Kathrin**, **Jochen**, **Sebastian**, **Claudia**, **Jing**, **Biswajit** and **Michi** for very funny years and unforgettable lunch breaks. Special thanks go to **Sebastian**, who I know since we started our diploma studies in Kaiserslautern and who made many hard and intensive times endurable for me. You always helped me with scientific problems as well as “outside-lab issues”. I would never have come that far without your support. Thank you so much for being a great friend and I hope we will never lose track of each other.

Scientific work would never been possible without some distraction from people who are not part of the scientific community. Therefore, I want to thank all of my friends, especially **Patrick** and **Benny** who initiated many funny activities and gave me plenty of great days.

I would never have come to this point in my life without the help of **my parents**. Thank you so much for bringing me up and for your ongoing support. I appreciate that you always enabled me the things I needed or wanted and made me to the man I am.

Last, but not least, I want to thank my wife **Martina**. You always endured my unsteady mood swings throughout the last years and covered my back whenever I needed your help. You always encouraged me to go on, so that I could achieve more than I expected. Finally, you gave me our wonderful daughter **Helena**, who holds my heart and lights up every day of my life. Thank you so much for being my wife and bearing me as I am.